



**Politecnico
di Torino**

Politecnico di Torino

Master's degree in Energy and Nuclear Engineering

Renewable Energy Systems

A.Y. 2023/2024

March/April 2024 Graduation session

OpenModelica-based modelling and simulation of a laboratory- scale district heating system

Supervisors:

Prof. Vittorio VERDA

Prof. Elisa GUELPA

Giulia MANCÒ

Gianmarco PRESO

Candidate:

Giovanni CHIAPPETTO

Table of Contents

Table of Contents	I
Abstract	III
List of Figures	IV
List of Tables	VI
Acronyms	VII
1. Introduction	1
1.1. Master thesis' structure	2
1.2. District heating: state-of-the-art and future development	3
1.2.1. Heating demand impact on European energy consumption	3
1.2.2. DH working principle and main components	6
1.2.3. DH primary energy mix in Italy and Europe	8
1.2.4. DH technological evolution.....	10
1.2.5. DH's potential and role in future energy systems	13
1.3. The concept of Digital Twin	16
1.4. Modelica language and its applications	19
1.5. District heating in the Modelica community	24
2. The Energy Center's district heating laboratory	26
2.1. Location and purpose of the laboratory	27
2.2. System layout and its components	28
2.2.1. Heat generation and primary circuit layout	29
2.2.2. Substations layout and relative secondary circuit	35
2.2.3. Thermal energy storage in secondary circuit 2.....	42
3. Building the digital twin	47
3.1. Software and libraries employed	48
3.2. The methodological approach	50
3.3. The digital components and their configuration	52
3.3.1. Primary circuit components	53
3.3.2. Substations and secondary circuit components.....	57

3.4.	Setting the system’s operational parameters	61
3.4.1.	Air heater: assessing the performance.....	62
3.4.2.	Substation heat exchanger: assessing the performance.....	63
3.5.	Summary of models created	66
4.	Simulations and results	71
4.1.1.	Setting the simulation environment	71
4.2.	Model 1: basic system layout	72
4.2.1.	Simulation 1: system cold start.....	72
4.2.2.	Simulation 2: preheating the primary circuit.....	77
4.2.3.	Simulation 2B and 2C: different primary supply temperatures...	82
4.3.	Model 2: basic system layout - enhanced primary circuit modelling.	85
4.3.1.	Simulation 3, 3B: the effect of pipes’ discretization level	87
4.3.2.	Simulation 4: investigating temperatures on the return side	90
4.4.	Model 3: sensible thermal energy storage study	92
4.4.1.	Simulation 5: comparing with experimental data.....	92
4.4.2.	Simulation 6: the effect of discretization level of the TES.....	95
4.5.	Model 4: the complete model	100
4.5.1.	Simulation 7	100
4.6.	Observations	104
5.	Conclusions	105
	Ringraziamenti	106
	References	107

Abstract

The goal of this thesis is to model a laboratory-scale district heating system to help test its performance and simulate different scenarios and configurations. The experimental system in question is located inside the Politecnico di Torino laboratories and it was built to replicate on a smaller scale the characteristic behaviour of a district heating system. Heat generation is accomplished with a natural gas water heater. The primary circuit is composed of a small network of steel pipes which distributes hot water to two secondary circuits. Each of the two secondary circuits features a substation, composed of a plate heat exchanger and a circulation pump, and an air heater to simulate heat load. A thermal energy storage system is also present in one of the two secondary circuits.

This work aims at creating a “digital twin” of this system, coupling each component present in the real setup with a digital one, trying to preserve their specific characteristics and features in the most accurate way possible. The foundation is OpenModelica software, an open-source Modelica-based modelling, compilation, and simulation environment, which enables the study of complex multi-domain physics systems.

The core of this project is proving the feasibility of digital twin modelling using open-source software, highlighting the eventual advantages and weak points of this method. A step-by-step explanation is provided, including the construction of this model using mostly Buildings and Modelica Standard Library components, commenting on their implementation and behaviour inside the model itself, while mentioning the problems encountered and their relative fixes.

Finally, the results of different simulations are showcased including a default system configuration and a few other ones, such as one setup that includes the sensible thermal energy storage, or one with different operational parameters, such as temperatures and mass flow rates.

List of Figures

Figure 1-1 Cross-sectorial study on heating in the EU [7]	4
Figure 1-2 Share of energy carrier by country for the final heating and cooling demand for all sectors in 2015 (EU-28) [8]	5
Figure 1-3 Space and water heating demand in Italy in 2018 [10]	5
Figure 1-4 Simplified district heating diagram (adapted from: [57])	6
Figure 1-5 Possible district heating sources [57]	7
Figure 1-6 Energy mix of Italian district heating networks in 2020 [12]	9
Figure 1-7 Evolution of DH technology [17]	11
Figure 1-8 Minimum recommended level of district heating adoption according to the HRE 2050 scenario [19]	13
Figure 1-9 Total operating district heat pipelines in Europe [9]	14
Figure 1-10 Evolution of DH in Italy, in extension, energy and heated volume [%] [10]	15
Figure 1-11 Number of Digital Twin related publications by year [59].....	17
Figure 1-12 The physical-to-virtual and virtual-to-physical twinning process [1]	18
Figure 1-13 Modelica logo [2]	19
Figure 1-14 A screenshot from OMEdit showing a model from the project	22
Figure 2-1 Primary circuit layout.....	30
Figure 2-2 Front plate of water heater with gas burner in front	31
Figure 2-3 Distribution network pipes - detail on supply and return junction.....	33
Figure 2-4 Distribution network pipes - detail on primary branch towards substation 2 – before insulation application.....	33
Figure 2-5 Primary circuit circulation pump [42]	34
Figure 2-6 Secondary circuit 1 diagram	36
Figure 2-7 Substation	37
Figure 2-8 Brazed plate heat exchanger	38
Figure 2-9 Air heater components.....	40
Figure 2-10 Air heaters placement	40
Figure 2-11 Secondary circuit circulation pump [47].....	41
Figure 2-12 Secondary circuit 2 diagram.....	43
Figure 2-13 TES placement in the laboratory.....	46
Figure 3-1 MBL water heater component icon	52
Figure 3-2 Effect of numerical diffusion for on temperature modelling in pipes [60]	55
Figure 3-3 Air heater modelling	59
Figure 3-4 HEX scheme	65
Figure 3-5 Model 1	67
Figure 3-6 Model 2	68

Figure 3-7 Model 3	69
Figure 3-8 Model 4	70
Figure 4-1 Normal system operation – bypass not active	72
Figure 4-2 SIM 1 - temperatures along primary circuit supply side	73
Figure 4-3 SIM 1 - water heater inlet and outlet temperatures.....	73
Figure 4-4 SIM 1 - temperatures along primary circuit return side	75
Figure 4-5 SIM 1 - temperatures along primary circuit return side - closeup ..	75
Figure 4-6 SIM 1 - Temperatures at 4 sides of substation 2 HEX.....	77
Figure 4-7 System operating with substation bypass (preheating phase).....	78
Figure 4-8 SIM 2 - temperatures along primary circuit supply side	78
Figure 4-9 SIM 2 - temperatures along primary circuit return side - closeup ..	79
Figure 4-10 SIM 2 - temperatures along primary circuit return side.....	79
Figure 4-11 SIM 1 – 2 – Water heater power output comparison	80
Figure 4-12 SIM 2 - Temperatures at 4 sides of substation 2 HEX	80
Figure 4-13 SIM 2, 2B, 2C - primary circuit supply temperature comparison..	82
Figure 4-14 SIM 2, 2B, 2C Air heater output temperature comparison.....	83
Figure 4-15 SIM 2, 2B, 2C - water heater power output comparison	83
Figure 4-16 Thermocouples placement along primary circuit	86
Figure 4-17 SIM 3 - Temperatures along return side primary circuit [nSeg = 10].....	88
Figure 4-18 SIM 3B - Temperatures along return side primary circuit [nSeg = 2]	88
Figure 4-19 SIM 3 - Temperatures along supply side primary circuit [nSeg = 10].....	89
Figure 4-20 SIM 3B - Temperatures along supply side primary circuit [nSeg = 2]	89
Figure 4-21 Alternative primary layout with additional bypass valve.....	90
Figure 4-22 SIM 4 - temperatures along primary circuit return side with modified primary configuration	91
Figure 4-23 SIM 5 – TES supply and return temperature – comparison with experimental data	93
Figure 4-24 SIM 5 - temperature evolution along height	94
Figure 4-25 TES experimental test - temperature evolution along height.....	94
Figure 4-26 SIM 6 - temperature evolution along height [nSeg = 4]	96
Figure 4-27 TES model configuration	96
Figure 4-28 SIM 6 - temperature evolution along height [nSeg = 70]	97
Figure 4-29 SIM 6 - TES behaviour	99
Figure 4-30 SIM 7 - TES thermocouples reading.....	101
Figure 4-31 SIM 7 - Water heater power output.....	101
Figure 4-33 SIM 7 - Air temperature at air heater output	102
Figure 4-32 SIM 7 - Temperatures at substation 2 HEX.....	102

List of Tables

Table 2-1 Water heater specification [41].....	31
Table 2-2 Distribution pipes specifications.....	32
Table 2-3 Primary circuit circulation pump specifications [42]	34
Table 2-4 Substation specifications	38
Table 2-5 Substation heat exchanger specifications [45]	38
Table 2-6 Air heater specifications [46]	39
Table 2-7 Secondary circuit circulation pump specifications [47]	41
Table 2-8 TES thermocouples placement.....	45
Table 2-9 Thermal energy storage specifications [50]	45
Table 3-1 PC specifications.....	49
Table 3-2 Air heater off-design performance calculation [46].....	62
Table 3-3 HEX Effectiveness values calculated with TRS	65
Table 3-4 HEX design conditions [45]	65
Table 4-1 General simulation settings	71
Table 4-2 SIM 1 parameters	72
Table 4-3 SIM 2 parameters	77
Table 4-4 SIM 2, 2B, 2C parameters	82
Table 4-5 SIM 3, 3B parameters	87
Table 4-6 SIM 4 parameters	91
Table 4-7 SIM 5 parameters	93
Table 4-8 SIM 6 parameters	96
Table 4-9 SIM 7 parameters	100

Acronyms

AH	Air Heater
CHP	Combined heat and power
DC	District cooling
DH	District heating
DHC	District heating and cooling
EC	European Commission
HEX	Heat exchanger
MBL	Modelica Buildings Library
MSL	Modelica Standard Library
nSeg	parameter for the number of segments
OM	Open Modelica
OMEdit	OpenModelica Connection Editor
OSMC	Open-source Modelica Consortium
RES	Renewable energy sources
SIM	Simulation
TES	Thermal energy storage
TFC	Total final gross energy consumption
TRS	Thermal Resistance Scaling
VM	Virtual Machine
WH	Water Heater

1. Introduction

District heating can be a great way to increase energy efficiency in the heating and cooling energy market. It can be coupled with RES and other waste heat sources to recover energy that would be otherwise wasted. Its centralized layout can act very effectively and can accelerate the adoption of new technologies, which would imply high investment costs for single users if implemented separately. However, being a legacy technology, DH's full potential is yet to be completely exploited. A new generation of this system, that guarantees higher efficiency, and more sustainability can play a central role in future energy systems. That is why DH is currently an important research topic in the field.

To serve this purpose, Politecnico di Torino built into one of its facilities a small-scale district heating system, with which it is possible to study the behaviour of the network under different conditions and when coupled with thermal storage or other innovative appliances.

The work focuses on creating a digital model of this very system, to provide an easy and flexible way of testing it with different configurations. Our goal consists of building a “digital twin” of the system [1], i.e. a model capable of representing each one of the components of the real system and simulating their behaviour as accurately as possible.

The digital model created could eventually be employed to provide insights on the system's behaviour under various scenarios eliminating the need for expensive or burdensome physical tests. These simulations can be run providing different operational conditions, like varying mass flow rates, temperatures, or other parameters, or could also be employed to assess whether the coupling of new machinery is convenient.

1.1. Master thesis' structure

This paper develops in the following chapters:

- *INTRODUCTION*: the concept of district heating and its role in the actual and future energy system in the EU and Italy is presented. Then, the definition of digital twin is discussed and, finally, the Modelica language [2], on which the project is based, and its applications are introduced.
- *THE PHYSICAL SYSTEM*: the structure of the real system under analysis is described, including its various components and their relative operational principle. The location and purpose of the laboratory are also reported.
- *BUILDING THE DIGITAL TWIN*: the tools and software used to build the digital model are presented. This section explains which models are built and why and the methodological approach to the problem is also reported.
- *RESULTS OF THE SIMULATIONS*: in this section, the results of various simulations are showcased and commented along with the proposal for further developments. A few problems
- *CONCLUSIONS*: a summary of the project is reported, highlighting the strongest and weakest points of the followed approach

1.2. District heating: state-of-the-art and future development

1.2.1. *Heating demand impact on European energy consumption*

Climate change is undoubtedly one of the biggest challenges our society has to face, demanding fast and incisive actions from us all. Energy efficiency and global adoption of innovative and sustainable heating and cooling systems are paramount in tackling the rapid growth of this destructive phenomenon. In this context, district heating and cooling can play a major role in reducing the environmental footprint of human activities.

The heating and cooling sector alone accounts for about 50% of the total final gross energy consumption (TFC) in the EU [3]. For this reason, the European Commission (EC) has published many reports in recent years on this very topic, considering it among the most urgent thematic in various plans to transition to more sustainable energy sources, such as the Energy Efficiency Directive [4], REPowerEU Plan [5] or the “Clean Energy for all Europeans” package [6]. Despite the importance of updated insights on the problem, it is quite a difficult task to gather information about energy consumption for heating and cooling and, especially, on the share of renewable energy in the sector, as statistical data can be fragmented or submitted to variable European directives for their calculation. However, a sense of the impact of this final use on overall energy consumption can still be understood.

The most up-to-date data obtained from the reports committed by EC show that 3445 TWh were consumed in the region in 2017 to meet heating demand [7]. The report also states that, considering a cross-sectorial approach, that includes residential, industrial, and commercial & public services, space heating and water heating account respectively for 42.4% and 5.0% of the total final gross energy consumption in 2017, with 23.1% of energy spent covered by renewable sources. In addition to these figures, the paper highlights also that 67% of heating demand comes from the residential sector, where investments in energy efficiency can show a slower rate of adoption. Regarding energy sources employed in the sector, more than 43% of the demand is covered by natural gas, followed by biomass and fuel oil, in similar percentages, around 15% [7]. In the following plots (Fig. 1.1), these partitions are described in greater detail.

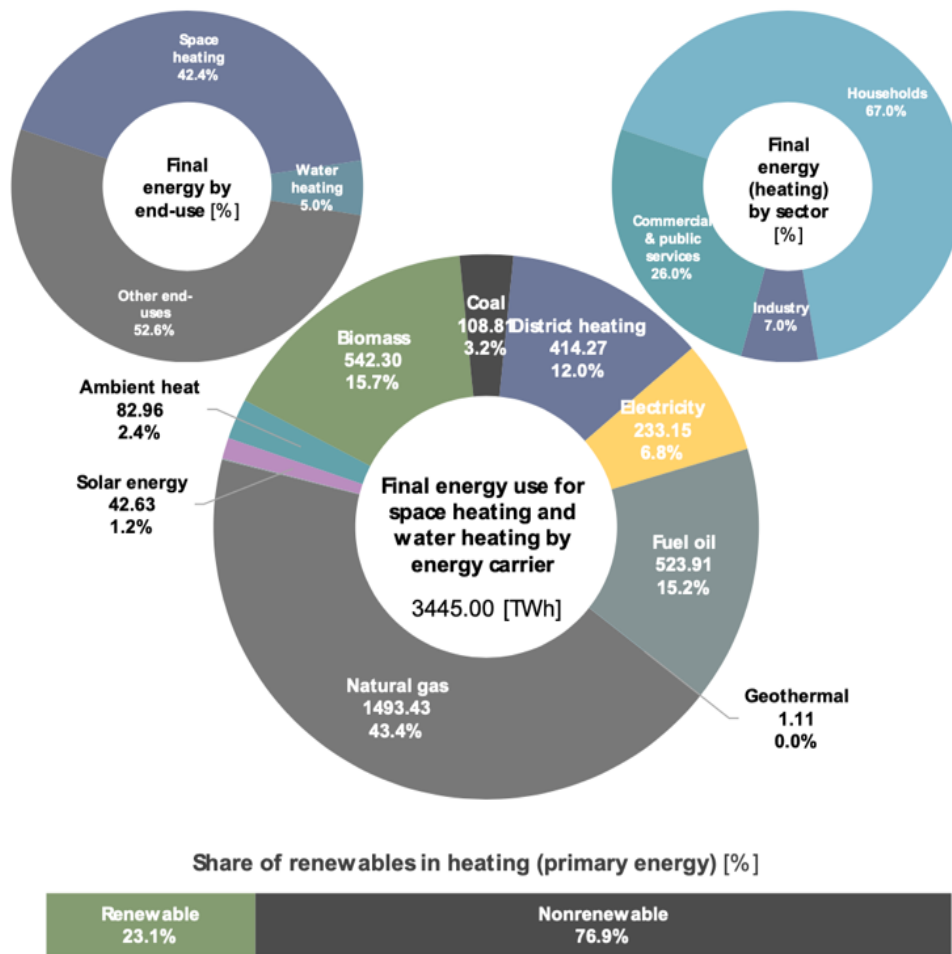


Figure 1-1 Cross-sectorial study on heating in the EU [7]

In the plot above, district heating is included in the share of energy sources and accounts for 12% of final energy use, while direct natural gas and fuel oil consumption still covers more than 43% and 15% respectively. The project Heat Roadmap Europe project tracked the adoption of DH in the region, also exploring the feasibility of future scenarios in which it plays a more prominent role in the heating supply. From Fig. 1-2 it can be noted that northern countries such as Denmark, Sweden and Finland were leading the district heating market in 2015. This is due to the very early adoption of the technology, which in turn means that DH systems in these countries can sometimes feature older plants and distribution systems, lowering the overall efficiency [8] [9].

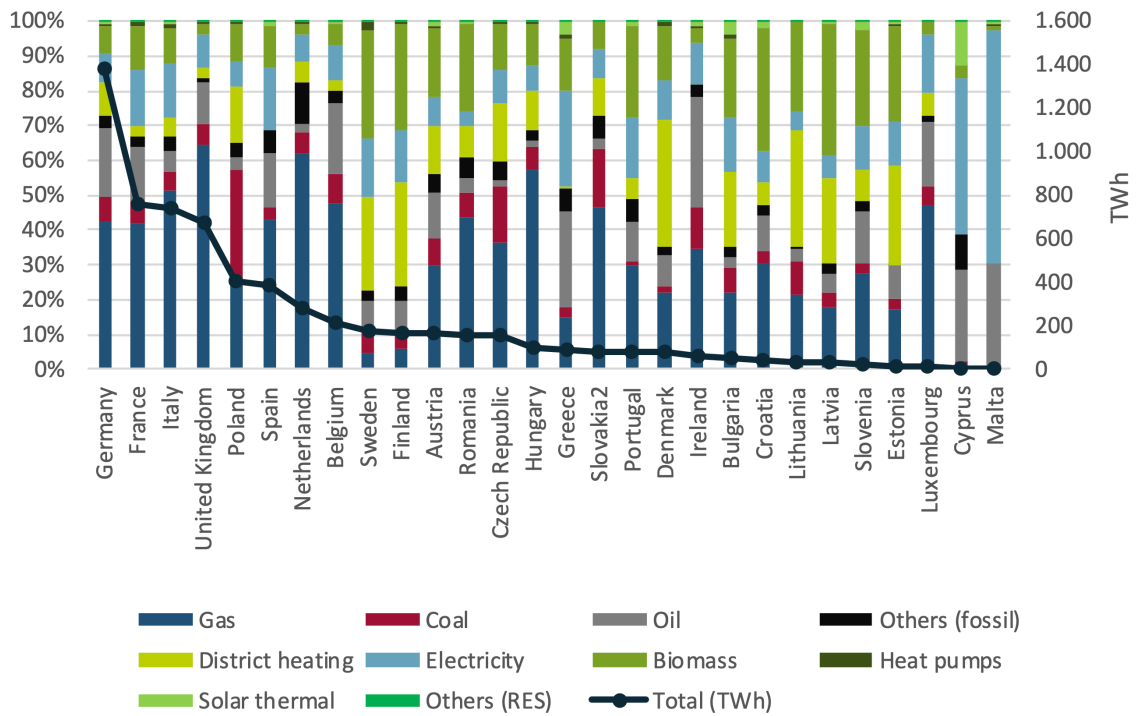


Figure 1-2 Share of energy carrier by country for the final heating and cooling demand for all sectors in 2015 (EU-28) [8]

Unfortunately, if compared to these countries, DH in the Italian heating market is far less significant. The latest data available show that the share of district heating on the total energy consumption for heating and cooling only accounted for 3% of total energy consumed in space heating and water heating in 2018, out of 366 TWh overall, as can be seen in Fig. 1-3. As in other European countries, most of the demand is met via direct consumption of natural gas, which covered even 60% of total energy consumption in the sector, followed by biomass at 13% and an encouraging 13% in heat pumps [10]. Other shares of energy in the mix are shown in Fig. 1-3.

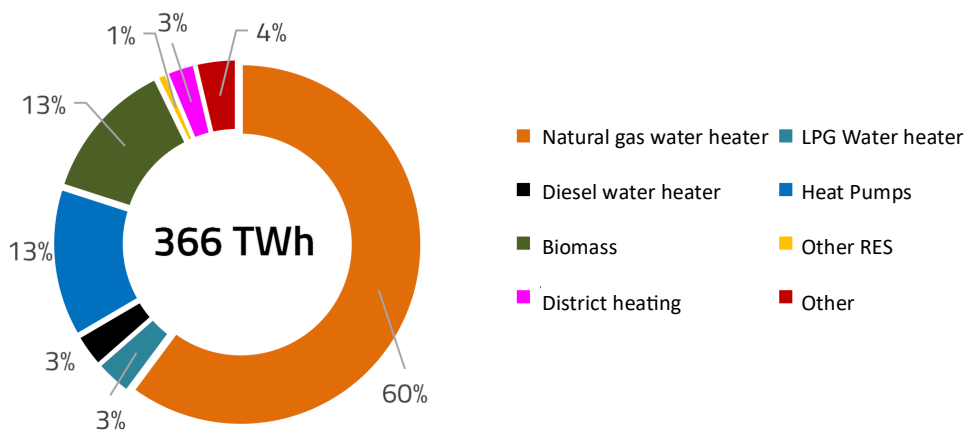


Figure 1-3 Space and water heating demand in Italy in 2018 [10]

1.2.2. DH working principle and main components

Another crucial aspect that must be considered when talking about the potential of district heating and its weight on the energy mix is the source of heat itself. To do so, it can be useful to recall the working principle of district heating.

District heating is based on the separation between generation and consumption of heat. In conventional heating systems heat generation happens locally at the building level. It can be centralised, serving multiple apartments or independent, where each household is served by its own heater. This happens in commercial or public buildings as well. These systems consist generally of water boilers, powered mainly by the combustion of fossil fuels such as natural gas or oil, or the combustion of biomass, like wood. Newly designed buildings might also be fitted with newer heat generation solutions such as electric heat pumps or solar collectors. Regardless of the source and the technology applied, heat is generated at the user level and is transferred to space heating components, like radiators or radiant floors, or air-based systems such as fan-coil units. In this way, each building's heating system is isolated and independent from one another.

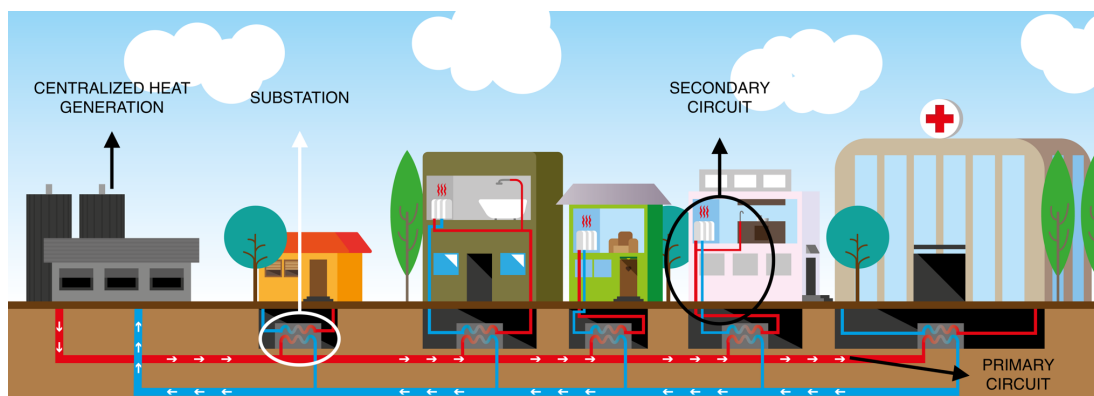


Figure 1-4 Simplified district heating diagram (adapted from: [57])

The fundamental concept of district heating is to decouple the heat generation and consumption, by concentrating the heat generation towards a centralized system. In most district heating systems, heat generation is centralized in a large plant, with eventual smaller back-up plants spread around the network, mainly to assist during heavy load or to guarantee the target temperatures in the furthest region of the network. Typically, heat is generated in CHP plants, where heat is recovered during electricity generation in thermoelectric power plants, but this can also be accomplished through bespoke water heaters, without electricity generation.

Once heat has been generated in the form of hot water, it is transferred to the users through a distribution network made of insulated steel pipes buried into the ground. This network spreads from the central heat generation plants and connects through smaller pipes to the buildings, and it is called the “primary circuit”. The

primary circuit is divided into a supply side, carrying hot water from the plant, and a return side, carrying colder water that is circulated back at the plant to restart the cycle.

The hydraulic circuit on the user’s side is called the “secondary circuit”. The link between these two circuits is called substation. Similarly to electric grids, the substation is responsible for taking energy from the main distribution network and transferring it to a lower level. In DH systems, the substation manages and controls the amount of heat transferred from the primary circuit to the secondary one and it is fundamentally composed of a thermal energy meter, a district heating controller, and a heat exchanger. The heat exchanger takes heat power from the primary circuit and transfers it to the user’s secondary circuit which is supported by a circulation pump.

From here on the hot water is sent to the building’s heating system, just like in any other conventional heating system, as mentioned earlier. In a way, the substation substitutes the local heat generation of conventional heating systems. In Figure 1-4 a simplified graphical representation of a DH system is proposed.

While the fundamental concept of this technology has remained the same, in the recent years the inclusion of alternative heat generation solutions has been investigated. Along with more sustainable heat generation plants, powered by solar or geothermal plants, waste heat recovery from data centers or industrial process could be implemented. These concepts upgrade the conventional DH design by including multiple heat generation distributed throughout the territory, accomplishing a better integration with RES and waste heat recovery. In this way DH can become a true player in the energetic transition towards sustainable energy systems. In fig. 1-5 a summary of these concepts is proposed.

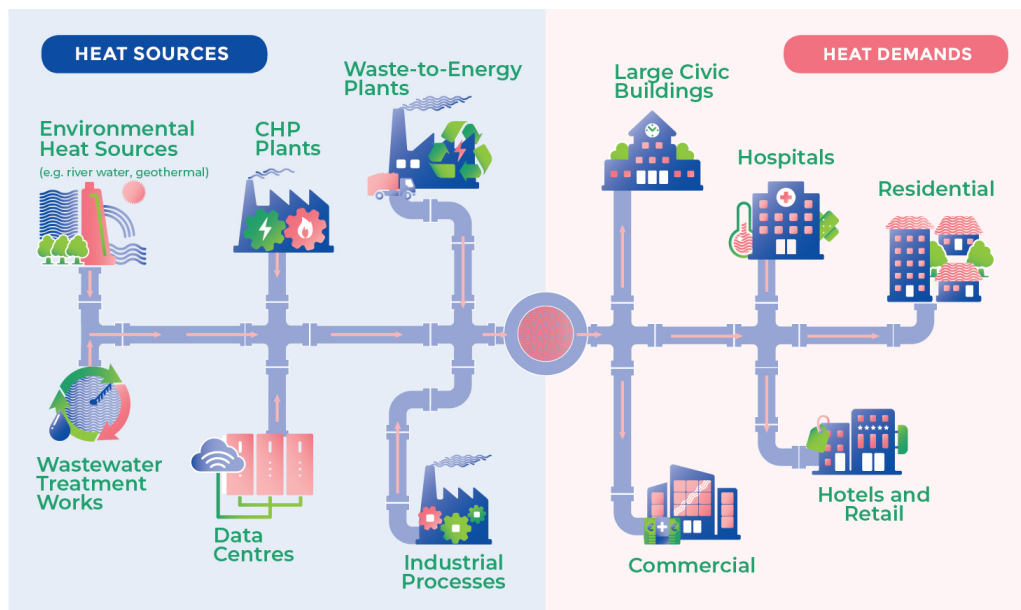


Figure 1-5 Possible district heating sources [57]

1.2.3. DH primary energy mix in Italy and Europe

Typically, DH energy is sourced in “Combined Heating and Power” plants or CHP plants, namely thermoelectric power plants, powered by fossil fuels, in which the waste heat produced during the thermodynamic cycle is partially recovered and transmitted into the DH network. Since the early concepts of district heating, this has been a great way of increasing the efficiency of these power plants, recovering precious heat that would be otherwise wasted. When this kind of implementation is not possible, DH can be powered by a “Heat Only” layout, where generation is still centralised but powered traditionally, as in local heat generation, via gas-powered water boilers or similar appliances.

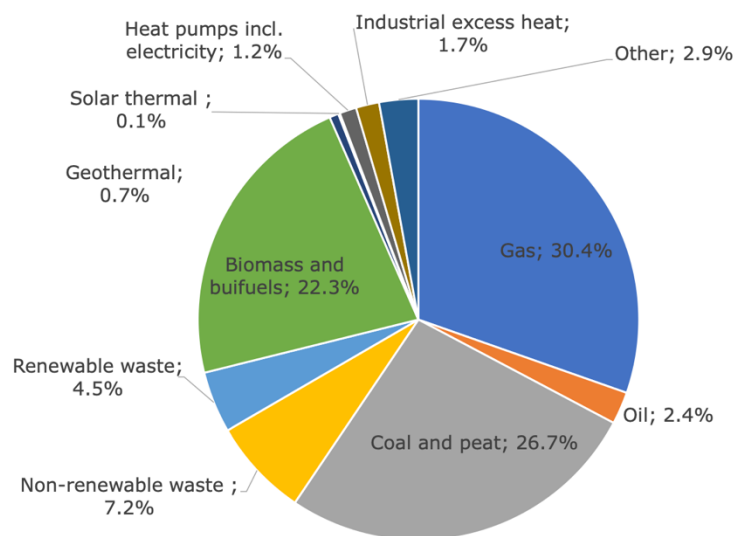


Figure 1-5 Energy mix of European district heating systems in 2018 [11]

This aspect can be controversial. On one hand, DH can dramatically increase the efficiency of the entire system when compared to multiple smaller local generation systems, on the other, these layouts can still be tied to fossil fuels consumption, requiring an update to fit into the transition to carbon-free energy sources. From Figure 1-5, it can be acknowledged how district heating is still very much dependent on this kind of traditional generation. In 2018 more than half of the total energy mix for the supply of district heating networks in Europe was covered by fossil fuels, namely natural gas, coal, and oil [11]. Coming back to the Italian district heating market, a similar situation is present. In 2022, according to GSE, total energy fed into the DH grid reached 11.9 TWh, of which 64% was sourced by CHP plants, the rest being covered by heat-only systems. Fossil fuels in primary energy consumption stand at approximately 74%, mainly consisting of natural gas [12]. Fig. 1-6 shows Italian DH energy share. There are two notable exceptions: Tuscany DH networks are mostly powered by geothermal energy and mountain regions like Valle d’Aosta or Trentino Alto Adige where a substantial share of biomass consumption is observed [12].

The data just reported show how district heating systems in Europe and Italy are still conventional systems, tied mainly to the consumption of fossil fuels or biomass, which, despite being efficient overall and a much better alternative to conventional heating systems, do not fit into a true decarbonisation scenario. District heating can be central in improving the energy efficiency at a wider scale, by cutting emissions generated by multiple buildings. However, the need for new configurations for DH rises. Systems that can take advantage of renewable energy sources or that can collect waste heat from multiple sources can further enhance the benefit of this technology, helping the adoption of new technologies at a wider scale.

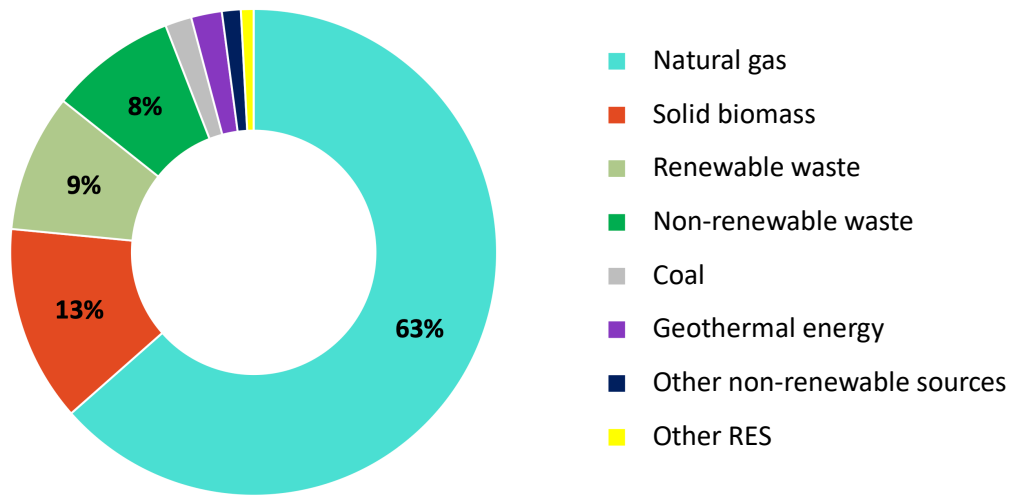


Figure 1-6 Energy mix of Italian district heating networks in 2020 [12]

To address this necessity, multiple research projects and working groups founded by the EU were born in the last years, to help create datasets and insights about the topic and try to develop a new concept of district heating [13]. Some of these projects are WEDISTRICHT [14], which experimented with the development of advanced configurations and technology, Heat Roadmap Europe [15], whose efforts concentrate on providing data and insights to policymakers and regulators about the possible integration of DH in the heating market or HeatNet NWE [16], which tested the feasibility of new generation DH through 6 pilot networks in different European cities. These projects are united by the development at multiple levels of the so-called 4th and 5th generations of district heating systems [13].

1.2.4. *DH technological evolution*

Being a well-established technology, that dates back to the end of the 19th century, district heating has been indeed classified into different generations, depending on the technology employed, the source of heat generation and the operating temperatures [17]. They can be summarised in the following points:

- **1st GENERATION**

Steam is used as the carrier fluid, fed into pipes laid in concrete ducts and heat is generated by coal combustion. This first iteration proved to be unsafe and poorly efficient, due to very high pressures and temperatures. Almost all the existing 1st gen systems were converted to newer setups [17].

- **2nd GENERATION**

This generation extended from the 1930s to the 1970s and featured pressurised hot water over 100°C as the carrier. CHP plants, running on coal and oil were on the generation side [17].

- **3rd GENERATION**

Born in the 1970s it is the typical configuration used today in DH systems worldwide. It is based on water below 100°C as the carrier, flowing into pre-insulated pipes buried into the ground. This generation was created in response to the oil crisis, which required highly efficient systems. CHP plants powered by fossil fuels are still the main source of heat, typically from coal, oil, and biomass. In the last years, these configurations have been retrofitted to accommodate new heat production technologies such as geothermal and solar [17].

- **4th GENERATION**

This is the current step in the development of district heating technology. The frontier of this evolution is integrating renewable energy share in the source mix, eventually replacing carbon-intensive ones, all while maintaining high flexibility. Systems can be categorised as 4th generation when they can operate with low primary temperatures, reduce losses in the distribution network, recycle heat from low-temperature sources such as solar or waste heat, and ensure sustainable economics for both the user and the operator. In addition, this generation started including the related technology of district cooling [17].

- **5th GENERATION**

This term comprehends all the possible future development of the technology, as there is still no consent on the definition. Generally, these systems are a big evolutionary step, as they detach from the main concept of technology. If 4th generation still features the basic setup, and range of applications, trying to enhance the efficiency, 5th generation includes new aspects such as hybrid applications for heating *and* cooling, brine as carrier fluid and ultra-low operating temperatures, not suitable for current systems [17].

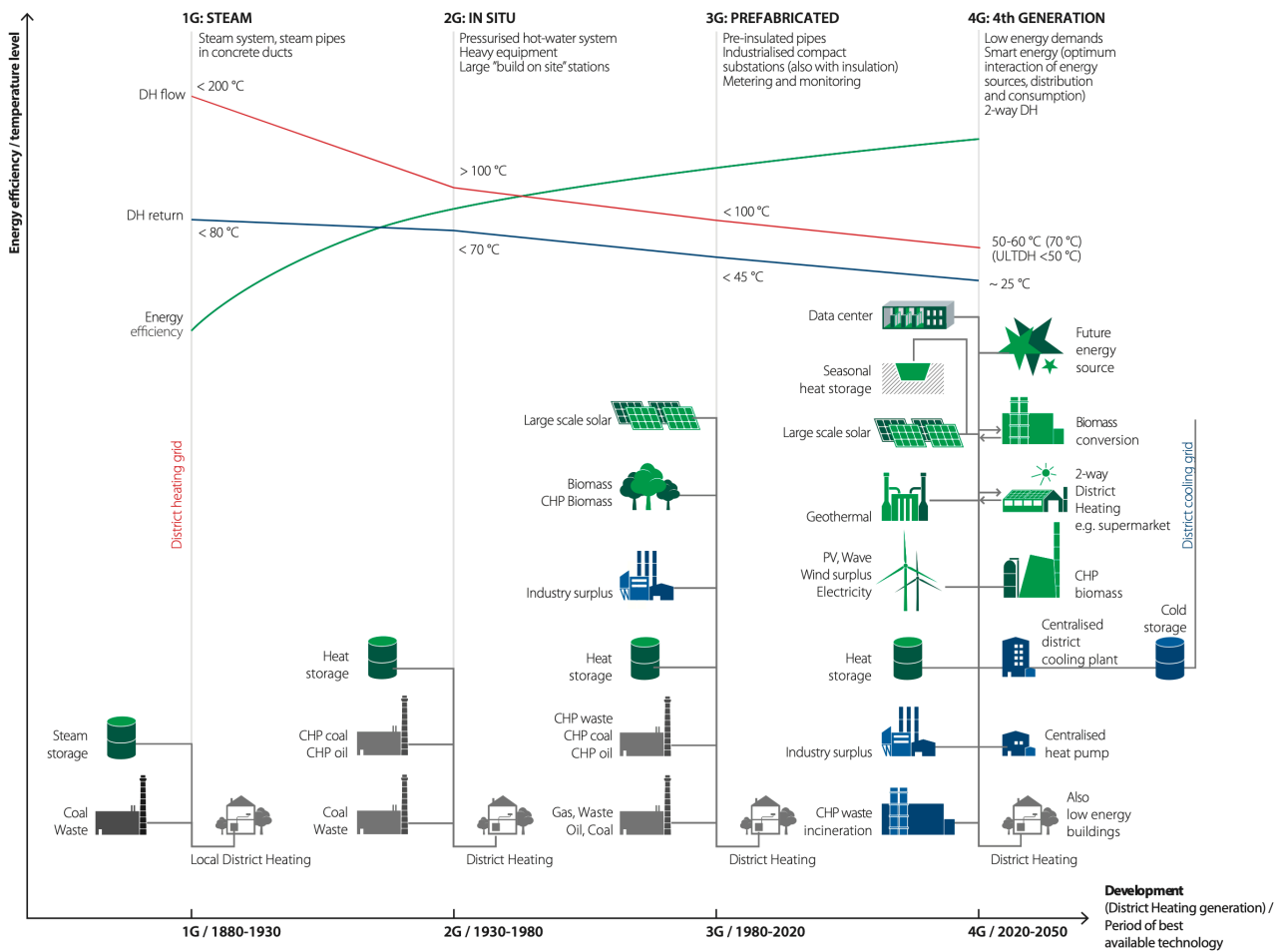


Figure 1-7 Evolution of DH technology [17]

The district heating technology is on the verge of a new era, with the coming of 4th generation systems. In Fig. 1-7, these new concepts are shown, and are based on lowering as much as possible the supply operational temperatures of the flow on the primary side, from around 100 °C in conventional systems to as low as 50° – 60°C in new ones. Lowering the supply temperature enables the coupling of DH networks with waste heat recovery such as data centre excess heat or with waste/biomass incineration, extending the employment of future low-temperature heat sources and enabling a better synergy with future renewable energy sources, such as a broader

use of heat pumps. These can also be an opportunity to further recover heat that is not technically recoverable with current setups. Lower heat losses in the distribution lines are another key advantage of this concept together with increased efficiency overall. Yet, it must be considered that the current district heating source is mainly covered by combustion-driven heat generation, which will have to be limited in the future both for the reduction of available biomass and landfill waste available for incineration and to fulfil total decarbonisation goals. New sources such as seasonal heat storage, where applicable, or 2-way district heating in supermarkets and similar commercial/industrial businesses could be employed.

However, this change in operational temperatures could also require intervention on the users' side, to adapt incompatible heating systems, such as old radiators with insufficient heat transfer surfaces, designed with high temperatures in the fluid carrier in mind. Anyway, many studies demonstrated that, excluding critical cases, actual heating systems can be coupled successfully with low-temperature DH [18]. This is supported by the fact that heating systems are designed with peak heat load in mind, although they operate typically in the range of 0-80% of the maximum demand. Current heating systems proved to sustain heating demand in normal conditions with the temperature at radiators as low as 45°C [18]. According to this evidence, heating systems should be sized and designed considering the typical heat load, and provide additional power only when truly needed, via an increased DH supply, or local heating provided by electric cables wound to supply pipes. These interventions could keep the costs of the transition under control, where extended retrofitting is not possible or economically viable [18]. These findings also apply to domestic hot water supply, which can be easily sourced by 4th generation DH systems without special requirements [18]. The overall system efficiency could also be increased with newly designed pipes in the distribution stage, with double-pipe systems which can reduce heat losses by 6-12% over traditional twin-pipe configuration [18].

1.2.5. DH's potential and role in future energy systems

All these advancements in DH technology were proven not only to be technologically viable but even economically favourable according to multiple studies [18] [9]. Actual DH networks and buildings can be upgraded to the new generation without significant investments. This is true despite the cost needed to upgrade existing distribution grids, retrofit older heating systems in buildings and finance new heat generation sites, as the savings due to higher efficiency and lower production costs, together with the benefits of system integration, assure a balanced investment [18].

These recent developments in the field brought some researchers to analyse the potential of district heating, and its integration into existing and future energy markets. Studies such as Heat Roadmap Europe or others funded by the EU found that DH could not only be a key technology to rely on but even provide better performances when compared to different decarbonisation scenarios. For example, when envisioning a scenario where heat pumps and DH together replace current heat generation systems, heat savings can reach 50% while reducing costs by 15% when compared to electricity-only heating systems scenarios [8] [18]. Another report from the EU showed that, when comparing DH with the possible electrification of the category, the first showed a much better primary energy factor of 0.79 compared to 2.22 of electricity, with the 2017 energy mix. This means that to provide a unit of final energy (heating), such as 1 kWh, DH heating requires only 0.79 kWh of primary energy [7].

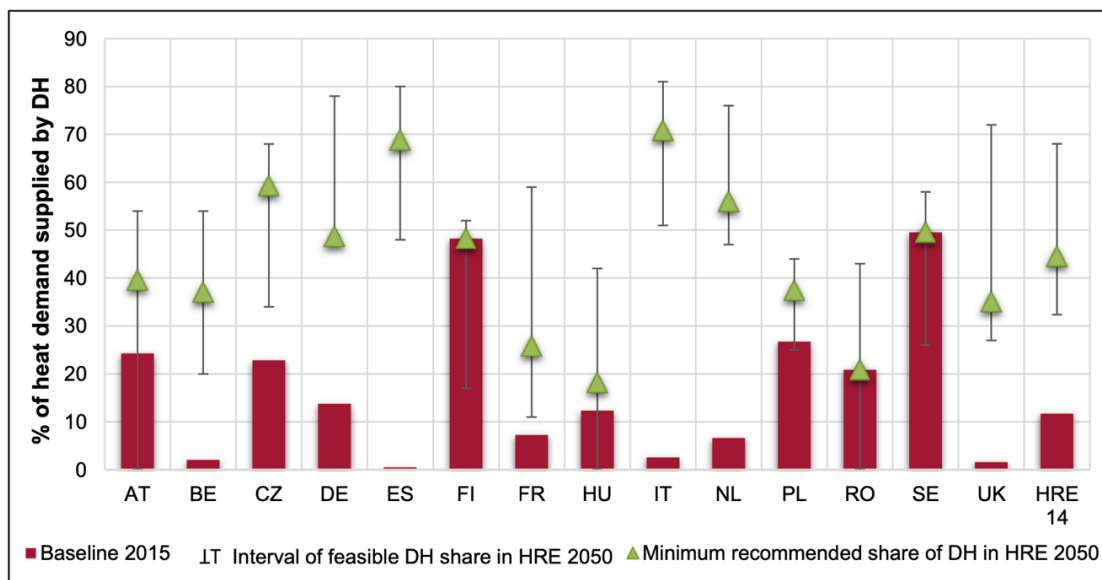


Figure 1-8 Minimum recommended level of district heating adoption according to the HRE 2050 scenario [19]

Future energy scenarios such as the one proposed in Heat Roadmap Europe forecast a potential DH adoption from the actual 12% up to 32-68% of total heating demand, with a recommended share of 45% to be reached in 2050, while trying to maintain a total investment cost of 0.5% on total annual energy system expenditure, showing how the potential of this technology remains still untapped [7] [19].

Although these scenarios envision a massive adoption of this technology, pointing at future targets that can appear distant and ambitious, as presented in the following figures, DH's presence in the European energy market keeps growing at a considerable rate. The total length of DH networks reached 200,000km in 2019, growing by 35% since 2005, supported by investments of 6 billion USD per year, as in Fig. 1-9 [9].

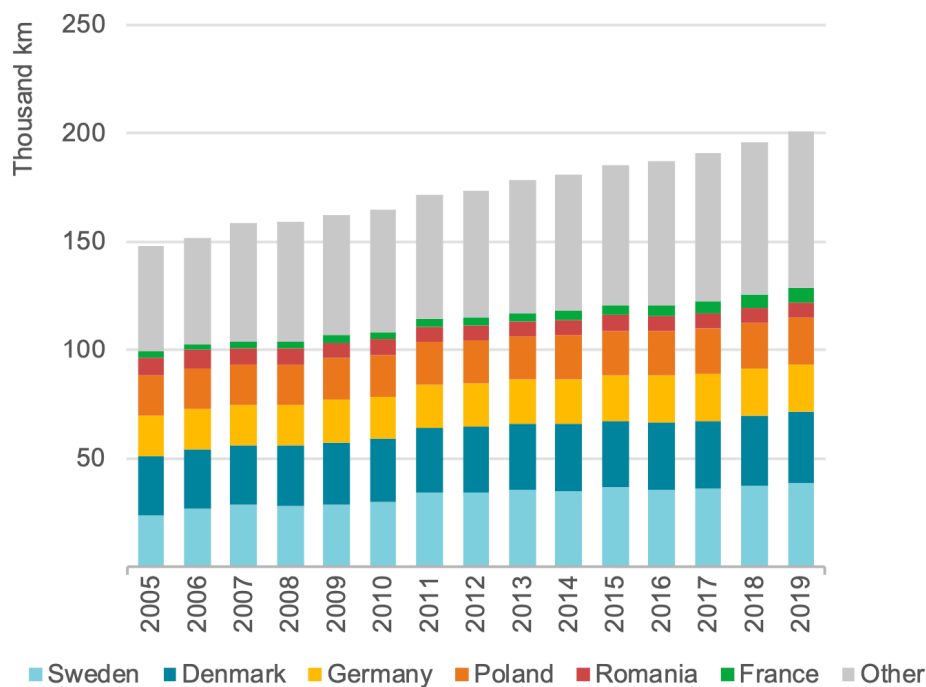


Figure 1-9 Total operating district heat pipelines in Europe [9]

This general increase in DH installation is also found in the Italian heating market. According to GSE, in 2018 networks' extension increased by 308% since the year 2000, as it is shown in Figure 1-10 [10]. The authority also reported that in 2018 total energy technically deliverable via DH systems could potentially exceed 57 TWh, more than 5 times the actual value [10].

Despite these promising facts, data report a slow integration of waste recovery, RES, or other sustainable energy sources in the European DH energy mix. Russian invasion in 2022 uncovered the fragility of an energy market mostly based on natural gas consumption and accentuated the need for a fast and reliable transition to new systems. Following these concerns, the plan REPowerEU was implemented. It outlined a clear path to detach from problematic energy supplies such as Russian-

derived natural gas, accelerate progress in the RES field, and contain even more ambitious targets towards carbon neutrality in 2050. Thanks to these efforts, in 2022, 41GW of photovoltaic power was added to the grid and RES reached 39% of total energy consumption [20]. Italy’s interpretation of these efforts is called “PNRR”, the national plan of public investments conceived to advance the transformation of the energy sector, aligning with European guidelines. Its section dedicated to energy efficiency in buildings accounts for more than 15 billion EUR, with district heating playing a central role [21].

However, the 40% RES share of total energy spent in heating and cooling by 2030, envisioned in the 2030 Climate Target Plan is looking very challenging as current adoption is stuck at about 20% and will require massive investments and a change in the regulatory and incentives field [22]. As DH technology clearly demonstrated its competitiveness and adaptability, it is up to regulators and operators to act together to create a more integrated and sustainable energy market in the future.

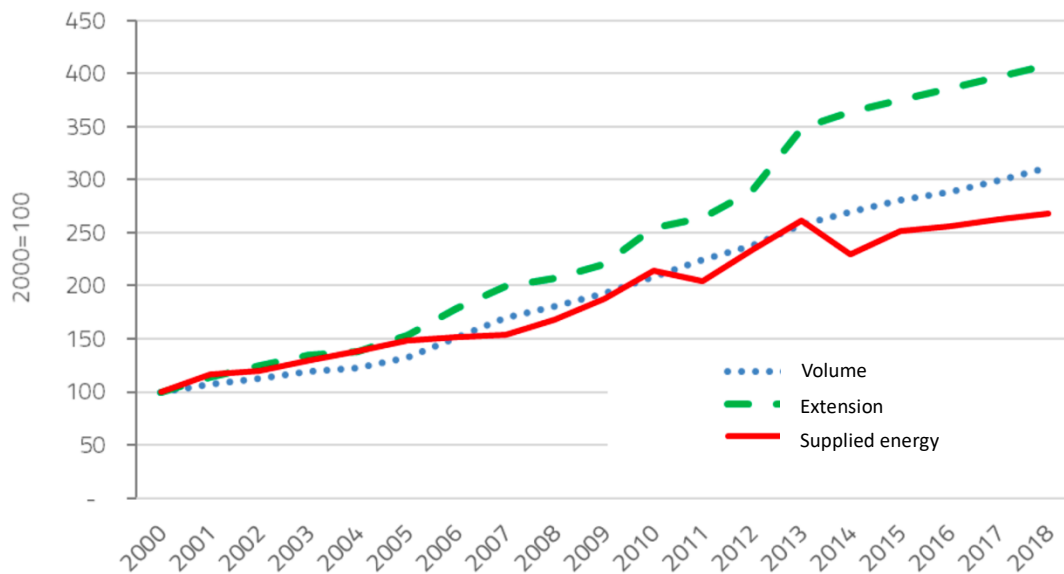


Figure 1-10 Evolution of DH in Italy, in extension, energy and heated volume [%] [10]

1.3. The concept of Digital Twin

As said before, the goal of this project is to create a so-called “digital twin” of the network, transferring each one of its components into our model. This demands a holistic approach to the problem, as multiple physical variables must be correctly calculated and represented. Multi-domain physical calculations are required, from fluid dynamics to thermodynamics, always maintaining a proper correlation to the real system.

Despite being a great ally when designing and operating various systems, the interest in digital twin technology has increased just in the last few years. The first definition of this concept was given by Prof. Grieves during a course at the University of Michigan in 2003 about product life cycle management [23]. Since then, many definitions have been proposed, depending on the field of application or the objective, but a digital twin can be described as a virtual counterpart of a physical entity, the *“full-element reconstruction and digital mapping of the working status and work progress of the physical entity of the product in the information space”* [23]. It consists of a multi-physics, multi-scale, realistic, dynamic simulation model that can be employed to simulate, diagnose, predict, and control the evolution of products in real environments [23].

The first application of this concept can be found in the defence and aeronautic market. NASA was one of the first to believe in the capability of this approach in the design and management of products, as testing and trials for aerospace-grade machinery imply the difficulty of recreating operating conditions and massive costs, especially when failure occurs. One example can be rocket-launch testing, where the failure rate can be high and produce catastrophic effects. With NASA, also the U.S. Air Force showed interest in this concept, as they were looking for a cleverer way of predicting and monitoring aircraft’s life and maintenance [23]. The technology and information consulting firm Gartner Inc., included the digital twin in the top ten strategic technologies for 2016 and 2017, as part of the future key technologies to shape the evolution of the defence and aerospace industry [23].

However, the advantages of this concept can improve performance and cut costs in virtually every engendering and design field, i.e. for product manufacturing, energy systems and many others. It can assist not only in the design and test phase but also give insights during maintenance, enabling fast identification of failures and better comprehension of product ageing. The Digital twin can indeed be included in the list of technologies and approaches that are at the base of a new era for the industry of all sectors, called “Industrie 4.0”, in which the digital world is embraced and applied to every step of the production, from the design phase until the decommissioning [24]. In the first stages, the concept of digital twin was seen as a collection of specific and separate digital models that were developed during product development, uncoupled from the data gathered in real utilisation scenarios.

On the contrary, in the last years, the interest in this technology has seen a notable increase, being cited more and more in technical papers and employed in the field as a key part of the design and management process, with dedicated and complete models built for the purpose of simulation [24]. Figure 1-11 reports the evolution of the digital twin concept in scientific literature.

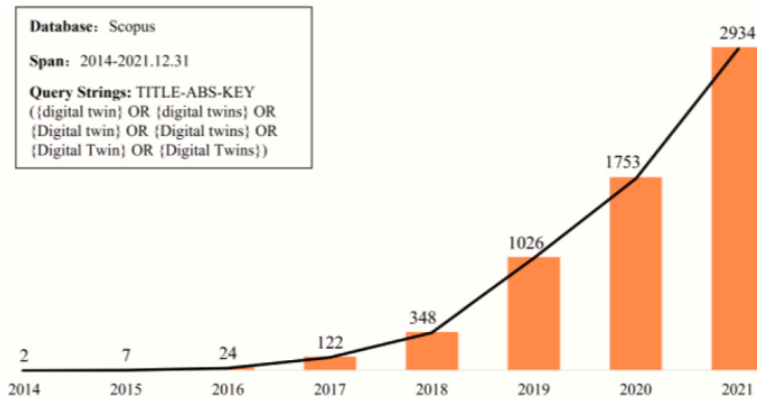


Figure 1-11 Number of Digital Twin related publications by year [59]

A digital twin approach should have at least these four elements: digital model, linked data, identification, and real-time monitoring capabilities [23]. Through these parts, a link between the physical entity and the virtual model should be achieved, with a two-way connection. On one hand, the virtual model is built on the characteristics, parameters and data gathered from the machinery and components of the physical system, both during the design and operation phases. On the other, the physical equipment is adjusted and configured on the insights gathered from multiple simulations run in the virtual model. This back-and-forth connection is fundamental to increase the fidelity of the digital model and to improve its prediction. In addition, rapid implementation of the data produced in simulation can enhance the efficiency of the physical entity. This overall process can be called “twinning”, and it is graphically summarized in the next Figure (1-12) [1].

According to a literature review, digital twins are mostly employed in the manufacturing field, in correlation with smart industry practices or learning purposes [1]. Another widespread use of this technology is found in the building field, where Building Information Modelling (BIM) is at the centre of advanced research [1]. BIM was created to gather data about buildings and facilities and was largely driven by government legislation [1]. It consists of a platform in which all stakeholders can operate, across the entire building’s life cycle. This enables all the technicians and professionals involved in the design and maintenance of the building, to refer to a single source of information, which can represent in a three-dimensional way every critical aspect of the structure. It features 3 levels of integration, from the digital model, being the CAD model, to the Digital Shadow, containing data from the construction phase up to the Digital Twin, where the two-way data connection is put in order [1]. As it turns out, BIM is a specific

interpretation of the general concept of a digital twin and shows just how useful it can be when implemented correctly. Other sectors in which digital twins are currently employed are the automotive industry, 5G development, farming, and biomedical engineering [1].

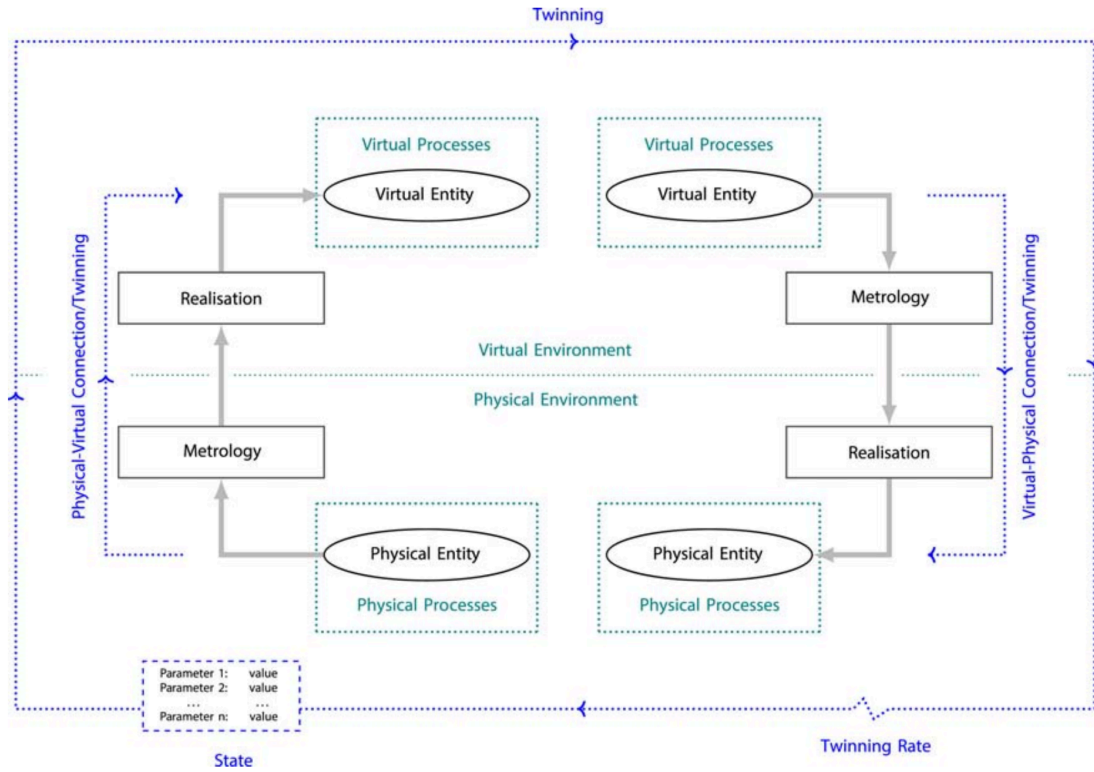


Figure 1-12 The physical-to-virtual and virtual-to-physical twinning process [1]

Summarizing, the digital twin method can reduce costs, risk and design time when employed in the design and production phase, improve reliability, and provide proactive and more precise maintenance and management of the assets, in the after-sale or operational phases [1]. However, a few drawbacks affect this method, one of which being the lack of detailed data about the physical entity, especially when in the operational phase, and resistance to implementing this approach in well-established professional workflows [1].

In the next section, the Modelica language and its application, the technical basis of this project, is described.

1.4. Modelica language and its applications

To build a digital twin of a district heating system a platform that can handle multi-domain and multi-scale variables. In our case, it must provide support for thermal and hydraulic calculations. Modelica language and its dependent libraries proved to be a perfect fit for our necessities.



Figure 1-13 Modelica logo [2]

Modelica is developed and maintained by The Modelica Association, started in 1996 by Hilding Elmqvist through the company Dynasim AB. Elmqvist conceived the language Modelica as the underlying base of the simulation and modelling environment Dymola during his PhD. The association consists of international public and private actors, mostly university laboratories and associations, or software houses. The association was founded as part of European ESPRIT programmes, a series of projects to advance research in information technology and relative applications [25]. The most notable participants in the project are: BMW, The Boeing Company, Siemens, and Bosch [25].

According to the Modelica Association's website, Modelica is a “language for modelling of cyber-physical systems, supporting the acausal connection of components governed by mathematical equation to facilitate modelling from first principles” [2]. It is an equation-based object-oriented language that enables the creation and re-use of models that can be recalled in larger subsequent models, easing the simulation of large complex systems, containing “mechanical, electrical, electronic, magnetic, hydraulic, thermal, control, electric power or process-oriented subcomponents” [2].

The basic Modelica object is the Model. It contains all the variables, parameters, and mathematical equations and expressions needed to describe the system under modelling [26]. The variables are typically real or integer, followed by parameters and constants. The other two built-in types are Boolean or character strings, as in other programming languages. As they typically refer to physics-related values, variables can have attributes that specify the unit of measure of a specific type of variable, ensuring better consistency within the model. Other kinds of attributes can indicate the minimum or maximum value allowed for a variable or they can specify a fixed initial value that is not modified by the compiler when translating the model. Parameters can be defined as variables already known, they

are our input data to the model and are not typically dependent on the evolution of it, despite being changeable each time a simulation is run. Constants, on the other hand, are fixed variables that are not modifiable once a model has been compiled and is ready for simulation [26].

Once all the variables have been defined, equations can be written in the model, to indicate how all the variables are supposed to interact with each other. In addition to basic mathematical equations, Modelica supports initial equations that define the initial condition of the model and also conditional equations, the typical if this then that kind of equation, which must contain variables with parametric variability [26].

The most powerful feature of this language lies in the ability to recall previously created models into a new one. In this way, complex systems can be subdivided into smaller entities and tested separately. Once the single component is created, with all the definitions and testing required, it can be included in a new model by “extending” it. In this way, the code remains easily readable and compact while enabling the user to compose large systems. Packages can also be employed to scale systems rapidly saving multiple lines of code. They can be defined as directories that contain a series of different Modelica entities, such as performance data about a component or physical values about the thermodynamic behaviour of fluids. These collections of pre-configured models and packages are called libraries. They are typically published with open-source licences. One of the essential libraries is the Modelica Standard Library. It provides a collection of pre-defined models and components that are in turn employed in many other libraries. It offers packages with data about the thermodynamic properties of many fluids such as water and air, physical constants such as gravitational acceleration, and almost every physical unit possible, inside the “SIunit” package. The library features many useful components, in the electric, hydraulic, mechanic and many other fields. Among these ready-to-use models, electrical components such as resistors and capacitors, mechanical systems such as springs and dampers, and hydraulic components such as pipes and pumps can be found. A description of the working principle of these components is usually provided with the model itself through annotations, explaining the assumption and configuration considered while coding. In addition, examples are commonly available to show a possible implantation of the model and its different possible configurations [26].

Coming back to the structure of the language, Modelica files could be edited via a common text editor, but to solve actual problems and exploit all its potential a modelling and simulation environment is needed. The platform or environment chosen must accomplish a series of tasks. Firstly, a graphical editor is advised as in complex systems the number of components and subsequent connectors tend to increase rapidly. A graphical interface can offer a comprehensive view of the whole system and make connections between the components more intuitive. In the background the editor will generate Modelica code while components are added to

the model, minimizing syntax errors, and making editing easier. The bare code is still accessible if needed. Then, the software will compile the Modelica code just generated and translate it into a computationally efficient form, ready to be simulated. During this step, the compiler will look for errors or lack of parameters and connectors, if present, and alert the user. Lastly, the tool must simulate the behaviour of the model, according to the simulation's parameters set and export the data for analysis or plot them directly into the simulation environment [27].

It is possible to take advantage of Modelica's capabilities through multiple modelling and simulation environments. Most of them are available as commercial software, such as Modelon Impact by Modelon, MapleSim by Maplesoft, Dymola by Dassault Systèmes, Wolfram SystemModeler by Wolfram or Simcenter Amesim by Siemens Software [27]. Dymola, as mentioned before, is one of the earliest implementations of Modelica and is now maintained by Dassault Systèmes which acquired the Dymola founder's company Dynasim AB. It delivers great performances, especially when dealing with very large models and can interface with MATLAB. Another well-established simulation environment is Modelon Impact by Modelon. It is defined as the next-generation system modelling and simulation platform, as it integrates many web and open standard technologies, making it both accessible and powerful. It features compatibility with many other languages and platforms, like Python and supports Functional Mock-up Interface, a standard developed by The Modelica Association which simplifies the creation and exchange of dynamic system models between platforms [27]. These systems can provide excellent performance and support and are indeed employed in many engineering and design firms around the world, in the automotive or manufacturing field.

However, these systems, despite offering many features and great support in the community, are generally very expensive and dedicated to commercial and industrial use or high-level research. That brought us to opt for the only completely open-source modelling and simulation platform based on Modelica, OpenModelica.

OpenModelica is developed and maintained by the Open Source Modelica Consortium (OSMC) and consists of a modelling and simulation environment based on Modelica, intended for industrial and academic usage [28]. While the cornerstone of this project was laid in 1998, the consortium was only born in 2007, by the joint venture of seven founding organisations. In the last year, the efforts and interest in the project increased consistently, with over 50 supporting actors joining the association. The long-term development of this software includes the ability to run optimisation and sensitivity analysis while keeping modelling and simulation at the core [29].

The mission of the OSMC association is to create a comprehensive environment both powerful and easy to use, that enables the modelling and simulation of complex physical systems, without burdening the user with complicated procedures. OpenModelica is built around its graphical editor and its simulation suite. In the graphical editor, called OMEdit the user can freely place the components from publicly available libraries and verify the connections to each other, without ever writing a single line of code. This enables quicker and easier implementation of models even by novices. The software takes care of generating Modelica code that accurately represents the system created in the graphical editor and then executes the compilation, through the OMC (OpenModelica Model Compiler) and, finally, the simulation of the model [29]. Figure 1-14 reports the user interface of the OpenModelica Connection editor.

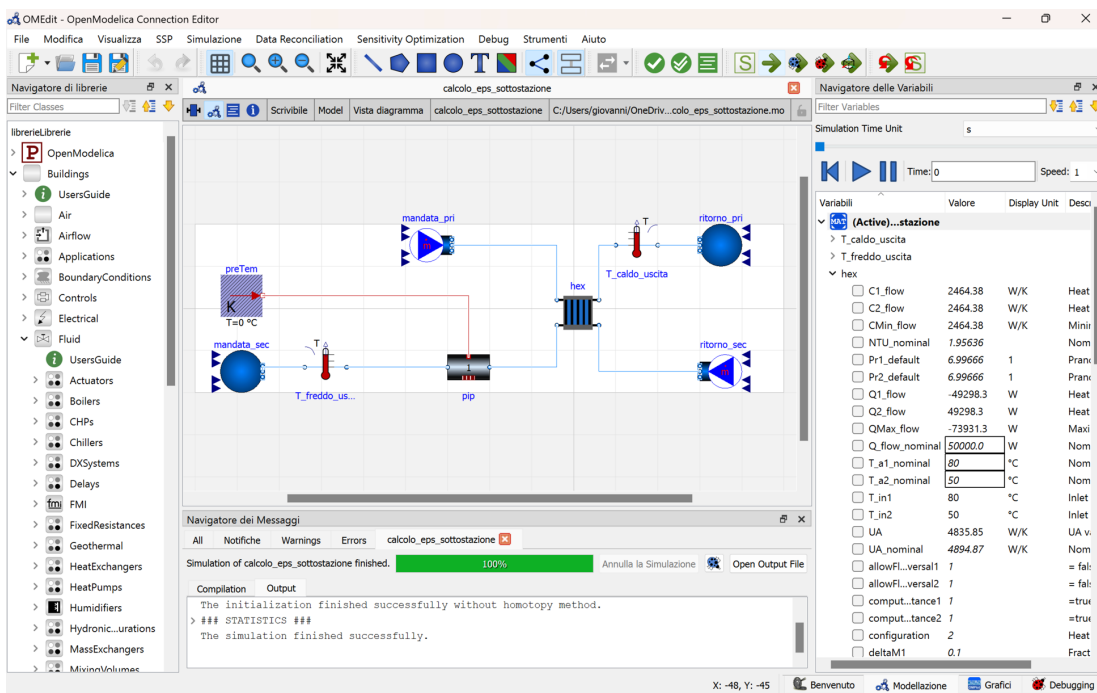


Figure 1-14 A screenshot from OMEdit showing a model from the project

Once the modelling and simulation environment has been chosen, it is time to choose the most adequate libraries on which to build our model. As previously mentioned, the Modelica Standard Library features models of many useful components, especially the ones in the fluid package, which consist of pipes, heat exchangers and other typical hydraulics. However, after some testing, the Modelica Buildings Library (MBL) proved to be the most complete and accessible. According to The Modelica Buildings Library website, the MBL is “a free open-source library with dynamic simulation models for building and district energy and control systems” [30]. The library was created, and it is currently being developed by researchers at the Lawrence Berkeley National Laboratory (LBNL), at the University of California. At its core is another Modelica library, the IBPSA Modelica Library, founded indeed by the IBPSA (International Building Performance Simulation

Association), as one of its many projects intended to advance the research and adoption of the simulation of buildings' performances [30].

The Buildings library is probably the best open-source Modelica library to model the components and overall performances of many building-related applications such as HVAC systems, hydraulic circuits, and many others. In addition to the flexibility of having multiple components at hand, the library offers a detailed user guide and many examples to better approach its implementation in new models. Moreover, the library can generate reliable results as its components are supposedly tested at the FLEXlab (Facility for Low Energy Experiments in Buildings) at the LBNL [30].

1.5. District heating in the Modelica community

As explained in the previous sections, Modelica and its complementary tools and libraries can be a solid basis for modelling and simulating complex physical systems. District heating fits perfectly among the various scenarios Modelica can handle. Many projects regarding the simulation of district heating networks and their inner components using the Modelica environment are found in the literature. These projects show different methodological approaches. Some of them end up in the construction of a full-fledged Modelica library for the purpose, while others focus more on study cases and rework other libraries' components.

One of these libraries is “DisHeatLib”, conceived by the researchers at the Integrated Energy System departments (IES) of the Austrian Institute of Technology (AIT) [31]. Although it was last updated more than 2 years ago, the library is based on the Modelica IBPSA project and offers a complete set of bespoke components to model typical district heating systems, such as substation models, a “dual pipe” component to model the primary circuit and some tools to simulate the user’s heat demand. However, this library was built to be used in Dymola modelling environment, and, while it is possible to explore the components in OpenModelica, it is not currently capable of running on the latter environment [32].

Another bespoke library is “dhcSim”, developed at the Hermann-Rietschel-Intitut of the Technical University in Berlin and it is based on the Modelica Buildings Library and Modelica Standard Library [33]. Unlike DisHeatLib, which offers finer and more detailed components, the focus of this library is shifted to the network level, ignoring the behaviour of smaller, single components that could make the model too complicated. Four main components are available: consumer, central producer, decentral producer, and network controller. They contain all the fundamental components needed to simulate the system’s behaviour, especially when a high-level overview of the entire system’s performance is required [33].

These libraries are just two examples taken from the Modelica community which is actively developing and testing solutions to model DHC systems more efficiently and accurately. Modelica proved to be instrumental in some recent case studies, including some that focused on modelling innovative DHC designs, studying by-directional substations. As discussed by Abugabbaraa et al. [34], new generation DHC could include decentralized heat and cool generation with heat pumps and chillers installed at the building level, all integrated with the main network to recover waste heat. Modelica allowed experimenting with these concepts, simulating an 11 buildings cluster efficiently and accurately [34]. Maccarini et al. [35] demonstrated the reliability of Modelica-based simulations to investigate the potential energy savings related to 5th-generation DHC configurations. They focused on a case study located in Denmark, experimenting with lowering the supply temperature in the secondary circuits, studying the impact on the overall network. To build the model, they employed components available in the Modelica Buildings Library, e.g.

circulation pumps and heat pumps while also creating custom ones, e.g. a component that simulates thermal dissipation from the pipes to the ground [35]. Similarly, Modelica was employed by Gautier et al. [36] to assess the feasibility of a geothermal district heating and cooling system. They evaluated the performance of the system and its resilience during a simulated 5 days heat wave, which are becoming more and more common due to climate change. As for the majority of DHC simulation projects, Modelica Buildings Library was chosen as the foundation [36]. Two researchers from this project, Michael Wetter and Antonine Gautier, collaborated on two other projects. In the first one [37], they conceived a new modelling approach for DH networks, including steam thermodynamics, as most DH systems located in the US feature steam as the heat carrier. They were able to create an efficient framework for mixed media calculation unlocking massive time savings during complex simulations, e.g. reducing from 33 hours to only 1 hour for an annual simulation of 180 buildings DH network, when compared to available libraries such as MSL or MBL [37]. The other project of theirs [38] focused instead on building and releasing new components to support the simulation of district cooling applications, which are still rare in the Modelica community. They used a real case study set at the University of Colorado Boulder, as the base to develop the models, such as network piping hydraulics and specific cooling equipment, which were made available as part of the MBL 8.1 [38]. Concluding this overview on the last developments on the topic of DHC in Modelica, it is worth mentioning the work of Van der Heijde B. et al. [39], who developed a new pipe model called plug flow pipe. With this new concept, they were able to cut simulation time while keeping an accurate account of thermal and hydraulic losses, when compared to the MSL standard pipe, based on a finite volume model [39]. This model enables the simulation of complex conditions such as zero mass flow rate or flow reversal and has become indeed a key component of many DHC Modelica libraries [39].

Most of the projects mentioned above have the Modelica language as technical base, in the form of MSL and MBL or IBPSA project 1 library. This proves the flexibility and reliability of Modelica as a framework for developing DHC modelling and simulations. However, these last advancements were generally directed towards efficient simulation of large and complex systems, comprised of many substations and extended distribution networks, which in turn require computationally efficient modelling, especially due to complex fluid dynamics effects in piping. Furthermore, these libraries and frameworks were tested and conceived for perfect integration with commercial software like Modelon Impact or Dymola, which were mentioned in the previous section. In addition, OpenModelica still does not support all the packages related to DHC components, especially when dealing with the plug flow pipe model, which is largely adopted in DHC libraries due to its faster and more accurate performance in simulation. Keeping in mind that the project developed in this thesis aims at replicating every single component of the real system, and it is being developed in the OpenModelica environment, these bespoke libraries are not a good fit.

2. The Energy Center's district heating laboratory

In this section the real system considered in this project is described and analysed. First of all, the placement of the system inside the university's facilities and its purpose and goals are explained. Then, the most critical components will be described and compared to fully fledged district heating system.

2.1. Location and purpose of the laboratory

The Energy Center initiative was started in 2016 after a joint venture between Politecnico di Torino and the regional and urban governments with funding from the public and private sectors, from philanthropic banking foundations of Fondazione CRT and Compagnia di San Paolo. The goal of this project is the creation of an interdisciplinary research lab focused on the energy sector, the Energy Center Lab, and a facility, called Energy Center House, in which to host laboratories and offices to accelerate the development of new technologies. The building is located in the offing of the Politecnico's campus and hosts the offices of various private companies and start-ups, in order to strengthen the collaboration between the public academic world and the private industrial and commercial sector. In this facility are located 450 m² of laboratories, including the one containing the experimental DH system used as case study.

The laboratory was conceived by the energy department of the Politecnico, known as DENERG, with the first design proposed in 2021. It is placed in a spacious warehouse next to the Energy Center's central building and it was built to provide a test bench for studying innovative solutions in district heating, in the context of 4th and 5th-generation DH development [40]. It was conceived as a small-scale district heating network, with piping running all around the perimetry of the warehouse and two substations, featuring one water-fed air heater each, to represent the heat demand at the user's side. While not supplying real heat demands, the plant was built to represent a real network on a much smaller scale, that can be operated just like a real district heating network, with its own primary and secondary side circuits, the heat generation and all the other main components.

The ultimate goal of this system is to study innovative thermal storage, such as sensible stratified heat storage or the ones based on latent heat. Furthermore, performance analysis on both the thermal and hydraulic sides can be carried out to investigate the impact of various operational parameters such as mass flow rates or water supply temperature setpoints. Different heat sources could also be tested, such as solar-based generation or electrical heat pumps. In addition to these aspects, this system can also help study and test software-based approaches to district heating development, like the creation of high-fidelity digital twins.

Moving in this direction, the laboratory-scale network, being equipped with various sensors such as thermocouples, can provide essential data gathered during different system configurations, to assess the reliability and fidelity of digital models and simulations, as in the two-way twinning process explained in the previous section.

2.2. System layout and its components

As introduced in the previous sections, a district heating system is based on the concept of decoupling heat generation and consumption. While conventional DH systems feature a centralized heat generation design, consisting of CHP plants or bespoke water boiler, newly design concepts consider a more evenly heat generation to unlock better integration with RES and waste heat recovery. Nevertheless, heat generation is still typically carried out in specialized plants and then transferred and distributed to the users.

The distribution is granted by a network of insulated ducts, that spread from the central heat generation to the various users, forking into smaller ducts and connecting to each building through junctions. From there the final pipe segment branches out and connects to the substation. The substation is located in the users' premises, typically in the buildings' basements and it is typically made of a plate heat exchanger, a thermal energy meter used for billing and a district heating controller, consisting of a system of valves and actuators that control the amount of energy transferred to the secondary circuit.

The substation makes the transfer of thermal energy possible, and it is the link between the primary circuit, i.e. the distribution network linked to the central heat generation, and the secondary circuit, i.e. the hydraulic system supporting heating and domestic hot water.

The objective of the laboratory built in the Energy Center is to represent all the fundamental components of a typical DH network on a smaller scale. Its components were selected to substitute real district heating components, trying to replicate the behaviour of a typical network, creating a sort of mock-up, while respecting spatial and financial constraints.

Its overall structure can be divided into 4 main parts:

- Heat generation
- Primary circuit – distribution network
- Substation 1 and relative secondary circuit
- Substation 2 and relative secondary circuit

2.2.1. Heat generation and primary circuit layout

The primary circuit of this network consists of insulated steel pipes which contain water as carrier fluid. Hot water is provided by a natural gas-fuelled water heater which injects hot water directly into the distribution pipes.

As in every district heating system, the supply and return sides can be distinguished in the primary circuit. The supply pipe brings hot water from the water heater towards the two substations, while the return pipe gathers colder water from the two substations towards the water heater, completing the distribution circuit.

On the supply pipe, two nodes or junctions are found. At these nodes the primary network branch out towards the substation via a similar pipe, only smaller in diameter. In the first node encountered a smaller pipe branches out vertically and connects the primary network to the substation 1, which transfers heat to a secondary circuit equipped with an air heater to simulate a typical heat load. At the second node a smaller pipe branches out vertically and connects the primary network to the substation 2, which transfers heat to a secondary circuit equipped with the same air heater of substation 1 and an insulated vessel for sensible thermal energy storage.

Right after the second node, the supply side pipe ends in a shut-off valve that connects the supply side pipe to the return pipe. From there on, travelling backwards along the return side pipe, the same nodes are found, first the second node from substation 2 and then the one from substation 1 until reaching the circulation pump that supports water flow. As on the supply side, at the nodes the smaller pipes coming from the substation connect to the main return pipe.

From there the last leg of the return pipe connects to the water heater inlet and the circuit is closed.

The Figure 2-1 reports a graphical representation of the primary network.

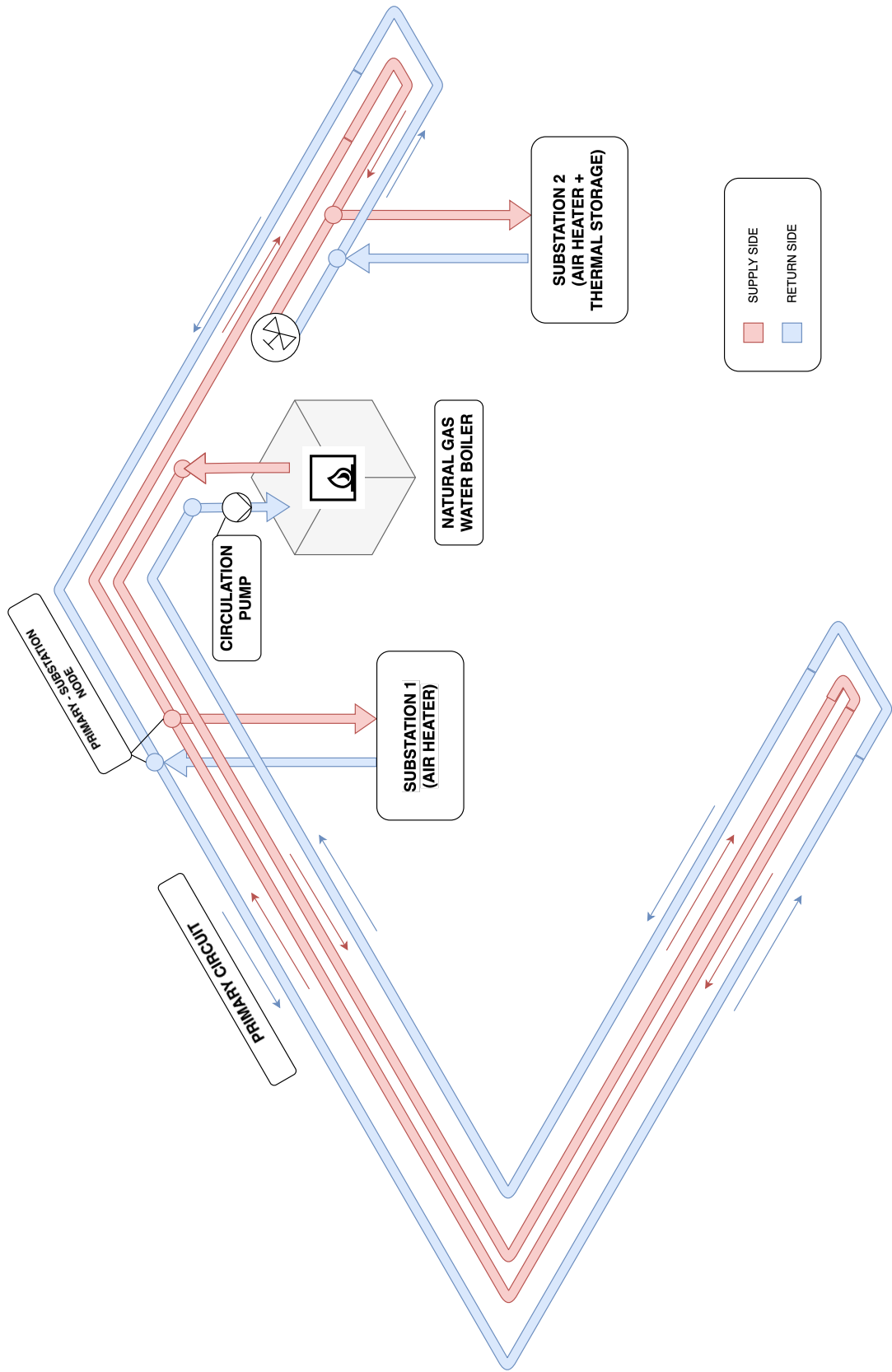


Figure 2-1 Primary circuit layout

Water heater specifications

In this system, heat generation is provided by a traditional heat-only design, consisting of a 40 kW Johannes methane-fed water boiler, whose specifications are in the following table (2-1) and some pictures are provided in Figure 2-2. Data was acquired from the water heater data sheet [41].

Table 2-1 Water heater specification [41]

<i>Model</i>	Johannes AR-NOx 34H
<i>Rated thermal power</i>	42.5 kW
<i>Useful thermal power</i>	40 kW
<i>Fuel</i>	methane
<i>Type</i>	Pressurized steel water heater with forced draught gas burner (Johannes JIM 6 GAS)
<i>Efficiency at 100% load</i>	93.63%
<i>T_{supply, max}</i>	90°C
<i>Pressure drop (water side)</i>	15 mbar



Figure 2-2 Front plate of water heater with gas burner in front

Primary circuit specifications

Heated water, the temperature of which is controlled by the set point of the boiler, is directly injected into the distribution network. The distribution network is purposely longer than needed, to replicate the typical layout of a real district heating network. The increased total length of the pipes allows the study of thermal and hydraulic losses along the distribution network. The pipes' specifications are reported in the table (2-2) below. The pipes are placed along the walls of the warehouse, folding on themselves to increase overall length while keeping the entire system as compact as possible, gathered into a corner of the room. Both supply and return ducts are fitted with thermowells along their entire stretch in which thermocouples are placed to monitor temperature changes along their elongation. Data about pipes was gathered from available CAD files.

A summary of their specification is available in the following table (2-2). The junction between the main primary circuit and primary-substation segments can be observed in Figure 2-4, where smaller vertical pipes branch out from the horizontal primary circuit pipes. In particular, this image shows the pipes before the insulation install.

A more recent picture is available in Figure 2-3, showing the detail of the valve joining supply and return sides is shown, together with the primary-substation segment now fully insulated and covered by the aluminium finish.

Table 2-2 Distribution pipes specifications

<i>Material</i>	Steel pipes with superficial anticorrosion coating
<i>Diameter (primary circuit)</i>	DN 40 ($d_i=42.5$ mm)
<i>Diameter (connection between primary and substation)</i>	DN 32 ($d_i=36.6$ mm)
<i>Length (supply + return)</i>	approx. 117 m (from CAD measurements)
<i>Insulation layer</i>	30 mm
<i>Insulation material</i>	80kg/m ³ mineral wool $\lambda=0.038$ W/mK
<i>Covering</i>	Aluminium sheet
<i>Typical operating pressure</i>	2.5 bar



Figure 2-3 Distribution network pipes - detail on supply and return junction

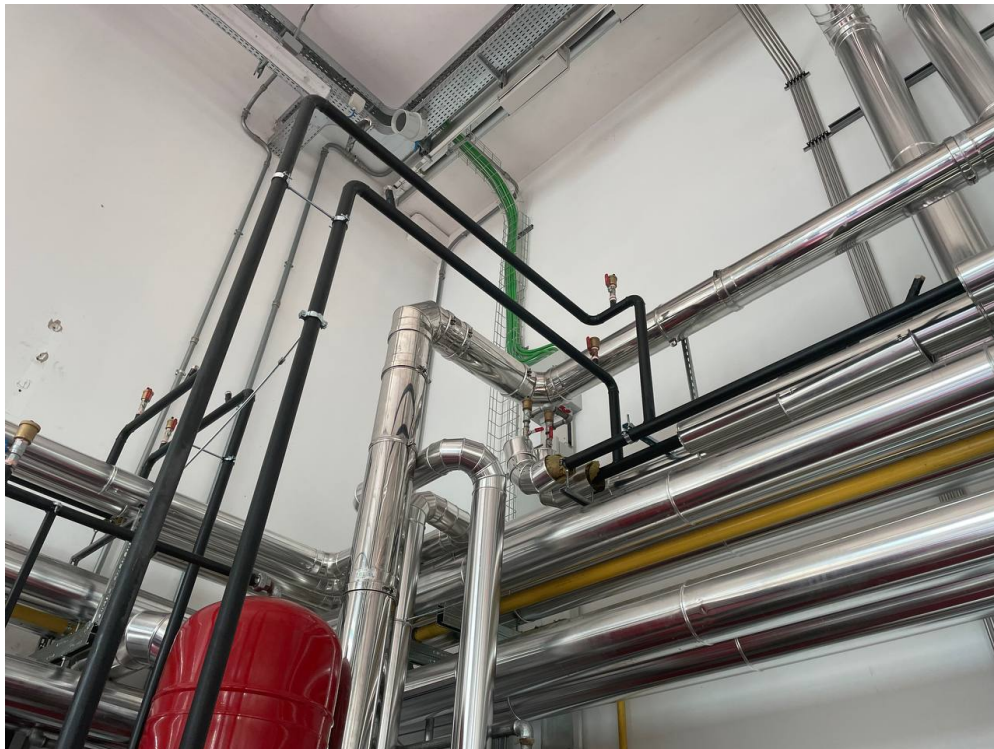


Figure 2-4 Distribution network pipes - detail on primary branch towards substation 2 – before insulation application

Circulation pump specifications

The circulation pump is placed right before the attachment of the return side primary circuit pipe into the water heater. It is designed to ensure constant circulation of the carrier fluid into the primary circuit, according to the system's heat demand. Its working point is selected considering the mass flow rate needed and the total pressure losses along the network, both distributed, due to friction in pipes and local, due to components such as heat exchangers or valves.

The model in question is a wet rotor in-line circulation pump, which, compared to dry rotor design, provides higher efficiency, lower maintenance costs, and lower noise level. Compared to the dry rotor design, this pump is equipped with a rotor immersed in the fluid, with the electric motor fully insulated, eliminating the need for a ventilation fan, as the fluid directly acts as the coolant. The weak spot of this type of circulator lies in airing, when air leaks into the circuit, exposing the pump to rapid and destructive wear to moving parts. The circulator is configurable in various modes, and it has been set for a typical working point, whose data is reported in the table below. A summary of technical data is available in table 2-3.

Table 2-3 Primary circuit circulation pump specifications [42]

<i>Model</i>	Wilo Premium Smart Stratos MAXO 30/0.5-14 PN10-R7
<i>Pipe fitting</i>	DN40
<i>Function mode</i>	Variable differential pressure
<i>Maximum operating pressure</i>	1 MPa
<i>Fluid temperature</i>	-10°C to +90°C
<i>Working point flow rate</i>	4.92 m ³ /h
<i>Working point hydraulic head</i>	11.63 m = 1.14 bar
<i>Working point electrical power</i>	300 W (240 V)



Figure 2-5 Primary circuit circulation pump [42]

2.2.2. *Substations layout and relative secondary circuit*

After the primary circuit and heat generation, substations and their correlated secondary circuit are the other essential parts of every district heating system. The substations transfer heat power from the distribution network to the heating system of the building or facility where they are placed. The basic layout is comprised of a heat exchanger, typically of the plate type, a district heating controller, that manages the amount of fluid directed to the HEX, in turn managing the amount of heat transferred, and a thermal energy meter, used for accountability purposes.

From the substation the secondary circuit begins, and it is essentially a local distribution network supported by a circulation pump that distributes heat from the substation towards the heating system of the building, which can present various configurations, such as radiators, floor radiant or fan coils. It may be also equipped with additional systems, for instance a thermal energy storage or a domestic water heater.

In Figure 2-6 an overview of the main component of substation 1 and its secondary circuit is available.

Smaller pipes for the supply and return side branch out from the primary network, as seen in Figure 2-4, and attach to the substation's plate heat exchanger. Two valves, working together, manage the supply of hot water to the substation. As it will be further explained in the next sections, the bypass valve links the supply and return sides of the primary network, bypassing indeed the substation. It springs into action when the network needs to recirculate the carrier fluid excluding the substations, or when a single substation's hot water demand drops towards nought. The other valve is placed before the heat exchanger inlet on the hot water side, to regulate the supply. Once hot water has been processed in the (HEX) heat exchanger, it re-enters the primary circuit on the return side. The secondary circuit is filled with water as carrier fluid as in the primary. Following the same layout found in the primary circuit, a circulation pump is attached right before the inlet of the HEX on the cold side, to guarantee circulation. This pump can be regulated to adapt to the user's heat demand.

Downstream of the HEX, on the outlet of the secondary side, water, now heated, is sent along the circuit which supplies the heating system of the building. In our case, an air heater was fitted to the system to replicate the user's heat demand. As it will be described in more detail in the following pages, the air heater is nothing but a water-air heat exchanger, supported by an air blower to ensure airflow. Its presence in this very configuration was not meant to satisfy the heating demand of the warehouse it is placed in, but rather to replicate in a single component the heat load of a typical heating system, which would normally be comprised of radiators or other similar devices. Once the water has been cooled in the air heater, it is circulated back through the circulation pump towards the plate heat exchanger and the cycle repeats.

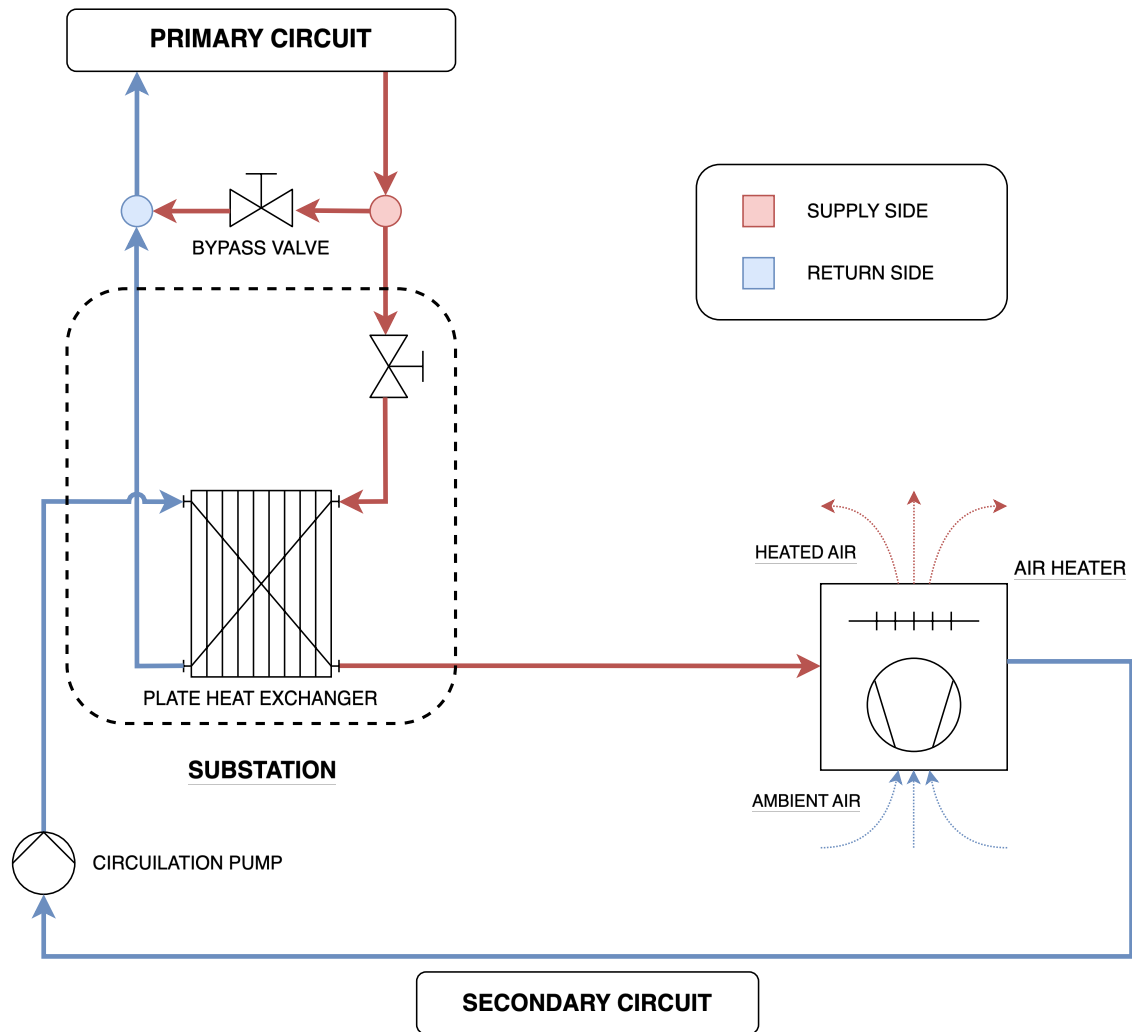


Figure 2-6 Secondary circuit 1 diagram

Substation

The substation installed in both secondary circuits is the “MOLE” model from the manufacturer Amarc DHS, specialized in district heating substations. It is no longer in production, so the documentation available is limited to a technical scheme listing the main components. This kind of substation is very common for domestic and small commercial use, as it is compact and easy to install on the wall. In this design is compatible with most hydronic heating systems and feature a metal case which contains all the required equipment [43].

In Fig 2-7 a photo of the actual substation placed in the laboratory is shown. The two vertical pipes belong to the primary network and are directed from/towards the nodes as seen in Fig. 2-4. The two horizontal pipes belong to the secondary circuits. The plate heat exchanger is placed inside the metal box down right. On the rightmost vertical pipe the electric valve controlling the flow of hot water from the primary network is present, as well as all the sensors such as thermocouples and flow meter that are connected to the control box on the upper right part. There the district heating controller and the thermal energy meter are placed. From those interfaces the setpoint for the secondary circuit can be managed and the amount of heat transferred to the secondary circuit can be read.

Typically, these substations control the amount of heat transferred by regulating the valve placed on the supply side of the primary network, as it can be seen in Fig. 2-7. The supply temperature on the secondary circuit is the target, and it is calculated considering a climatic curve based on the external temperature. Mass flow from the primary is regulated until this temperature is matched.



Figure 2-7 Substation

During the modelling, these control systems and sensor were not included, as the mass flow rate and, in turn, thermal power were regulated manually.

Table 2-4 Substation specifications

<i>Model</i>	AMARC DHS “Mole” – compact wall mounted
<i>Power</i>	20 kW – heating only

Plate heat exchanger specifications

The plate heat exchanger is the heart of the substation, transferring heat between the primary and secondary circuits. They have two inlets, one for hot water from the primary circuit and one for cold water from the user’s heating system and two outlets, one for cold water directed to the primary circuit on the return side and one for hot water ready to serve the building’s heating system. The HEX installed in both Substation 1 and Substation 2, as in most DH systems, is a brazed plate heat exchanger from Alfa Laval. It enhances the concept of the gasketed type heat exchanger by soldering shut the plates together, increasing reliability and enabling even more compact designs [44]. In the following table (2-5) there is a summary of its specifications and Figure 2-8 shows an image of the HEX from the producer’s catalogue.

Table 2-5 Substation heat exchanger specifications [45]

<i>Model</i>	Alfa Laval CB30-24H
<i>Type</i>	24 copper-brazed stainless steel plates HEX
<i>Maximum pressure loss</i>	20 kPa
<i>Rated power</i>	50 kW
<i>Rated mass flow rate hot side</i>	2156 kg/h
<i>Rated mass flow rate cold side</i>	2154 kg/h
<i>ΔT hot side</i>	80 → 60 °C
<i>ΔT cold side</i>	50 → 70 °C



Figure 2-8 Brazed plate heat exchanger

Air heater specifications

The air heater represents the user's heat demand in this laboratory-scale system. It is used to dissipate a variable amount of heat by warming ambient air using hot water supplied by the substation. It was not conceived to heat the laboratory, as it is only a placeholder to simulate a typical heating load. In a real DH system, it would be substituted by a hydronic system with radiators or floor heating or by mixed water-air for space heating. However, as the purpose of this experimental DH system focuses on studying the performance of the network and its main components, there is little interest in analysing the performance of this air heater, which is only considered as a heat load.

The air heater consists of a water-air heat exchanger and an air blower to support air circulation. The heat exchanger is made of an array of steel tubes with aluminium fins in which hot water from the secondary circuit is circulated. The air blower is placed right behind this array. This specific air heater is produced by Sabiana and features some technical advantages compared to the competition such as a reduced number of tubes, each one with a larger diameter, to reduce resistance to airflow and make maintenance and cleaning easier. To improve air circulation and cleaning the fins attached to the tubes are more spaced out and being thicker, they are less prone to damage. The single-speed electric motor makes the power regulation possible only by changing the hot water supplied to the air heater. In table 2-6, a summary of its specifications is available. Figure 2-9 shows in detail all the air heater's components and Figure 2-10 shows the placement of one of the two air heaters in the laboratory.

Table 2-6 Air heater specifications [46]

<i>Model</i>	Sabiana ATLAS 46A32SX
<i>Electric motor speed</i>	1350 rpm
<i>Poles</i>	4
<i>Material</i>	Stainless steel tubes with aluminium fins
<i>Air flow rate</i>	2915 m ³ /h
<i>Thermal power (rated)</i>	20.85 kW
<i>Outlet air temperature (rated)</i>	35.9 °C
ΔT_{water}	10 °C (85 → 75 °C)

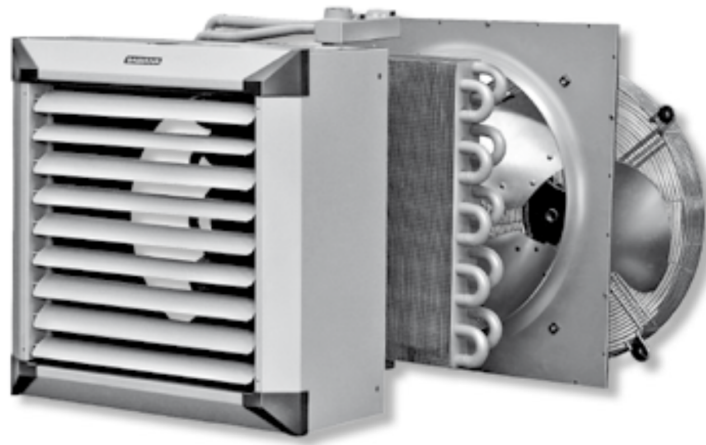


Figure 2-9 Air heater components



Figure 2-10 Air heaters placement

Circulation pump specifications

The circulation pump supporting the secondary circuits is from the same brand and features the same working principle as the one supporting the primary circuit. The model is slightly different. Here is reported a list of its specifications.

Table 2-7 Secondary circuit circulation pump specifications [47]

<i>Model</i>	Wilo Stratos 32/1-12 PN 6/10
<i>Pipe fitting</i>	DN32
<i>Function mode</i>	Variable differential pressure
<i>Maximum operating pressure</i>	0.6 - 1 MPa
<i>Fluid temperature</i>	-10°C to +90°C
<i>Working point flow rate</i>	2000 l/h
<i>Working point hydraulic head</i>	5000 mm
<i>Working point electrical power</i>	60 W (240 V)



Figure 2-11 Secondary circuit circulation pump [47]

2.2.3. *Thermal energy storage in secondary circuit 2*

The secondary circuit 2 replicates the basic layout of the first one, featuring the same model of substation, circulation pump and air heater. The only difference between the two lies in the presence of a sensible thermal energy storage (TES).

The TES installed is integrated into the secondary circuit by means of additional shut-off valves that can exclude different parts of the circuit to make it work in different modes. Depending on the operational configuration, i.e. whether the storage is being charged, discharged, or excluded, different legs of the circuit have to be opened and closed. Therefore, an additional circulation pump is also needed when the one supporting the substation is excluded. In Fig. 2-12 the layout is represented.

As in other kinds of energy storage, such as batteries in electric grids, thermal energy storage can increase the efficiency of the entire DH network by providing more flexibility to the system, and a plethora of advantages [48]. TES is especially useful when used to shave the peaks in the demand curve. As electrical system, a DHC systems work best when the demand curve following smooth, ideally constant, trend, turning on a more manageable and predictable system. In real systems, however, peak loads, that are registered during the day, e.g. in the morning when users turn on the heating systems and during the colder periods of the season, introduce momentary spikes in the demand curve. This in turn requires an overestimation of heat generation capacity, both in local backup systems, such as water heater placed at the user's premises, and in centralized generation, worsening the operational efficiency and increasing installation costs [48].

Therefore, a smart employment of TES technology can [48]:

- Increase the flexibility of the whole system, making it more efficient and resilient to sudden changes in the demand curve
- Decrease the use of back-up boilers or chillers
- Decouple the instant of thermal generation and usage, enabling a better management of heat production, shifting it when it is most convenient
- Increase the share of RES, capturing for instance excessive energy even if it is not currently required by the users
- Enable the expansion of current networks without heavy changes to the design

Furthermore, TES can consist of different technologies, such as sensible, latent, or chemical thermal storage, and many others [48]. It can also vary depending on the installation site, as it can be integrated directly into the primary network, flanking the heat generation or at the user's premises, integrating into the secondary circuit.

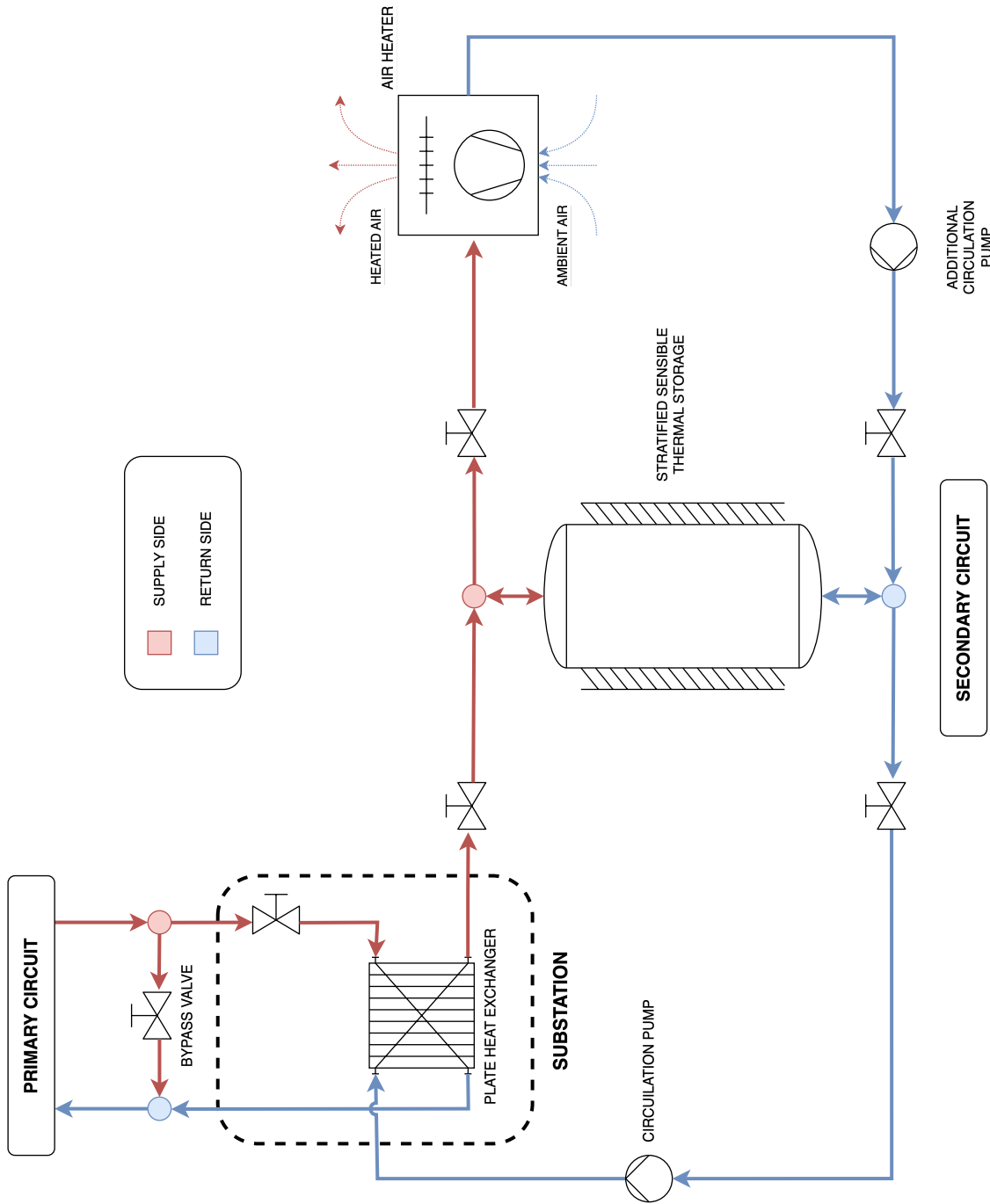


Figure 2-12 Secondary circuit 2 diagram

Thermal storage specifications

Our experimental system is equipped with a sensible TES which stores energy directly by accumulating hot water into a thermally insulated pressure vessel and keeping it hot for extended periods. It can provide hot water to the building's heating system, substituting, or integrating heat withdrawn from the primary network.

The one installed in the laboratory is an insulated carbon steel tank, pressurized with water that is recirculated in a closed loop. In this setup, water is circulated from the tank to the substation's heat exchanger for charging or to the air heater for discharging. The fluid carrier must be recirculated into an air-tight circuit to prevent oxidation and corrosion.

Unlike other TES it is not equipped with any internal heat exchanger. Those designs feature a spiral-shaped coil in which a carrier fluid from a separate loop is being circulated. In this way the TES can be charged or discharged indirectly, keeping the two circuits hydraulically separated. Those systems are mainly employed for domestic hot water production or coupled with solar panels.

Another important aspect of sensible TES is the thermal stratification which occurs when inside a hot water storage, fluid at slightly different temperatures stratifies, with colder water falling at the bottom and hotter water rising to the top, separated by an intermediate region called thermocline. Like any fluid, water at different temperatures presents slight differences in density values. This triggers buoyancy effects which generate the stratification effects. If the TES is not being charged or discharged, the stratification effect eventually disappears and the fluid becomes fully mixed, with the formation of a single layer at average temperature [49]. This effect has great benefits on the thermodynamic performance of the TES, as it becomes able to supply water at a higher temperature for longer periods if compared to fully mixed vessels. In this way, the TES can support more effectively the heat demand and improve heat transfer during charging.

The TES under evaluation is equipped with multiple inlets and outlets to enable the withdrawal and injection of water at different heights and, in turn, at different temperatures. However, it is charged and discharged through the top and bottom inlet only, while three of the ports along the side are currently equipped with one thermocouple each for temperature detection. These sensors were employed during an experimental test about the performance assessment of the TES, as, by detecting temperature at different levels, the stratification effect can be better investigated. This test will be described and simulated in Chapter 4. In table 2-8, the summary of the TES' dimensions is reported

Table 2-8 TES thermocouples placement

<i>Total height</i>	2115 mm
<i>Top thermocouple</i>	1725 mm
<i>Middle thermocouple</i>	1400 mm
<i>Bottom thermocouple</i>	340 mm

As it can be seen in the simplified diagram available in Figure 2-12, the insulated tank is connected to the secondary circuit via additional branches controlled by valves and supported by an additional circulator. In this way, multiple configurations are deployable:

- CHARGING MODE
There is no heat demand, the substation supplies hot water directly to the thermal storage until it reaches the setpoint temperature.
- DISCHARGING MODE
The substation is excluded and the user (in this case, the air heater) is provided with hot water previously accumulated in the TES. This configuration can be ideal for short periods when the user's heat demand is low, or as a fallback option in case of faults in the primary circuit or when the network has low capacity due to high demand.
- TES EXCLUDED
The storage is in standby mode, the air heater is supplied with hot water directly from the substation

The model installed in the system features the following specifications (table 2-9). A picture of the TES is available in Fig. 2-13.

Table 2-9 Thermal energy storage specifications [50]

<i>Model</i>	TML Industrie Pufferspeicher PF 01500 F
<i>Max operating pressure</i>	4 bar
<i>Max operating temperature</i>	95 °C
<i>Capacity</i>	1472.4 l
<i>Type</i>	Closed loop tank
<i>Internal HEX coil</i>	Not present
<i>Material</i>	Carbon steel
<i>Insulating layer thickness</i>	130 mm
<i>Insulating material</i>	Flexible polyester + external PVC coating



Figure 2-13 TES placement in the laboratory

3. Building the digital twin

In this chapter the realisation of the digital model will be discussed, describing the tools employed and the choices made to represent each physical component as accurately as possible. The approach taken to comply with the task is described and explained. The modelling of critical components such as the substations' heat exchangers and the air heaters will be analysed in greater detail.

3.1. Software and libraries employed

As introduced before, this project has been carried out using Modelica as the foundation, thanks to its affinity to model complex multi-domain physical systems. However, as discussed in the previous section, many well-known Modelica-based modelling and simulation suites like Modelon Impact and Dymola are available under onerous licenses, making them suitable only for high-level commercial or research uses. Affordability and ease of use are two key objectives for this project, making open-source software the only way to go. OpenModelica proved to be the perfect choice as it offers a free, fully-featured and user-friendly way to create digital models of physical systems, from modelling up to simulating and plotting results.

The core of the suite is “OMEdit”, the OpenModelica Connection Editor, which is the graphical editor in which components can be placed and connected to create the model. This enhances greatly the usability of the software, making the modelling process more intuitive and minimizing errors related to direct scripting, which is still available and useful for some applications. However, OMEdit provides only the basic modelling environment, and it has to be completed by the true potential of Modelica-based modelling: publicly available libraries. When the software is first started only essential add-ons are available in addition to the latest release of the Modelica Standard Library (MSL), which already offers a wide range of components ready to use.

Additional libraries can be downloaded and installed via the built-in library manager. As anticipated before, there are many free libraries built for Modelica applications, covering virtually every physical system configuration.

The ones employed in this project were:

- Modelica Standard Library (MSL) (v.4.0.0) [51]
- Modelica Buildings Library (MBL) (v.10.0.0) [30]

Only a few control components were sourced from the MSL, while almost every other one was sourced from the MBL.

The MBL was conceived for the accurate representation of buildings’ energy and control systems, such as HVAC systems, energy storage or thermal analysis of rooms and spaces, and was, therefore, the perfect foundation for this project [30]. It contains many packages, such as one for fluid applications, featuring piping, pumps, and hydraulic resistances, or one for thermal zone analysis, and even one dedicated to district heating modelling.

However, in the first steps of the modelling process, other libraries were taken into consideration, such as:

- ThermoFluidStream (v.1.1.0) [52], a new library based on an innovative computational scheme, yet not featuring all the components present in the MBL

- DisHeatLib v1.2.0 [31], made specifically for DHC application, but lacking full OM support
- The DHC package of MBL, not yet fully functioning and meant for large DH networks modelling

The last two libraries mentioned, along with other ones, provide specific components that enable quick and effective modelling of large and complex district heating systems, providing ready-to-use models of substations as well as components representing the heat generation or heat load. However, these libraries are built with large networks modelling in mind, focusing on being computationally efficient rather than customizable. For these reasons, these components could not satisfy the needs of this project, where precise and finely customizable modelling is required. The MBL proved to be more adequate for the scope as it offered single components such as pumps, heat exchangers and temperature sensors, unlocking the creation of a tailor-made model to mimic the real system as is.

During the course of this project, a few updated versions of OpenModelica and libraries were released, as their developments are supported by active communities. The latest versions were always used to showcase the potential of Modelica and benefit from the latest fixes. The software was entirely run on a virtual machine based on Windows 11, as support for MacOS was dropped due to low adoption.

However, VM can be used successfully for models limited in size and complexity and did not compromise the success of the project. A summary of the PC technical specifications is available in table 3-1. OpenModelica versions employed during the tests are: v1.21, v1.22.0, v1.22.1, v1.22.2. The final simulations were run using the latest version, v1.22.2.

Table 3-1 PC specifications

<i>Computer</i>	2020 Apple MacBook Air
<i>Processor</i>	ARM Apple Silicon M1
<i>Memory</i>	8 GB
<i>VM Software</i>	Parallels Desktop v19
<i>VM OS</i>	Windows 11 Pro for ARM
<i>VM RAM</i>	3 GB
<i>VM processor</i>	4 cores

3.2. The methodological approach

To build the digital twin it is necessary to couple each component present in the real system to its digital counterpart, trying to represent its features and behaviour as accurately as possible. However, to simplify the task and to unburden the model, some components present in the real setup were not included, focusing on the critical ones, providing a simplified, yet representative, version of the real system.

The analysis of the layout of the plant began with the study of the available CAD files and diagrams, from which essential information such as the scheme of hydraulic circuits and the dimensions of the pipework was gathered. Specifications about the components were collected from technical data sheets available online from the manufacturers' websites or already present at the laboratory.

Once the general layout and the specifications of the installed machinery were discerned, the modelling began with the selection of the digital components. To better understand which component is the correct fit, libraries are typically shipped with multiple examples for the various components, showing a batch of different configurations in which the component can be set. Along with these examples, a user guide is often attached to the component, giving insights on how to correctly use, and set it up. Furthermore, these user guides are also critical in understanding the physical concepts on which the components are designed and built by developers, even citing references to properly explain the validation process of the component. In this way, it is possible to understand and correct unexpected behaviour of the components and decide whether it can be a good fit for the real one. In addition, being these components models themselves, they can be explored by analysing their Modelica script and gathering information about their inner workings.

During this phase, multiple purpose-built models were created just to test whether the components were working as expected, to experiment with their performance and to assess unexpected errors or results during simulations. For example, a model was created expressly to test different kinds of heat exchangers available in the library, to understand which of those could correctly represent the one installed in the laboratory. In this phase, the components were placed in the final models and initialized correctly. In the following section, the selection and configuration of the most critical ones are discussed.

After this step, the models were ready to be simulated. There was therefore the need to find adequate inputs to the models, such as initial temperatures, mass flow rates or set points. For this purpose, a few scenarios were selected with proper operational parameters and tested in the simulations. Special case was provided to the study and modelling of both the substations' heat exchanger and air heater. The method followed during this phase is explained in section 3-4.

However, the performance of the models could only be compared to expected results as, at the time of writing, there is no data gathered during the real systems operation at all. Without dependable data the digital twinning process cannot be fully completed, as it is fundamental to compare the behaviour of the two systems, the digital and the physical one, and to iteratively tweak the model.

Although the components were selected from one of the most established Modelica libraries and are therefore already validated and can guarantee trustworthy results, only a proper comparison with real data can attest to the quality of the models. The only exception is the study of the sensible thermal energy storage, of which a limited collection of data gathered through a real test scenario was available. These data were employed to assess the accuracy of the model and will be discussed in the results chapter.

Once simulations were run, the most critical variables were exported in a CSV file and later ingested in MATLAB to generate the plots that are reported in the following chapter.

3.3. The digital components and their configuration

In this section a list of the components selected from the Modelica Building Library to build the models is reported. In the graphical editor, the components are available inside a sidebar called library navigator, in which the installed libraries are organized with a nested layout. Inside each library the main packages are nested, which in turn contain other sub-packages with the models of the components, the examples, and other tools such as packages containing physical properties of water and other media.

In the library navigator, all the components are listed and can be browsed and from there a view of each component's inner working can be opened. As each component is a model itself, it is possible to explore its inner components in the graphical editor. In this way, a better comprehension of the working principle of each component can be grasped, thanks to the user guide available on the side.

First of all, they are dragged from the navigator into the graphical editor, then they must be named and configured properly. By double-clicking on each component, the relative properties window appears in which the configuration and initialization of the component can be done. Each component features a number of required parameters which must be provided for correct operation and some optional ones, to further specify the behaviour of the component or to modify a default parameter.

Once all the necessary components are placed in the model, they can be easily connected to each other by using each components' connectors. As soon as they are moved into the editor, they are represented as a unique icon from which at least two connectors branch out. These connectors enable the connection between different components and different kind of information. When considering MBL fluid package, all the main components feature two fluid ports, an inlet, and an outlet, typically called port a and b, where fluid direction is intended positive from a to b. These enable the exchange of mass flow rate between components. Additional connectors might be present depending on the component's type. For example, the water heater (WH) component is equipped with two additional ones: a connector that takes a real number input for prescribing the set point and one that outputs the heat flow rate transferred to the fluid. In figure 3-1 the WH icon with its connectors is shown.

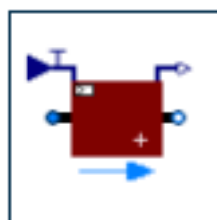


Figure 3-1 MBL water heater component icon

All the components feature a “medium” parameter that defines the substance which the component is working with. Apart from the air side of the air heater, all the components were configured selecting the “*Water*” package contained in the “*Media*” package of the MBL. It provides all the thermodynamics properties of water required for the simulation of the model.

In particular, this package models liquid water with constant density, as the medium model considering density variations with temperature can cause a great increase in simulation computing time [53]. This package also does not consider phase changes.

3.3.1. *Primary circuit components*

Boundary for pressure

The component “*boundary-pT*” from the package “*Fluid.Sources*” is used to prescribe ambient condition and “fill” the circuit with the correct medium, which is water in this case. It must be included in every circuit present in the model and fixes the boundary for temperature and pressure. It can be connected to any component present in the circuit, in this case it was connected to the inlet of the water heater. This component can also be considered as a source or sink for the medium, with its respective thermodynamic properties [53].

It was configured with the following parameters:

- Temperature: $T_{\text{start}}=15^{\circ}\text{C}$
- Pressure: 2.5 bar

These parameters represent the initial condition of the system, standing in 15°C room with all the components “at rest” at the same room temperature.

Water heater

The water heater was modelled with the “*Heater_T*” component from the package “*Fluid.HeatExchangers*”. It represents an ideal heater that control the fluid temperature at the outlet according to a prescribed temperature set point and specified thermal power. It regulates the thermal power transmitted to the fluid according to the current mass flow rate and temperature of the fluid at the inlet and it shows almost immediate response to change in these parameters. It provides little control on its operation, having almost no optional parameters to be configured.

For example, changes in efficiency due to reduced power are not considered in this component, nor are the minimum power threshold reachable by the real water heater. This component only provides an ideal source of heat with which the system can be tested, as no better alternatives are available so far in the MBL. A bespoke model should be implemented to enhance the representation of this component [53].

It was configured with the following parameters [41]:

- QMax_flow = 40.000 W - Maximum thermal power available, from data sheet
- dp_nominal = 15 mbar - Maximum pressure drop on the water side, from data sheet

Pipes

Pipes were modelled employing the “*Pipe*” component from the “*Fluid.FixedResistances*” package. It represents a pipe through finite volume discretization along flow path. It models the pressure drop due to the flow resistance and also heat exchange with the surroundings. For this reason, the component is equipped with a heat port with which a fixed temperature to model the temperature of external environment can be connected. It features an optional configuration in which each segment of the pipe is connected to its own heat port, to consider temperature differences along the length of the pipes. This can be useful when the pipe stretches along different environments at different temperatures, while in this case a unique external temperature was prescribed for the entire length [53].

The primary network was divided into two segments, one from the water heater outlet to the first junction that connects to the first substation, and one from this very junction until the end of the circuit, corresponding to the junction towards the second substation. This was required to insert the junction in between and allow the inclusion of a few temperature sensors. See Fig. 4-1 and Fig. 2-1 for reference. In Model 2 the numbers of pipes had to be increased, to allow the insertion of many temperature sensors placed along the pipes, see section 4-3. All the data for the configuration was gathered from the CAD files and other diagrams available at the lab.

Being developed using a discretization of the volume contained in the pipe, the level of discretization, i.e. the number of segments in which the pipes is divided for the simulation, called nSeg, directly influence the accuracy of the results and the behaviour of the model itself. If a higher discretion level is chosen, a more precise modelling should be accomplished, at the cost of simulation calculation time. When lower numbers of segment are set, indeed, the effect of numerical diffusion tend to “smooth” the hot temperature front entering the pipe, with temperature readings along the pipe increasing gradually before the fluid has reached that point. In the following Figure (3-2) a visual representation of the discretization effect is represented. However, Van Der Heijde et al [39] demonstrated that even with rougher discretization, a good accuracy is acquired. The impact of this effect on the results is discussed in section 4-3.

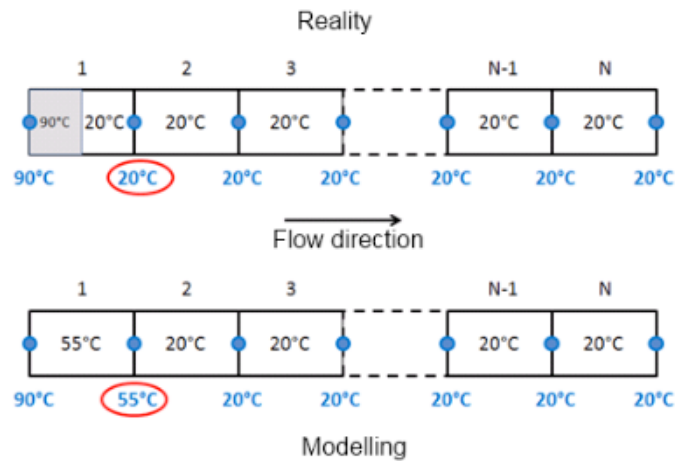


Figure 3-2 Effect of numerical diffusion for on temperature modelling in pipes [60]

The component was configured with the following parameters:

- nSeg = 10 (default) - number of segments for discretization. Changed to nSeg = 2 in Model 2, see section 4-3
- thicknessIns = 0.030 m - thickness of insulation
- lambdaIns = 0.038 W/mK - heat conductivity of insulation
- diameter = 0.0425 m (DN40) – internal pipe diameter
- length = 36.5 (WH > NODE A); 23.1 (NODE A > NODE B)

The component was connected to a prescribed temperature of 15°C on the exterior to model thermal losses, while head loss is automatically computed by the model considering the roughness of the material and the mass flow rate.

Circulation pump

The circulation pump was modelled employing the “FlowControlled_m_flow” component from “Fluid.Movers.Preconfigured” package. This model represents a pump with ideally controlled mass flow rate as input signal and pre-configured parameters [53]. A real input signal prescribing the value of mass flow rate required is sent to the pump via its m_flow_in connector. In this way, the correct pressure raise is supplied by the pump to ensure the prescribed mass flow rate.

This component was selected as it features several preconfigured parameters in order to avoid errors during simulation. By providing m_flow_nominal and dp_nominal values about the real pump, the model constructs a pressure curve, basing on default pressure curves data available in the MBL. In this way all the important parameters are set automatically, and anomalies are avoided. However, this can generate errors in the electric consumption estimations, as efficiency is computed basing on a generic curve [53]. The component can also estimate the heat transferred to energy transferred to the fluid and heat dissipation to the environment.

The component was configured with the following parameters:

- $m_flow_nominal = 1.37 \text{ kg/s}$ – nominal working point
- $dp_nominal = 1.14 \text{ bar}$ – nominal pressure raise working point

Temperature sensors

Temperature sensors were placed in critical points of the circuit, such as close to the water heater inlet and outlet and junctions with the substations' branches. In Model 2 additional ones were placed along the primary circuit to mimic the positioning of real ones.

The component "*TemperatureTwoPort*" from the package "*Fluid.Sensors*" was selected. It has two ports, so it has to be placed along the flow path, for example placing it between the outlet of a tube and the inlet of another one [53]. For this reason, in order to accommodate every thermocouple present in the real system, the pipes had to be subdivided into multiple segments, as these sensors can only be placed before or after a pipe, not along its length.

The presence of the sensor does not influence the fluid properties in any way.

It was configured with the following parameters:

- $T_start = 273.15 + 15 \text{ K}$ – initial guess value of temperature

Localized head loss

The component "*PressureDrop*" from the package "*Fluid.FixedResistances*" was selected to model the head losses due to curves along the primary network pipes. It calculates the pressure drop depending on the current mass flow rate, referring to the nominal one [53]. Nominal mass flow rate, the diameter of pipes and the data from the CAD files were employed to estimate, following the procedures described in the hydraulics handbook from the hydronics firm Caleffi [54].

The component was configured with the following parameters:

- $dp_nominal = 248 \text{ Pa}$ - single curve head loss.

Two components were used to model all the losses, summing all the curves present in between two nodes.

Junctions

The component "*Junction*" from the package "*Fluid.FixedResistances*" was selected to model the node where the pipes from the primary circuit branch out towards the substations. It features three ports to split the flow, each with a fixed resistance to model the head loss. It requires the configuration of expected mass flow rates and nominal head losses for each direction. To express expected flow direction is sufficient to provide a positive value for flows entering the component and negative for the ones exiting it. The same is true for values of head losses. The flow direction can also be "prescribed" to simply calculations for larger models [53].

The junction was set with the following parameters:

- $m_flow_nominal = [m_flow_port1, m_flow_port2, m_flow_port3]$ kg/s – values of expected mass flow rates for each port, depending on the junction modelled
- $dp_nominal = [dp_nominal1, dp_nominal2, dp_nominal3]$ Pa – values of expected head loss for each port, depending on the junction modelled. Similarly to the localized head losses, the pressure drops related to these junctions were calculated following the guidelines present in [54], resulting in an average pressure drop of 745 Pa.

Valves

The regulation and shut-off valves present in the systems were modelled employing the “*TwoWayLinear*” component from the “*Fluid.Actuators.Valves*” package. In addition to the conventional two ports for fluid flow, it features an input connector with which the position of the valve can be controlled, providing a real value from 0 (closed) to 1 (open). Depending on the valve, a different real input was connected to this connector. The model features also a filter that by defaults automatically smooth eventual step changes to the input value, avoiding errors during the simulation [53]. In addition, it can calculate additional head losses when the valve is partially opened.

It was configured with the following parameters:

- $l = 0.0001$ (default) - valve leakage (ratio between mass flow with valve fully closed and fully opened. Required to avoid instability to due decoupling of circuit segments
- $dpVale_nominal = 1738$ Pa – head loss with valve fully opened. Calculated with guidelines available in [54]

System-wide parameters

Unless otherwise specified, all the components’ parameters not mentioned were left as default. In addition, all the components required a mass flow rate initialization which was equal to the value of primary network mass flow rate for all the components. This value changed according to the scenario under consideration, as explained in section 3-4. The initial temperature was also set for all the components equal to the ambient temperature of $T_{start}=15^{\circ}\text{C}$.

3.3.2. Substations and secondary circuit components

Heat exchanger

The plate heat exchanger present in the substations was modelled using the “*PlateHeatExchangerEffectivenessNTU*” present in the “*Fluid.HeatExchangers*” package. It is the only component available in the MBL representing a plate heat

exchanger as the one found in the substation. The heat transfer is calculated through the definition of an efficiency value, as in the NTU method [53]:

$$Q_{HEX} = Q_{MAX} \cdot \varepsilon$$

The efficiency value was determined starting from the nominal case available in the HEX datasheet and then applying the thermal resistance scaling, as further explained in section 3.4.2. An automatic mode is also available in the component that feature a similar calculation to the one proposed here. Yet, as documentation on this component was limited, the manual definition of the efficiency value was preferred [53].

The component feature 4 fluid ports, corresponding to the inlet and the outlet on the hot and cold side respectively.

In addition to the value of effectiveness, the following parameters were set:

- `dp1_nominal`; `dp2_nominal` = 20 kPa – value for head loss on each side, set to the maximum value, as provided in the datasheet
- `m1_flow_nominal`; `m2_flow_nominal` – set to the value corresponding to either the primary or secondary side mass flow rate [45]
- effectiveness
- `configuration` = CounterFlow – parameter that specify the HEX operation, counter flow

More information on the heat exchanger modelling is available in section 3.4.2.

Circulation pump and pipes

The same component as the one employed in the primary circuit was utilized, with properly modified parameters.

Air heater

The air heaters present on each secondary circuit were modelled combining different components as no dedicated component was found in the MBL to represent it properly.

The basic component used is the “*DryCoilEffectivenessNTU*” present in the “*Fluid.HeatExchangers*” package. Similarly to the substation HEX, it represents heat exchange basing on the nominal heat transfer parameters and updating the performance for off-design cases [53]. Unlike the previous case, though, detailed data on the air heater performance was available in the data sheet, so the value of thermal power exchanged was directly provided during the configuration. More details on this procedure are available in section 3.4.1.

To model the air flow generated by the air heater’s fan, the components “*MassFlowSource_T*” and “*Boundary_pT*” from “*Fluid.Sources*” were selected. The first one was set to provide a constant mass flow rate of air at T=15°C according to

the air heater's data sheet, while the second one served as a sink towards directing heated air.

An image from the graphical editor is available in Fig. 3-3.

Similarly to the substation HEX, these parameters were set:

- $m1_flow_nominal$; $m2_flow_nominal$ – mass flow rate of air and water side, available in section 3.4.1
- $dp1_nominal = 4$ kPa – head loss on water side, as described in the data sheet for the according mass flow rate [46]
- $dp2_nominal = 0$ kPa – head loss on air side was not considered, as the air heater circulates ambient air
- configuration = CrossFlowUnmixed

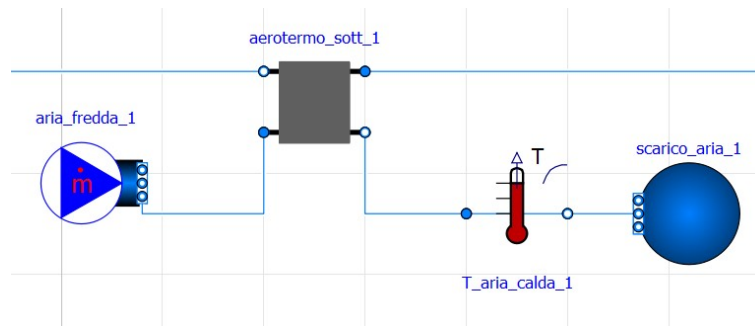


Figure 3-3 Air heater modelling

Thermal energy storage

The TES present in secondary circuit 2 was modelled using the “StratifiedEnhanced” component from “Fluid.Storage” package. It represents a stratified fluid storage vessel for thermal energy storage. To model the stratification effect, the tank is divided into several volumes, similarly to what is done in the pipe component. These volumes are stacked vertically along the height of the vessel and heat conduction is modelled in between them, as is the thermal dispersion from the fluid to the ambient [53]. The number of segments used to model the tank directly impact on the results and the behaviour of the component, as it will be investigated in section 4.4.

The component is fitted with two fluid ports, placed at the top and the bottom of the vessel respectively, and as many heat ports as the number of segments selected. These heat ports are directly linked to each segment and can be used both to detect the temperature of that very segment or to add heat to the segment, to represent, for instance, an electrical resistance heater. In addition, three external heat ports are present, one at the top, one along the side and one at the bottom, with which the surrounding temperature can be specified. In this way, the heat transfer with the environment is modelled.

Unlike the real TES, though, lateral fluid ports placed at different heights are not present in this component, so water can be withdrawn or poured through the top and bottom port only [53].

The component was configured with the following parameters [50]:

- $V_{Tan} = 1.4724 \text{ m}^3$ – volume of the vessel
- $h_{Tan} = 2.115$ – height of the vessel
- $d_{Ins} = 0.130$ – Thickness of insulation
- $n_{Seg} = 4$ up to 70 – number of volume segments for stratification modelling. See section 4.4
- $\tau = 1 \text{ sec}$ (default) – time constant for mixing – present but still not implemented at the time of writing
- T_{start} – initial temperature of the tank, set according to the case under evaluation
- $T_{Flu_start}[n_{Seg}]$ – this parameter accepts an array containing the initial temperature of each segment. In this way it is possible to express a gradient of temperature along the height of the TES as initial condition. This is useful to describe the tank status when it has not been fully charged or discharged, and in turn present different values of temperatures along the height.

The component was connected to the circuit through its top and bottom ports, the three external heat port were connected to the prescribed ambient temperature $T_{ext}=15^\circ\text{C}$. The internal heat ports were employed to connect three temperature sensors representing the three thermocouples placed in the real system. Their positioning was done considering their height on the side of the tank and matching them to the correct segment in the digital model, depending on the discretization level set.

3.4. Setting the system's operational parameters

After the selection and placement of every component, a crucial phase of the project was defining the operational parameters of the model as a whole. As there was no data available regarding the real operation cycles of the system, a method had to be established to assess which mass flow rate at the primary and secondary circuits was adequate and which supply temperature was required at the water heater outlet. This task was particularly delicate, as these variables condition the behaviour of each component systemwide, making the performance depend on each other. For this reason, the need to fix a few boundary conditions arose.

In this way, the calculation began with the assessment of the parameters required at the air heater and then proceeding back, calculating the heat demand at the substation and, in turn, at the primary circuit. The procedure started with imposing the thermal power required at each air heater. Thinking of configuring a real DH network, the user demand, here in the form of the air heaters, is the final goal for the optimization of the network and must be always met. Furthermore, the air heater's technical data sheet allowed for a precise definition of its performance as it included a list of correction coefficients to calculate the thermal output under different operational conditions, making it a solid basis on which to calculate the rest of the parameters.

Once thermal power at the air heater was known, the mass flow rate and temperature required at each secondary circuit were calculated under a few assumptions. These calculations are exposed in the next section.

In turn, as the secondary circuit requirements were set, the focus shifted to calculating the performance of the heat exchanger. As it has been discussed in the previous section, the heat exchanger model requires an input value for its effectiveness, as it does not support manual entering of parameters such as heat exchange area or the overall heat exchange coefficient. To calculate this parameter, the "*Thermal Resistance Scaling*" method was adopted, as it enables the prediction of a heat exchanger's performance in off-design conditions [55]. This approach was successfully employed by Ancona and others [55] in a project developed at ENEA intended to model a DH network in a similar fashion as this project. Their method consisted of considering the performance of the heat exchanger while under design conditions and then estimating the behaviour when fed with different mass flow rates or temperatures. This method is further explored in section 3.4.2.

With all this information, the mass flow rate and temperature required at the primary circuit could be evaluated and the relative parameters inserted in the model. This cycle was repeated to represent 3 possible cases, ranging from 70°C to 90°C at the primary circuit supply, with all the subsequent parameters. Further details are available in the results chapter.

3.4.1. Air heater: assessing the performance

The calculation of the air heater power output began considering the technical data sheet. The thermal power output was given for a design case that considers a $\Delta T_{water} = 10^{\circ}C$ drop on the water side, with a $T_{water,in} = 85^{\circ}C$ and $T_{air,in} = 15^{\circ}C$ as air inlet temperature with a volumetric flow rate of $\dot{Q}_{air} = 2915 \frac{m^3}{h}$. With these parameters the thermal output of $Q_{airheater,design} = 20.85 kW$ and the temperature of the air at the outlet $T_{air,out} = 35.9^{\circ}C$ were given. These data were followed by a list of correction coefficients, which depend on the temperature drop at the water side and the temperature of the air at the inlet, that enabled the calculation of the air heater performance in off-design conditions.

Three different scenarios were considered, varying the temperature of the water at the inlet, at $T_{water,in} = 60^{\circ}, 70^{\circ}, 80^{\circ} C$, keeping the same temperature drop of $\Delta T_{water} = 10^{\circ}C$. On the air side, the volumetric flow rate was kept constant, as the air heater's electric motor is fixed, and the same inlet temperature was considered. Off-design power output was calculated with the correction coefficient available. The mass flow rate of water for each case was approximated considering an ideal heat transfer between the water and air side, as no information could be found in the technical data sheet of the air heater. On the air side, considering 50% relative humidity and atmospheric pressure, and relative parameters for density and specific heat, the off-design outlet air temperature could be calculated. This information was not strictly needed to run the model, however, a sensor for output air temperature was included in the model, as a check measure. All data related to air heater performance were gathered from its technical data sheet and the results of calculations are reported in table 3-2 [46].

$$Q_{airheater,off-design} = Q_{airheater,design} \cdot \text{correction coefficient} [kW] \quad (3.1)$$

$$\dot{m}_{water} = \frac{Q_{airheater}}{c_{p,water} \cdot \Delta T_{water}} \left[\frac{kg}{s} \right] \quad (3.2)$$

Table 3-2 Air heater off-design performance calculation [46]

scenario	2	1	3	unit
$T_{water,in}$	60	70	80	[°C]
$T_{air,in}$	15	15	15	[°C]
Correction coefficients	0.62	0.77	0.92	[-]
$Q_{airheater,off-design}$	12.93	16.06	19.18	[kW]
\dot{m}_{water}	0.309	0.384	0.458	[kg/s]
$T_{air,out}$	27.9	31.1	34.2	[°C]

3.4.2. Substation heat exchanger: assessing the performance

As anticipated in the previous section, due to the design of the plate heat exchanger employed, a value for the effectiveness of the heat exchanger was required in the component configuration, according to the ε -NTU method. However, the effectiveness of a heat exchanger changes according to various parameters. As the overall system is supposed to operate under different conditions, such as different supply temperatures and different mass flow rates, a fixed value for the effectiveness could not be adequate. Conducting the thermal analysis of the HEX through the calculation of conventional fluid dynamic parameters was also not possible due to the lack of precise information about the geometry of the HEX.

For these reasons, the “*thermal resistance scaling*” (TRS) method was a good alternative for the evaluation of off-design behaviour. This method was employed by [55] to solve the same problem explained in this section. Ancona and others [55], developed a new HEX component model in Dymola environment and configured it according to the TRS method. In this project, inspiration was taken from their approach, although the value of effectiveness was inserted manually depending on the model configuration and not dynamically. The aim of the method was to provide three values for the effectiveness of the HEX, linking to one of the three power levels just considered for the air heater and presented in table 3-2.

The TRS method starts by considering the performance of the HEX in design conditions (table 3-4). In this case, the operational data provided in the datasheet of the HEX were taken as the reference condition on which the method was applied. The effectiveness (ε) of a heat exchanger according to the ε -NTU method can be defined as:

$$\varepsilon = \frac{1 - \exp\left(-\left(1 - \frac{C_{min}}{C_{max}}\right) NTU\right)}{1 - \frac{C_{min}}{C_{max}} \exp\left(-\left(1 - \frac{C_{min}}{C_{max}}\right) NTU\right)} \quad [-] \quad (3.3) [55]$$

In (3.3) $C = \dot{m} \cdot c_p \left[\frac{W}{K}\right]$ is the heat capacity of the hot or cold fluid running into the HEX respectively. The subscript min/max indicates the one with the highest or lowest heat capacity and, as water is flowing in both channels, is directly related to the fluid having the highest or lowest mass flow rate, as the specific heat is constant in both cases.

In (3.3) NTU stands for Number of Transfer Units, and it is a dimensionless parameter that, under fixed conditions, is directly related to the size of the heat exchanger and is defined as:

$$NTU = \frac{UA}{C_{min}} = \frac{\Delta T_{max}}{\Delta T_{LMTD}} \quad [-] \quad (3.4) [55]$$

To calculate NTU, a value of UA is required (where $U \left[\frac{W}{m^2K} \right]$ is the heat transfer coefficient and $A [m^2]$ is the total heat transfer surface) and can be calculated through the value of the total thermal resistance as in (3.5). The total thermal resistance consists of the sum of the two convective resistances, one for the hot and cold side, and the conductive resistance of the metal constituting the ducts of the HEX.

$$R_{T,D} = \frac{1}{(UA)_D} \left[\frac{K}{kW} \right] \quad (3.5) [55]$$

The thermal resistance scaling springs into action in this part of the calculation. First, the total resistance of the HEX under design conditions is calculated, then is divided into its three components, two convective and one conductive, using a factor found in [55], being:

$$\begin{aligned} R_{convection,hot,D} &= R_T \cdot f_{conv,h} \\ R_{conduction,D} &= R_T \cdot f_{cond} \\ R_{convection,cold,D} &= R_T \cdot f_{conv,c} \\ f_{conv,h} &= f_{conv,c} = 0.43 \\ f_{cond} &= 0.13 \end{aligned} \quad (3.6) [55]$$

Once all the resistances for the design (D) condition are individuated, the ones for off-design (OD) conditions are calculated taking into account the new mass flow rates of the hot and cold side in off-design conditions. The conductive resistance is not modified as it is not influenced by the different conditions.

$$\begin{aligned} R_{conv,h,OD} &= R_{conv,h,D} \cdot \left(\frac{\dot{m}_{h,D}}{\dot{m}_{h,OD}} \right)^{0.8} \\ R_{conduction,OD} &= R_{conduction,D} \\ R_{conv,c,OD} &= R_{conv,c,D} \cdot \left(\frac{\dot{m}_{c,D}}{\dot{m}_{c,OD}} \right)^{0.8} \end{aligned} \quad (3.7) [55]$$

As all the resistances have been updated, their sum is calculated to calculate the new total thermal resistance in off-design conditions and the relative UA value, according to (3.5). With this new UA_{OD} the NTU can be computed as well as the new value for the effectiveness, completing the analysis. However, at this point, only the mass flow rate on the secondary side of the HEX is known, as it has been calculated during the air heater analysis as in table 3-2. The mass flow rate of the primary side is still unknown, and it is required to complete the assessment of the effectiveness, as, without the two mass flow rates, the minimum heat capacity required in (3.4) is unknown. An iterative process was set up to find this parameter. Using a purpose-built model, different guess values for the mass flow rate of the primary were tested, repeating the calculation of the effectiveness each time, and inputting it into the

model. The supply temperature on the secondary side was considered the goal for the iterative process, with its value changing according to the scenario under evaluation, as explained in table 3-2. The results of this iterative process with all the parameters considered are summarized in table 3-3. In all the scenarios, according to the ones created for the air heater study, the supply temperature on the primary circuit is 10°C higher than the T_3 , i.e. the supply temperature on the secondary side, which is in turn the goal of the iterative process.

Table 3-3 HEX Effectiveness values calculated with TRS

scenario	2	1	3	unit
$T_1 = T_{supply,primary}$	70	80	90	[°C]
$T_3 = T_{supply,secondary}$	60	70	80	[°C]
$\dot{m}_{primary-side}$	0.185	0.220	0.290	[kg/s]
UA_{OD}	2552	2940	3496	$\left[\frac{W}{K}\right]$
ε	0.881	0.873	0.836	[-]

In the following table (3-4) the information relative to the design conditions, as provided by the HEX manufacturer, is reported.

Table 3-4 HEX design conditions [45]

Rated power	50 [kW]
$\dot{m}_{hot-side}$	0.598 [kg/s]
$\dot{m}_{cold-side}$	0.598 [kg/s]
ΔT hot side	80 → 60 [°C]
ΔT cold side	50 → 70 [°C]
UA (calculated)	5000 [W/K]
ε	0.665

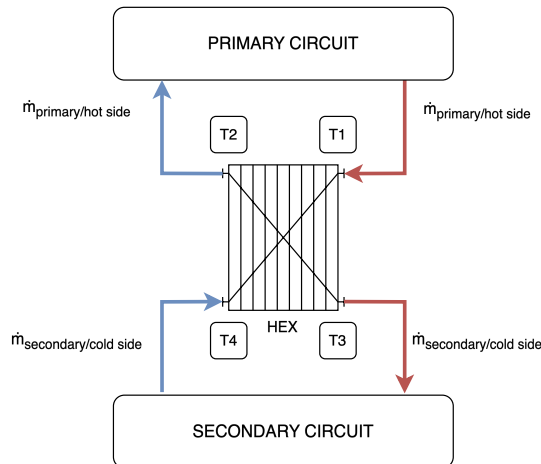


Figure 3-4 HEX scheme

3.5. Summary of models created

Here is a list of the four main models created during this project. The results of the simulations will be presented in the next chapter.

Screenshots from the graphical editor of all the models are available in Figures 3-5, 3-6, 3-7, 3-8.

MODEL 1: Basic system layout

This is the reference model on which the other ones are based. It features the primary circuit with relative heat generation and two identical secondary circuits supported by two identical substations. Heat demand is represented by the two air heaters, one for each secondary circuit. In this model, the TES is not considered.

MODEL 2: Basic system layout - enhanced primary circuit modelling

This model resumes Model 1, enhancing the modelling of the primary circuit. The pipework of the primary circuit was divided into many smaller units to allow the insertion of all the thermocouples placed in the real system configuration. In this way, the temperature can be detected at the exact spot as in the real system. Furthermore, this model was employed to experiment with the inclusion of a bypass valve, connecting the primary circuit's supply and return sides directly.

MODEL 3: Sensible thermal energy storage study

This model was created specifically to study the behaviour of the thermal energy storage present in the laboratory and compare its performance with the experimental data available. It includes the TES and a controlled discharge circuit only, to make the analysis easier and exclude other variables.

MODEL 4: The complete model

This model includes the knowledge gathered in the three previous ones and represents the complete system layout of the experimental system under analysis. The TES is included in the secondary circuit connected to substation 2.

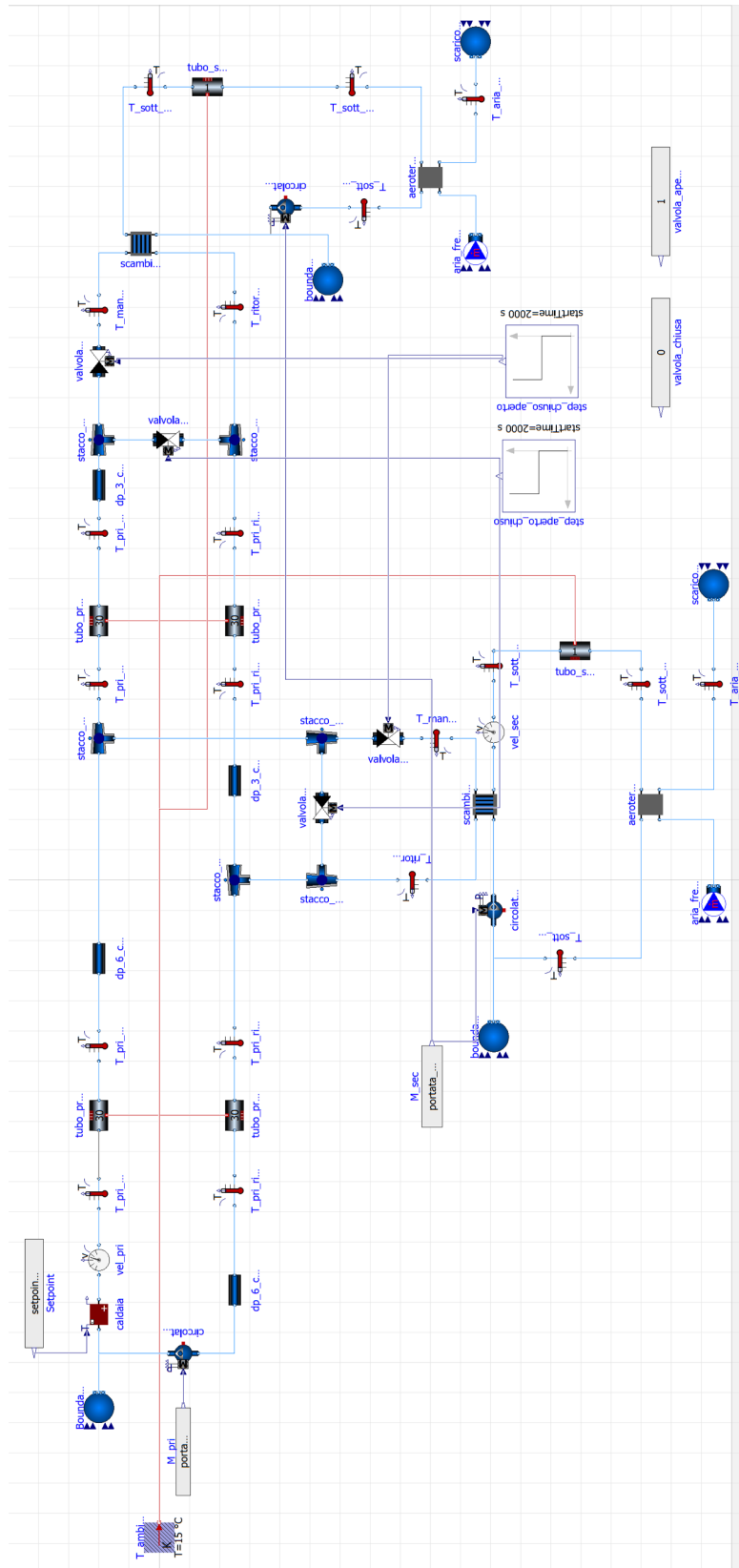


Figure 3-5 Model 1

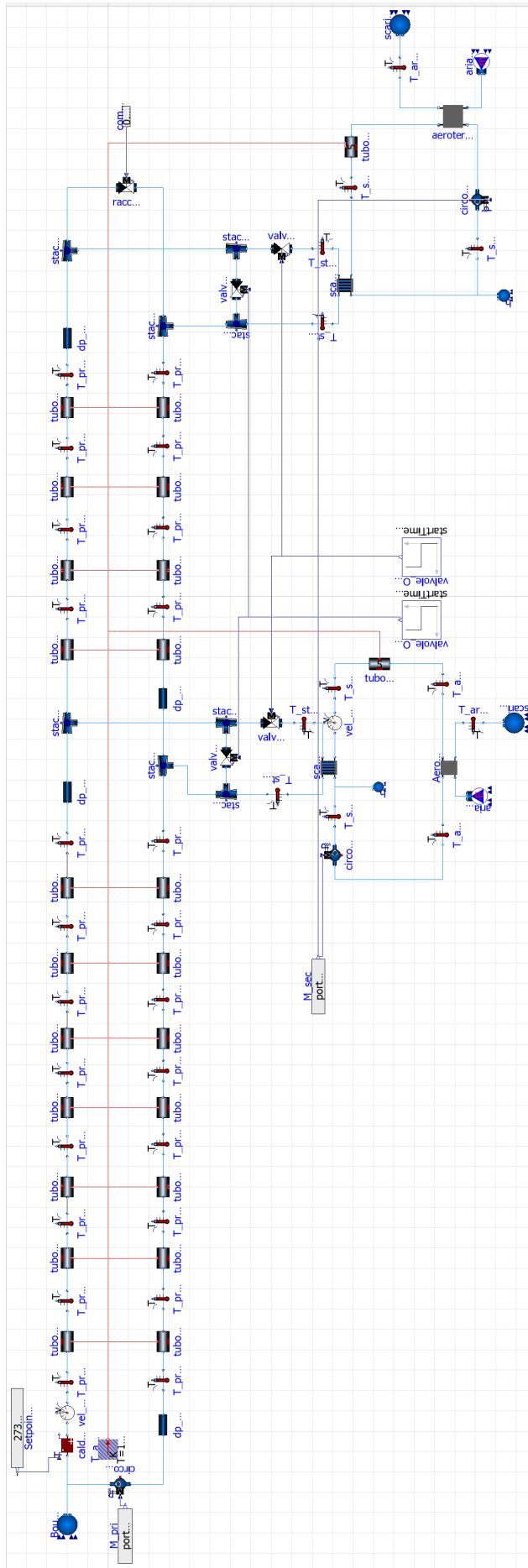


Figure 3-6 Model 2

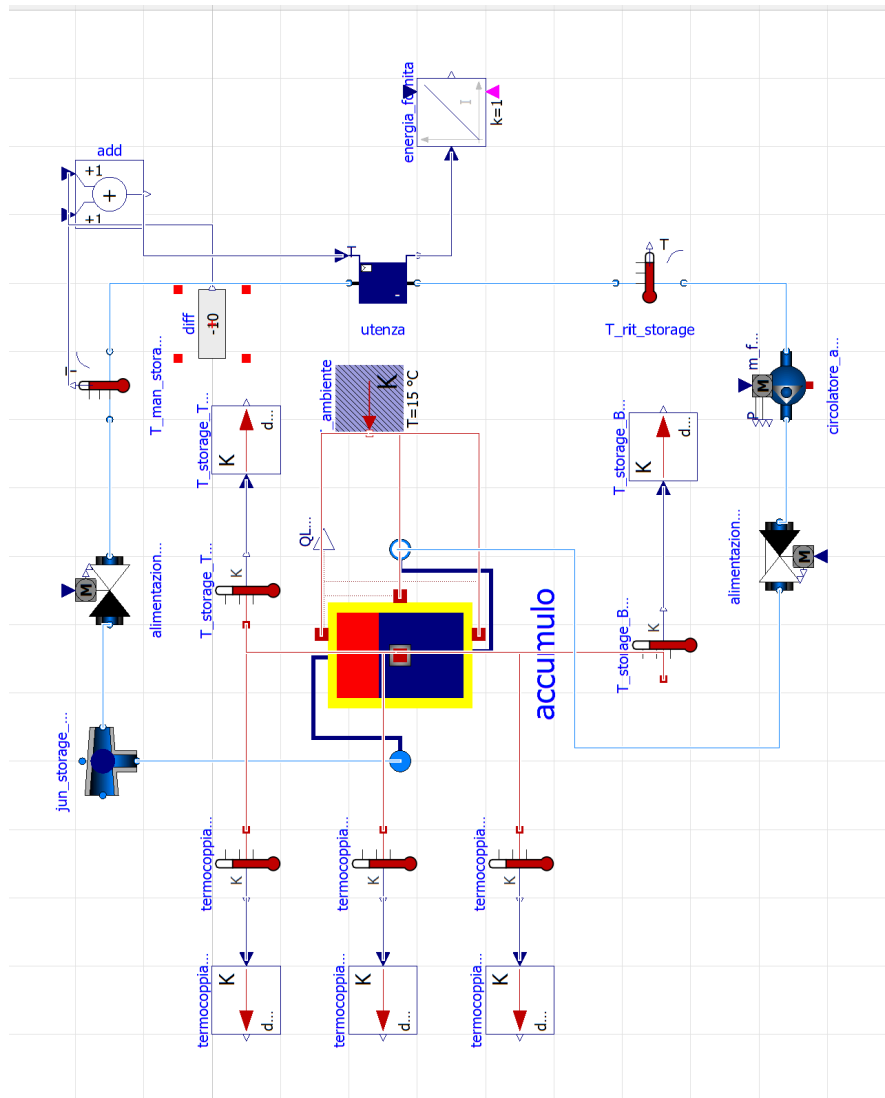


Figure 3-7 Model 3

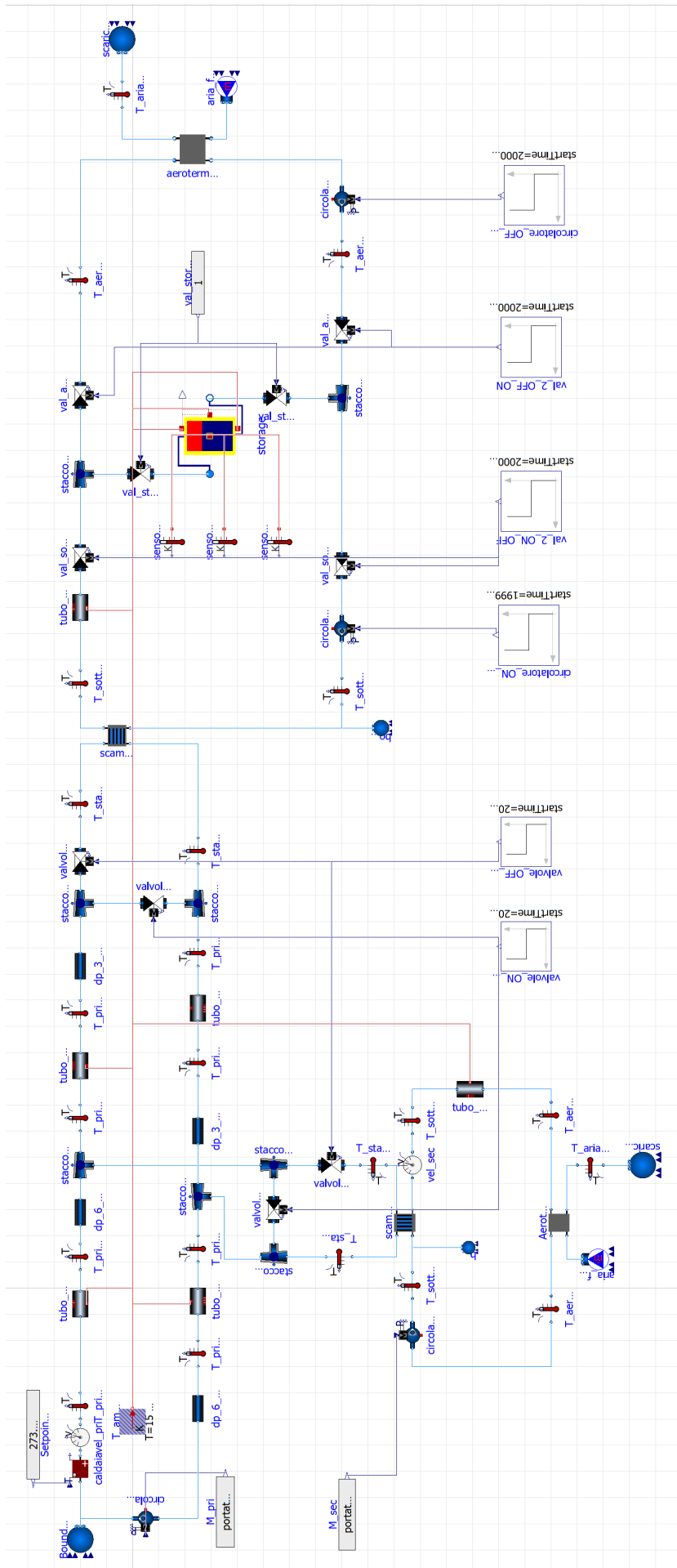


Figure 3-8 Model 4

4. Simulations and results

This chapter showcases the most interesting results collected during the testing and simulation phase of the project. Once the models were created, a few scenarios were conceived to test the behaviour of the model, looking for eventual anomalies in the components.

Predictably, the first obstacle encountered in this phase was the absence of data about the system's performance gathered during a real operation to refer to. Ideally, when a digital twin is under development, a mutual exchange of data and insights between the real and digital entity should take place, to perfect the prediction of real behaviour by the digital model. In this case, a few test scenarios were created to test the system under typical conditions and results were commented on the basis of expected trends, investigating the ones that reported particular or unexpected behaviour.

Therefore, the results reported in the following sections are intended to serve as a proof of concept, demonstrating the capability and the strength of this modelling approach, as they do not refer to any real operational configuration, with the thermal storage modelling being the only exception.

4.1.1. *Setting the simulation environment*

As previously explained, all the simulations were conducted in the OpenModelica suite, with the following parameters (table 4-1). The default solver, DASSL, was left unchanged, as being an implicit solver provides robust performance without being influenced by the time step, which, in this case, only controls the resolution of output results. The time step was selected as 1 sec, to provide a good resolution. The default value for the tolerance was also untouched, as during all the simulations the solver always managed to complete the task in a short time [56].

Table 4-1 General simulation settings

Solver	DASSL (default)
tolerance	10^{-6} (default)
Time step	1 sec
Start time	0 sec
Stop time (length)	variable

4.2. Model 1: basic system layout

4.2.1. Simulation 1: system cold start

In this simulation, a cold start of the system was performed. The circulation pumps of the primary circuit and secondary circuits are controlled through a constant flow rate and start circulating water in all three circuits. Water is circulated right away through the two substations, which in turn feed warmed water to the air heaters. The bypass valve that allows circulation in the primary excluding the substations is closed for the entire length of the simulation. In table 4-2, a summary of the simulation parameters is available.

Table 4-2 SIM 1 parameters

Simulation length	4000 seconds
T_{start}	15 °C
$T_{\text{setpoint,water-heater}}$	80 °C
\dot{m}_{primary}	0.45 kg/s
$\dot{m}_{\text{secondary}}$	0.384 kg/s
$Q_{\text{air-heater}}$	16.06 kW

This is the simplest configuration. Every component is set to its default parameters and the system is left operating for 4000 seconds. In the following pages, a selection of results is presented and commented on. In Figure 4-1, a schematic representation of the system's configuration is proposed.

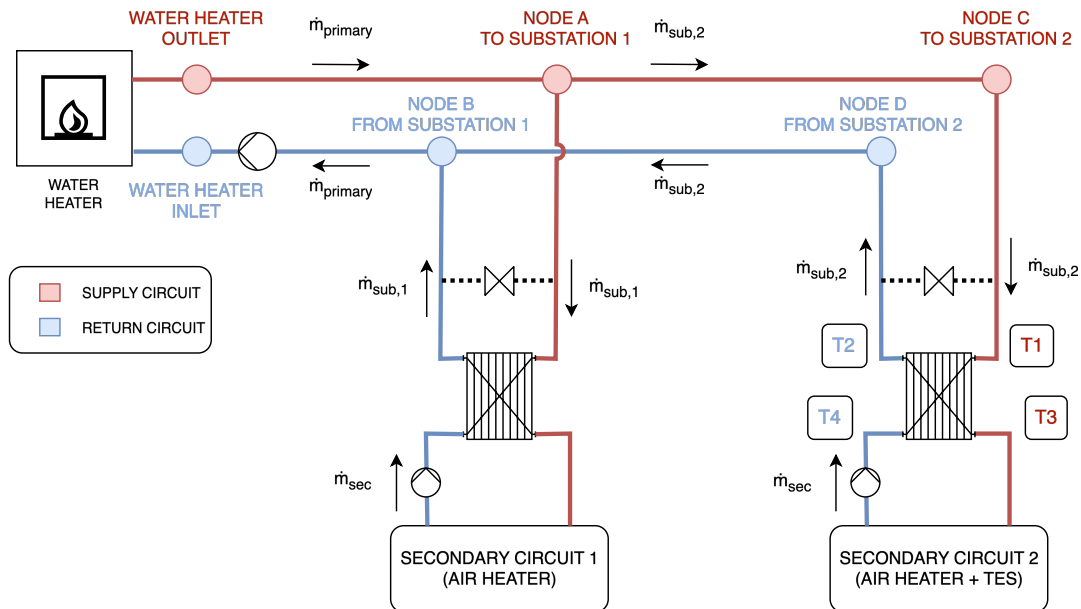


Figure 4-1 Normal system operation – bypass not active

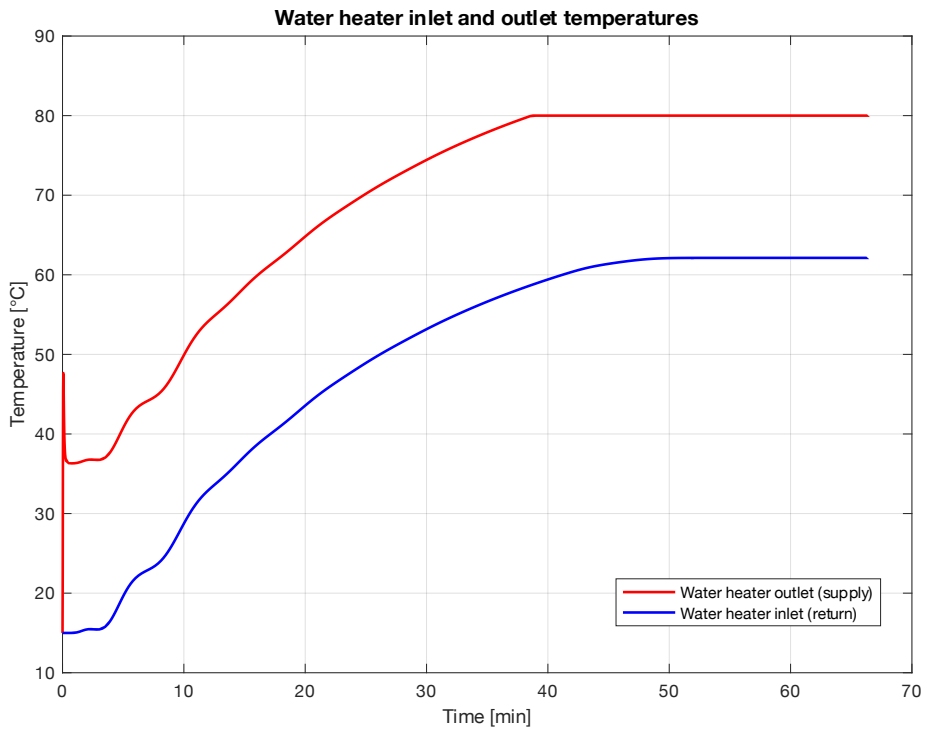


Figure 4-3 SIM 1 - water heater inlet and outlet temperatures

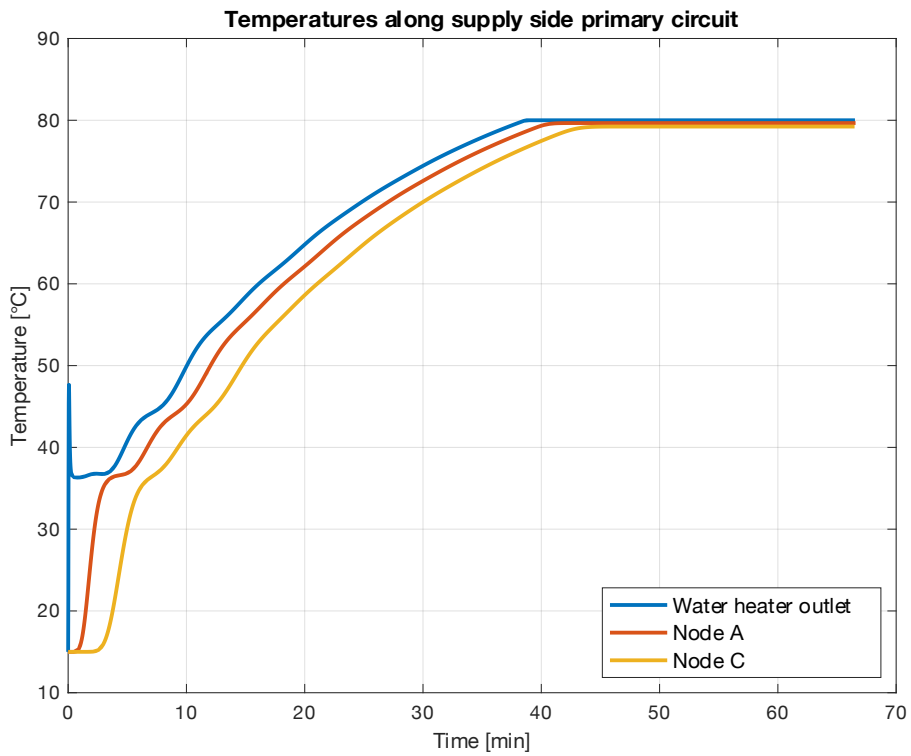


Figure 4-2 SIM 1 - temperatures along primary circuit supply side

This simulation was useful to investigate the transients involved in a cold start and to test the overall system in a basic configuration. The graphs shown in these pages report the readings from the temperature sensors placed in the primary and secondary circuits.

In Fig. 4-3 the inlet and outlet temperatures from the water heater are reported. A spike in the supply temperature can be noticed, reaching a maximum of 46°C. During the analysis of the CSV file reporting all the data points, the anomaly showed for a brief instant, lasting less than 9 seconds. This is probably due to instability during the initialization of the model and should be ignored, as the output stabilizes right after. A brief constant temperature segment can be seen and is due to the circulation of cold water into the primary circuit. As the circulation pump is started, all the water present in the pipes has to be warmed up from the initial $T_{\text{start}}=15^{\circ}\text{C}$. The water heater, at 40kW, with a constant mass flow rate, can provide a $\Delta T_{\text{water_heater}} = 20^{\circ}\text{C}$ maximum increase in temperature. As water is circulated and heated, the warm front is pushed further into the primary circuit, however, the residual cold water still present has to be warmed and this generates the constant output that can be noticed approximately for the first 5 minutes. By considering the water speed constant at 0.32 m/s and the total length of the primary circuit of about 120 m, taken from the CAD files of the system, an approximate time of 6 minutes is needed to cover the whole circuit.

Fig. 4-2 shows the temperatures detected by temperature sensors placed at the junctions between the primary circuit and the two branches that connect the primary circuit to the substations. As can be seen, node A starts detecting the increase in temperature first, as it is closer to the water heater. Likewise, node B starts detecting a constant temperature as the stagnant cold water is gradually swept away by the warm front from the water heater.

The primary circuit stabilizes after several minutes, with the supply temperature reaching the $T_{\text{setpoint}}=80^{\circ}\text{C}$ after almost 40 minutes and the return temperature reaching 62°C after almost 50 minutes. This long transient occurs as the substations are exchanging power with the respective secondary circuit from the first instant, cooling the water that is sent back at the water heater on the return side of the primary circuit. In this way, coupling the cooling effect from the substations and the initial state of the system, with all the components at $T_{\text{start}}=15^{\circ}\text{C}$, the water heater cannot supply water at the setpoint before the whole system reaches a stable condition.

In Fig. 4-2, by looking at the temperatures after the system has stabilized, the little thermal dissipation happening in the pipes can be noticed. It is very limited, as the furthest temperature reading only shows a decrease of 0.8°C compared to the water heater supply.

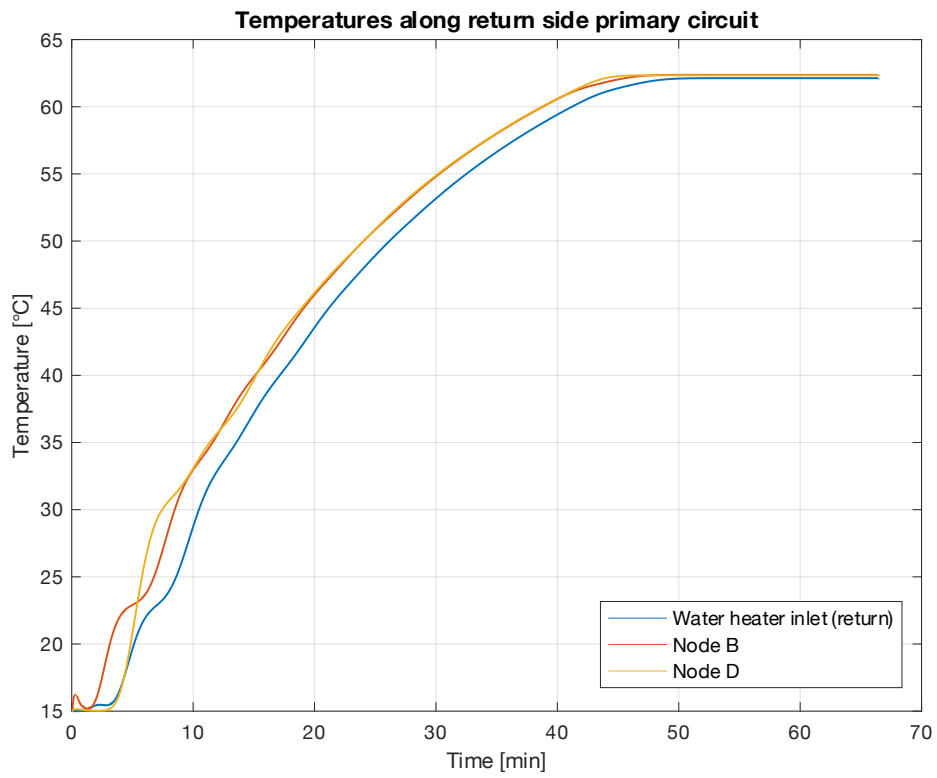


Figure 4-4 SIM 1 - temperatures along primary circuit return side

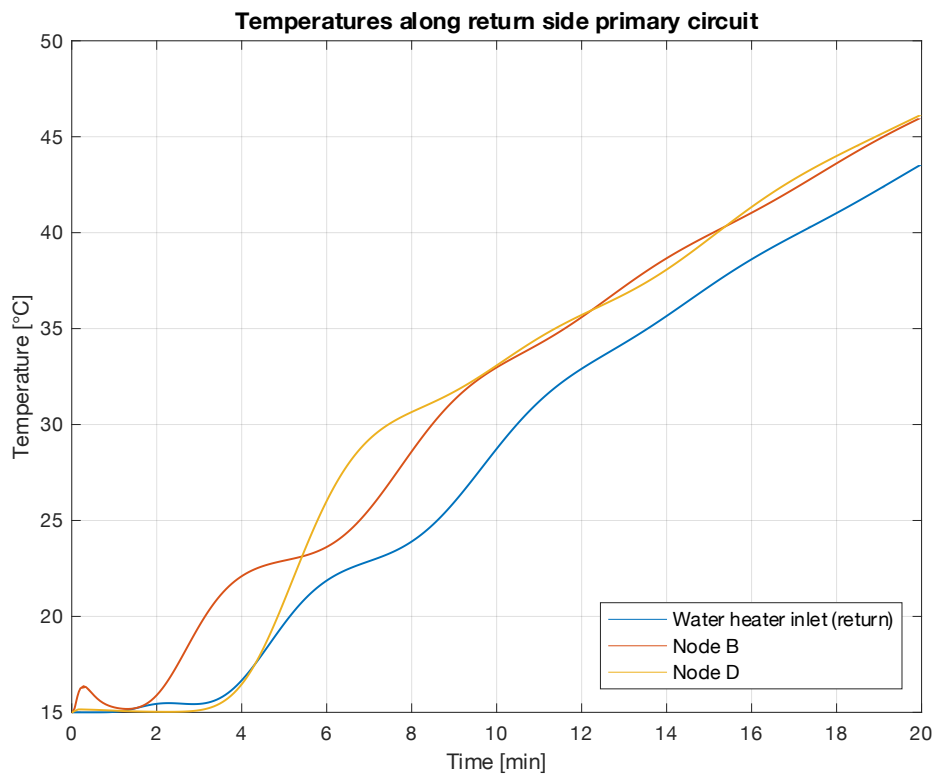


Figure 4-5 SIM 1 - temperatures along primary circuit return side - closeup

In Fig. 4-4 the temperatures from the same nodes on the return side are shown, with a closeup in Fig. 4.5, from which an interesting trend can be noticed. At node B, where the return mass flow rates from the two substations are mixed, the temperature rise anticipates the one in other nodes. This happens because, on the return side, node B is the first one to detect warm water from the water heater, as can be seen in Fig. 4-1. Then, as there are no further inputs or outputs between node B and the water heater inlet, the blue curve follows the trend of node B, just slightly delayed due to the additional pipe length. On the other hand, at node D a different behaviour is registered. As expected, for the first minutes the output of the sensor is constant as it is only detecting cold water circulating. As soon as the warm front reaches the sensor, the temperature increases sharply, without the momentary delay in increase that can be noticed between minutes 4 and 6 at node B. This is probably due to the segment of cold water still present between the two nodes that temporarily hinders the increase of temperature at node B. Since at node D all the cold water has already been swept by the warm front, this behaviour is not detected.

Furthermore, as will be discussed in the next sections, when discussing other simulations, a rippling effect can be noticed during the first 15 minutes of the simulations. This effect is especially noticeable in fig 4-2. This is due to the way pipes are modelled in the MBL “pipe” component. As anticipated in the previous chapter, the level of discretization selected alters the way temperatures are computed along its length, generating sudden changes in sensor readings, followed by a constant segment. A lower discretization parameter can be set to avoid this effect, at the cost of lower resolution in the results.

In Fig. 4-6 the temperatures detected at the 4 sides of the substation 2 HEX are presented. As expected, they show a continuous trend, as the HEX is constantly fed with water from the primary, since the initial instant of the simulation. The target temperature of $T_3=70^\circ$ is reached only after more than 40 minutes.

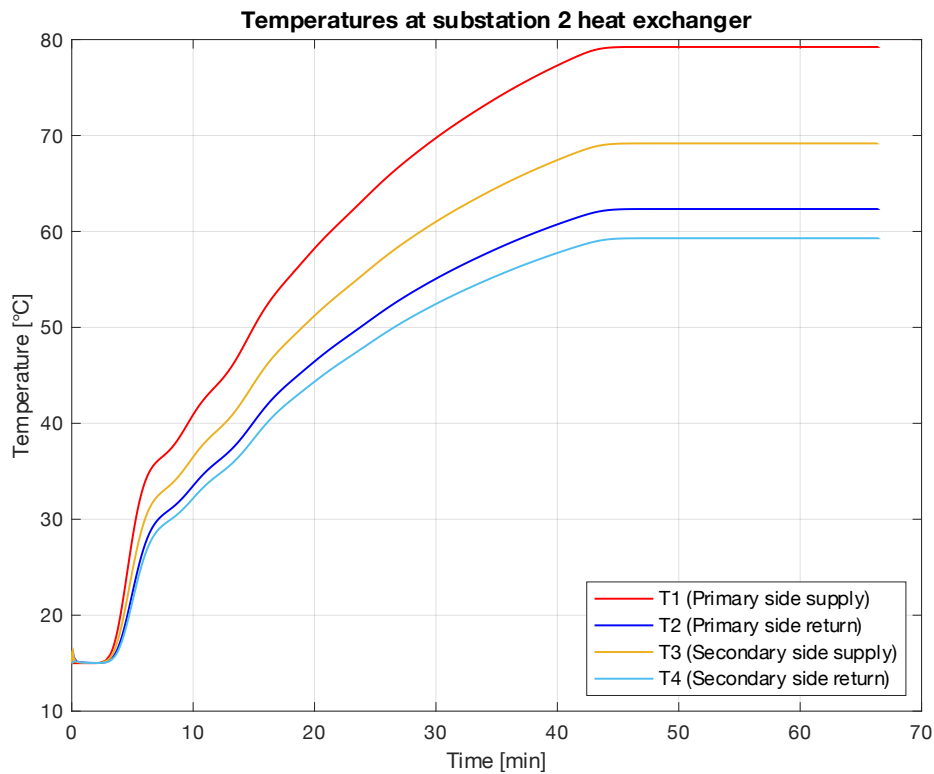


Figure 4-6 SIM 1 - Temperatures at 4 sides of substation 2 HEX

4.2.2. Simulation 2: preheating the primary circuit

In this simulation, a different configuration was tested. Instead of feeding water to the substations from the start of the simulation, a preheating phase was inserted, by exploiting the bypass valves linking the supply and return branches that connect the primary circuit to each substation. In this way, once the system is started, water is recirculated in the primary circuit and heated before opening the valves feeding the two substations. In this way, the time required to reach the setpoint temperature is much reduced and, by opening the substations' valves at a second time, the reaction of the model to sudden changes could be investigated.

In the following table, a summary of the simulation parameters is available.

Table 4-3 SIM 2 parameters

Simulation length	4000 sec
Preheating	2000 sec
T_{start}	15 °C
$T_{setpoint,water-heater}$	80 °C
$\dot{m}_{primary}$	0.45 kg/s
$\dot{m}_{secondary}$	0.384 kg/s
$Q_{air-heater}$	16.06 kW

In Figure 4-7, a scheme of the system working with the bypass at substations is shown. This configuration excludes the two substations, recirculating water only in the primary circuit. After about 33 minutes in this setup, the valves' positions are switched, as the substations are connected to the primary circuit and begin transferring thermal energy to their respective secondary circuits, coming back to the normal configuration seen in Fig. 4-1.

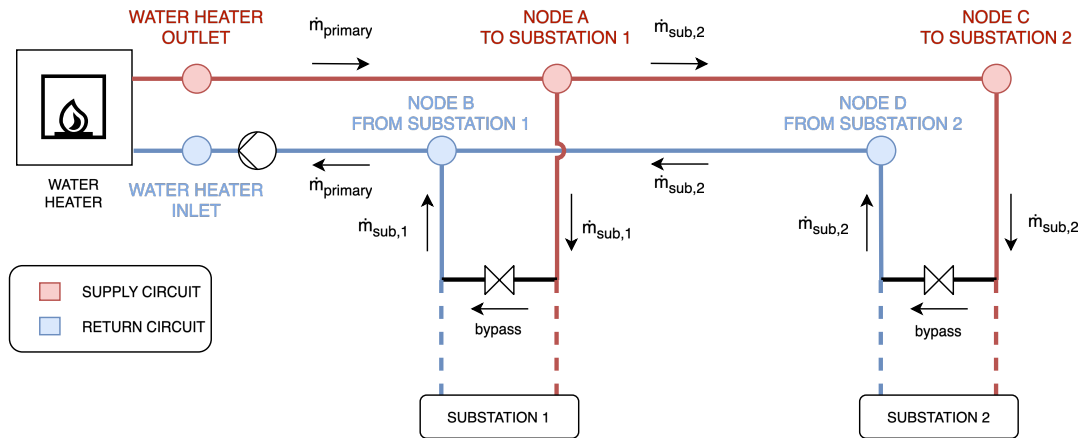


Figure 4-7 System operating with substation bypass (preheating phase)

This effect is clearly visible in the fig. 4-8, showing the temperatures detected on the supply side of the primary circuit, where the setpoint temperature is reached in less than 20 minutes, half the time required during simulation 1.

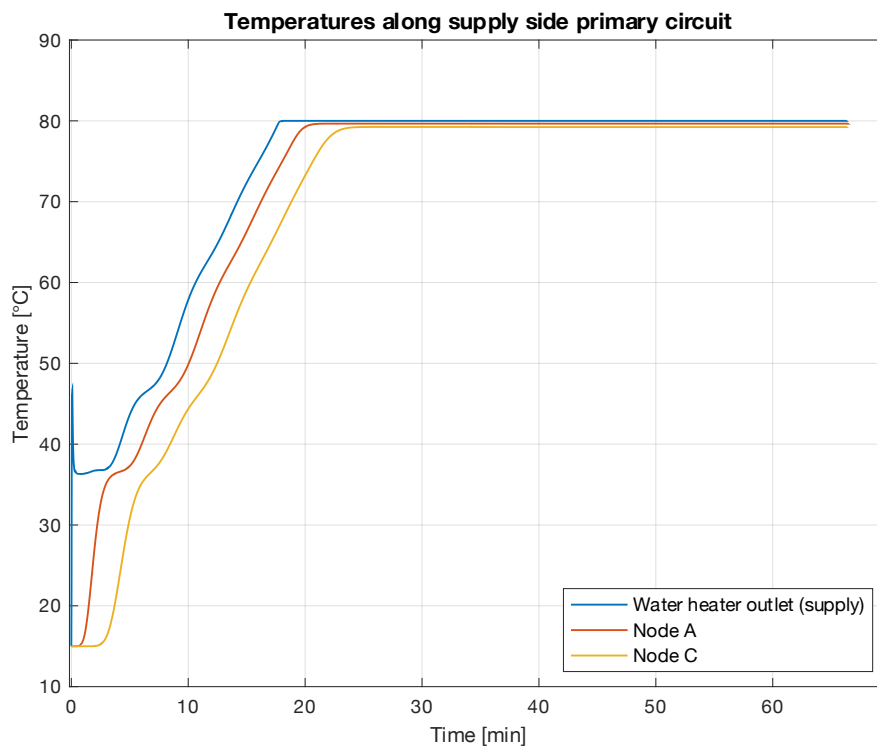


Figure 4-8 SIM 2 - temperatures along primary circuit supply side

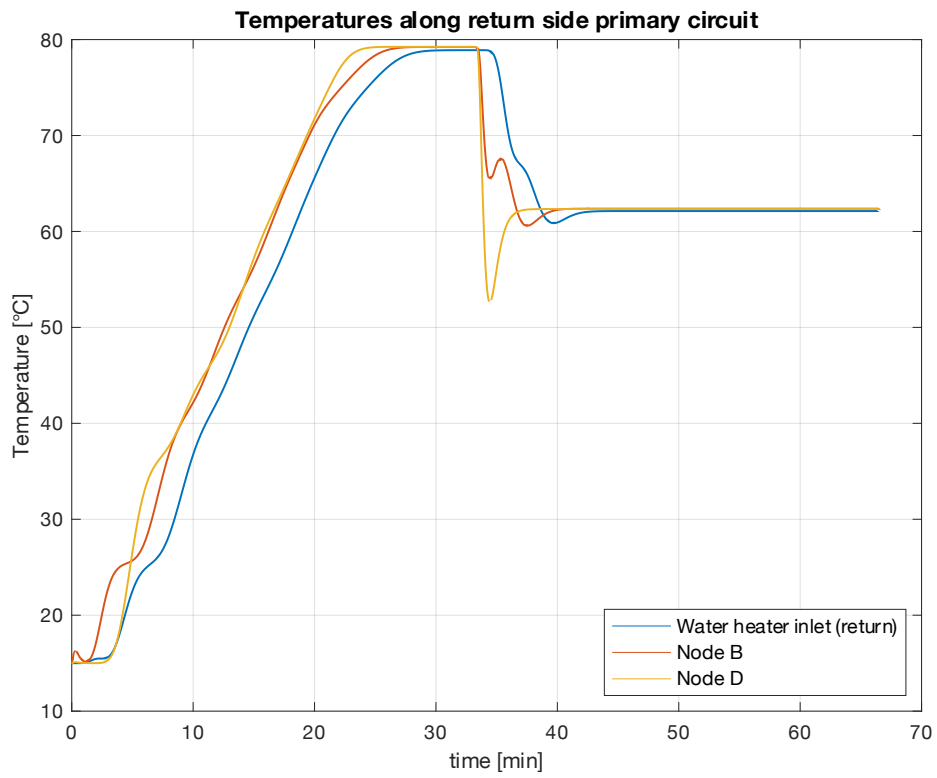


Figure 4-10 SIM 2 - temperatures along primary circuit return side

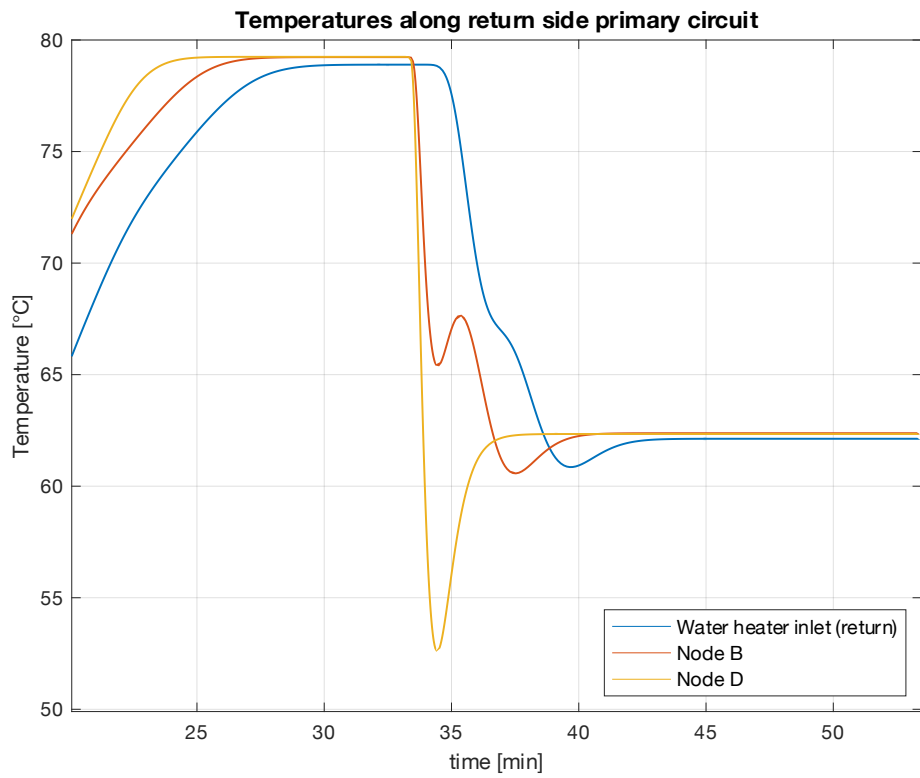


Figure 4-9 SIM 2 - temperatures along primary circuit return side - closeup

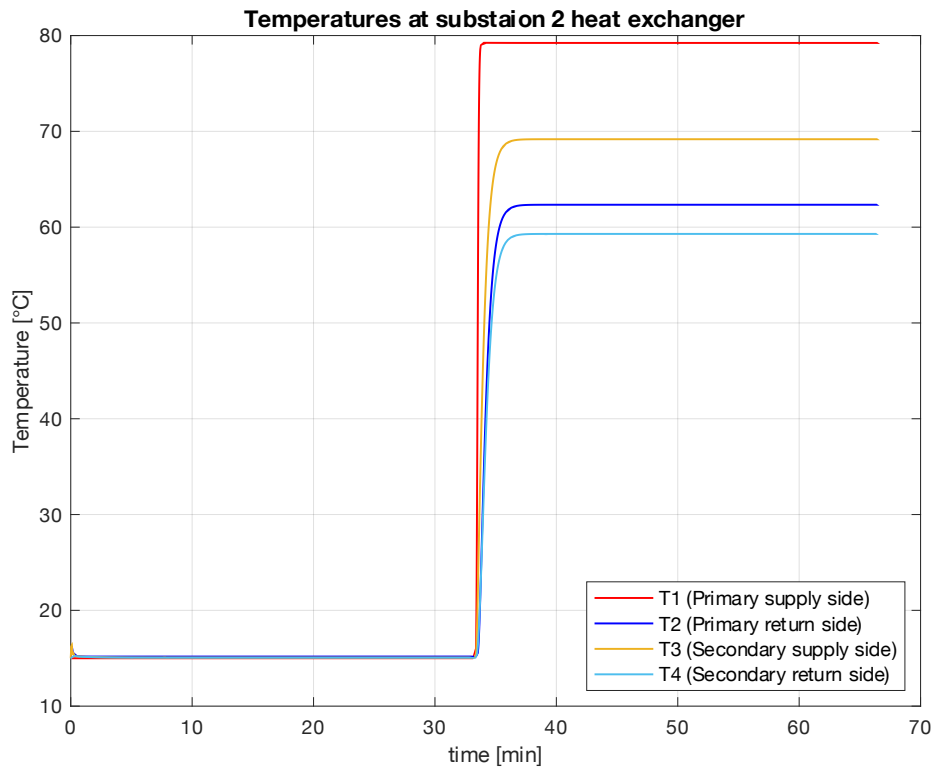


Figure 4-12 SIM 2 - Temperatures at 4 sides of substation 2 HEX

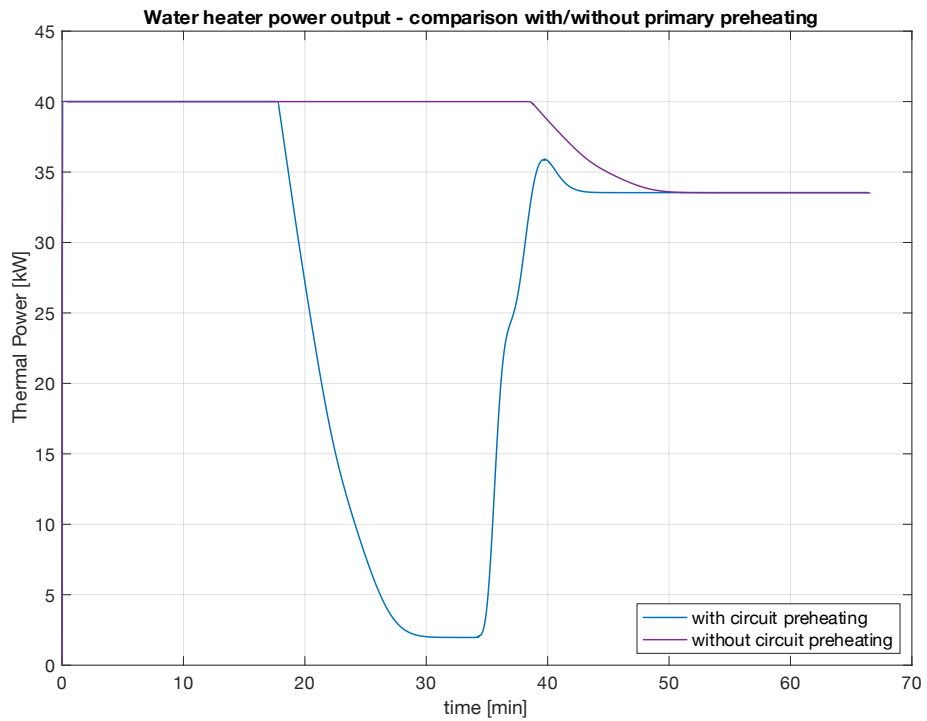


Figure 4-11 SIM 1 - 2 - Water heater power output comparison

In Figures 4-10 and 4-9, the readings from the temperature sensors on the return side of the primary circuits are shown. As expected, the delayed opening of the valves feeding hot water from the primary circuit to the substation has a noticeable effect on the readings. As soon as the valves are opened, a mass flow of cold water starts flowing from the substation branch into the return side of the primary which until this moment was recirculating hot water. At node D only water from substation 2 is flowing and the temperature drops briefly under 55°C . At node B the temperature drop is mitigated because, when valves are opened, there is still a volume of hot water between node B and D, that mixes with cold water coming from substation 1. In the next section, a different layout for the primary circuit is proposed to investigate further this effect.

In Figure 4-12 the temperatures at the 4 sides of the HEX of substation 2 are presented. Differently from simulation 1, in this case, the temperatures are constant at the $T_{\text{start}}=15^{\circ}\text{C}$, because the primary circuit is not supplying the substations with hot water. As soon as the valves are opened, the temperatures are set at the same values as in the previous simulation.

The effect of primary preheating is also clearly visible in Fig. 4-11, where the power output of the water heater in the two cases is compared. During SIM 2, where preheating is applied, the WH output quickly drops under 5 kW as soon as the $T_{\text{setpoint}}=80^{\circ}\text{C}$ is reached, whereas in SIM1 the output remains constant at maximum power of 40kW until the system reaches its normal operation after a long transient.

4.2.3. Simulation 2B and 2C: different primary supply temperatures

In simulations 2B and 2C the same system configuration from simulation 2 was tested, changing the temperature set-point of the water heater and, in turn, the power output at the two air heaters. Just like in the previous simulation, the system underwent a preheating phase until the T_{setpoint} of the water heater was reached. As in the previous scenario, the parameters for the heat exchangers and air heater were set according to the cases studied in sections 3-4-1 and 3-4-2. In the following table (4-4), a list of the most important parameters is presented.

Table 4-4 SIM 2, 2B, 2C parameters

Simulation	2	2-B	2-C
Simulation length	4000 sec	4000 sec	4000 sec
Preheating	2000 sec	2000 sec	2000 sec
T_{start}	15 °C	15 °C	15 °C
$T_{\text{setpoint,water-heater}}$	80 °C	70 °C	90 °C
\dot{m}_{primary}	0.45 kg/s	0.37 kg/s	0.58 kg/s
$\dot{m}_{\text{secondary}}$	0.384 kg/s	0.309 kg/s	0.458
$Q_{\text{air-heater}}$	16.06 kW	12.93 kW	19.18 kW

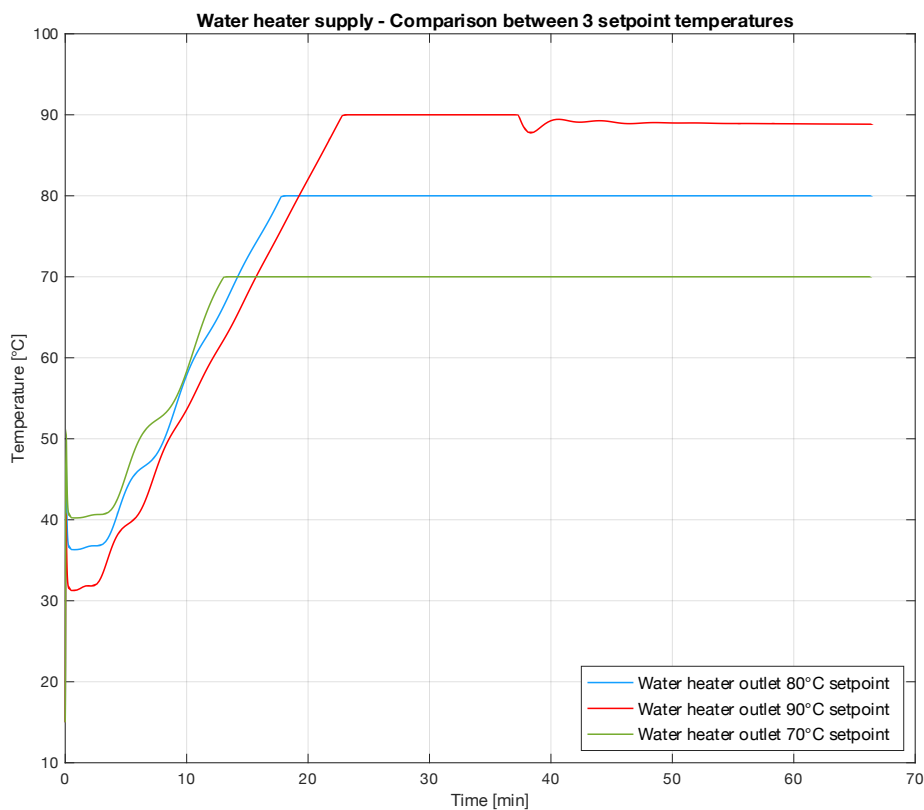


Figure 4-13 SIM 2, 2B, 2C - primary circuit supply temperature comparison

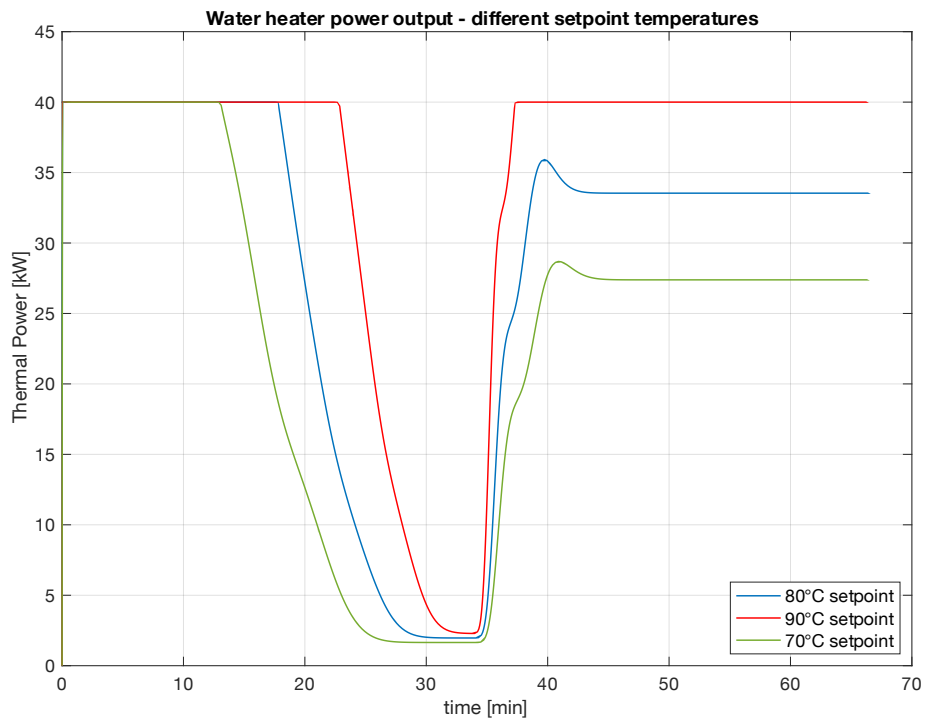


Figure 4-15 SIM 2, 2B, 2C - water heater power output comparison

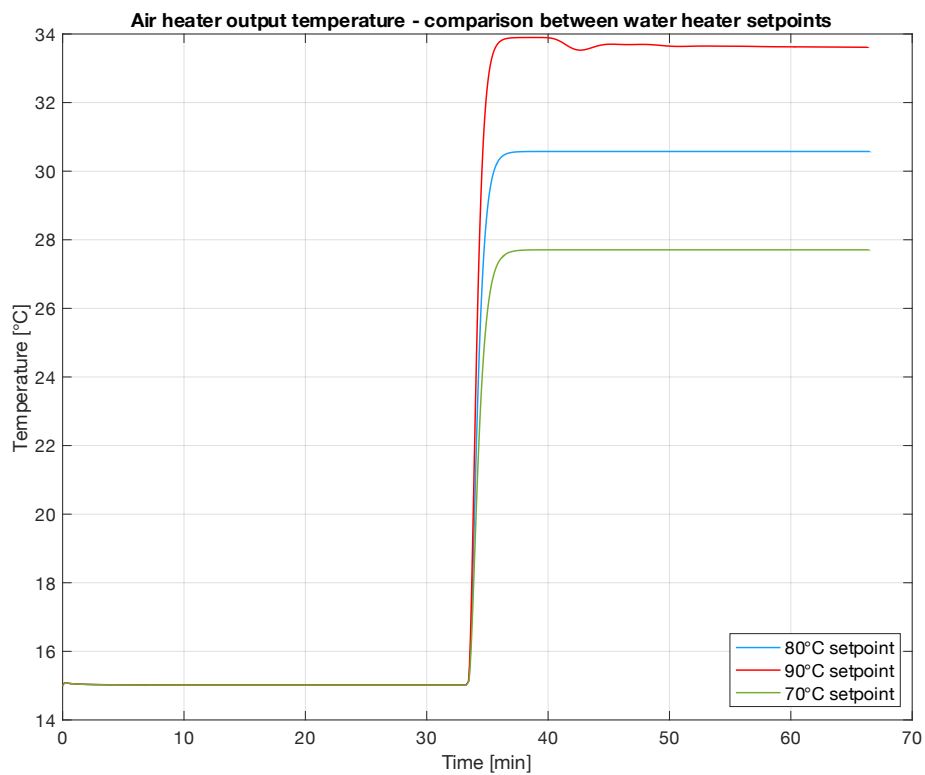


Figure 4-14 SIM 2, 2B, 2C Air heater output temperature comparison

These 3 simulations enabled the analysis of the model when configured with different supply temperatures at the primary circuit. In Fig. 4-13 the supply temperatures at the water heater outlet are compared. Predictably, in the simulation configured with the lowest supply setpoint of $T_{\text{setpoint}}=70^{\circ}\text{C}$, the target temperature is reached in about 14 minutes while in the one configured with the highest setpoint $T_{\text{setpoint}}=90^{\circ}\text{C}$, more than 23 minutes were required. This effect is not only due to the lower target temperature but also to a lower mass flow rate at the primary circuit, according to table 4-3.

As can be noticed in Fig. 4-13, in the case with a $T_{\text{setpoint}}=90^{\circ}\text{C}$, the supply temperature at the WH outlet showed a rippling effect as soon as the two substations were connected to the primary circuit, right after the preheating phase. This effect proves that the water heater cannot support properly the system in this configuration, as the increased power output at the air heaters provokes a higher decrease in temperature on the return circuit. This condition is attributable to the increased ΔT at its ends and the higher mass flow rate, compared to the other two setpoint temperatures. This behaviour is also confirmed by looking at the power output of the water heater shown in Fig. 4-15, as, after lowering once preheating is completed, it resumes full power, trying to reach the setpoint temperature.

This power deficiency is in turn transferred at the air heater's output air temperature, as in Fig. 4-14, where the corresponding line shows the same pattern noticed in Fig. 4-13. The air heaters, according to data calculated in the previous sections, are supposed to provide more than 19 kW of thermal power each. Their power draw, combined with thermal losses in the other parts of the system such as in the piping, are likely exceeding the maximum power of the WH, at 40 kW, generating this anomaly in the performance curves.

4.3. Model 2: basic system layout - enhanced primary circuit modelling

Model 2 enhances the modelling of the primary circuit of Model 1 by including all the thermocouples placed in the real system. As briefly anticipated during the description of the system in Chapter 2, along the primary circuit are placed 20 thermocouples, inserted in thermowells installed in the pipes. They are evenly distributed between the supply and return sides of the primary circuit, 10 on each side. They are installed in couples, detecting the temperature at the same spatial position, and reading the return and supply side temperature respectively.

These thermal sensors were placed in the real system to detect the temperature along the primary circuit, enabling the study of the propagation of a hot or cold front during possible transients generated by shifts in the system configuration, such as opening or closing a branch directed to a substation. In addition, they can be used to calculate the thermal dispersion of the pipework, by comparing temperatures in different parts of the circuit. However, as noticed in previous simulations, this thermal loss is limited, therefore the readings from these sensors should replicate the same curve only shifted in time due to the delay of the front in reaching the farthest thermocouples.

In Model 1, only two pipe components were needed for each side of the primary circuit. By looking at the model 1 overview, in Fig. 3-2, the first one ranges from the water heater to the first junction towards substation 1, while the second completes the circuit by ranging from the aforementioned junction until the second one towards substation 2. In model 1 temperature is only detected at the junctions, as real thermocouples are not considered. To accommodate the additional thermal sensors along the circuit, the two pipes were subdivided into smaller segments, so that a thermal sensor could be inserted in between at the right spot, according to CAD measures. Due to the component's design, it is not possible, indeed, to insert a sensor along its length, but only at its ends. The location and numbering of these sensors are better explained in Fig. 4-16, where a view of the primary circuit from above is presented.

However, despite replicating the same configuration seen in the previous ones, the simulations of this model reported some noteworthy results, especially showing the effect of the pipes' discretization level and helping the analysis of temperature readings on the return side. These results are shown in the following sections

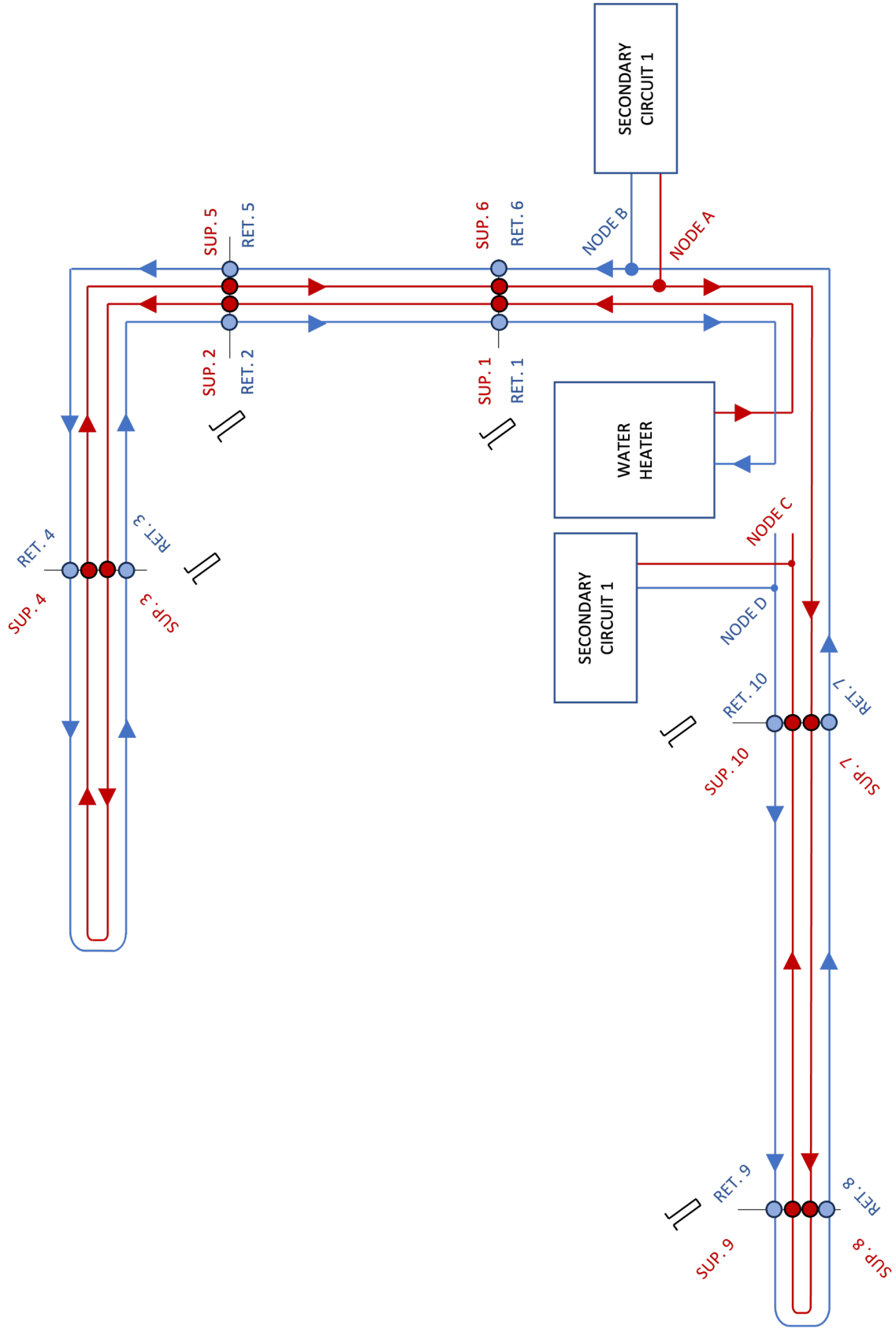


Figure 4-16 Thermocouples placement along primary circuit

4.3.1. Simulation 3, 3B: the effect of pipes' discretization level

Simulation 3 proposes again the configuration from simulation 2, with the primary circuit operating first isolated from the substations to preheat the fluid carrier and then opening the branches toward the substations after about 30 minutes.

As explained before, model 2 features multiple pipe segments instead of just two per side on the primary to accommodate the additional thermocouples. During the first simulation of this model, SIM 3, the level of discretization of the pipes was left at the default value, 10. As anticipated in section 3-3, this value sets the number of finite volumes in which the pipe is divided during the simulation to better represent the behaviour of the fluid during transients. Therefore, as the total number of pipe segments was increased in Model 2 with respect to Model 1, with equal discretization value, the total number of nSeg was much higher.

This not only slowed the compilation and simulation process of Model 2 but altered the results, showing an unexpected oscillatory behaviour in the temperature readings. To control this effect, a simulation with a lower number of nSeg was run, reporting more comparable results to the previous simulations.

In table 4-5, the SIM parameters are summarized.

Table 4-5 SIM 3, 3B parameters

Simulation	3	3-B
Simulation length	4000 sec	4000 sec
Preheating	2000 sec	2000 sec
T_{start}	15 °C	15 °C
$T_{setpoint,water-heater}$	80 °C	80 °C
$\dot{m}_{primary}$	0.45 kg/s	0.45 kg/s
$\dot{m}_{secondary}$	0.384 kg/s	0.384 kg/s
$Q_{air-heater}$	16.07 kW	16.07 kW
nSeg (each pipe component)	10 (default)	2

In Fig. 4-17 and 4-18, the readings of the thermocouples on the return side of the primary circuit are shown, while in Fig. 4-19 and 4-20 the ones from the supply side are shown. The impact of pipe discretization is clear. In SIM 3, the default number of nSeg coupled with the increased number of pipe components produce an unstable output on the temperature readings. On the other hand, in SIM 3B the discretization level was reduced at two nSeg per pipe, as the increased number of components is already sufficient to effectively model the behaviour of the pipework. However, a comparison with data from the real thermocouple should be done to assess which level of discretization is best to describe the transient states in piping.

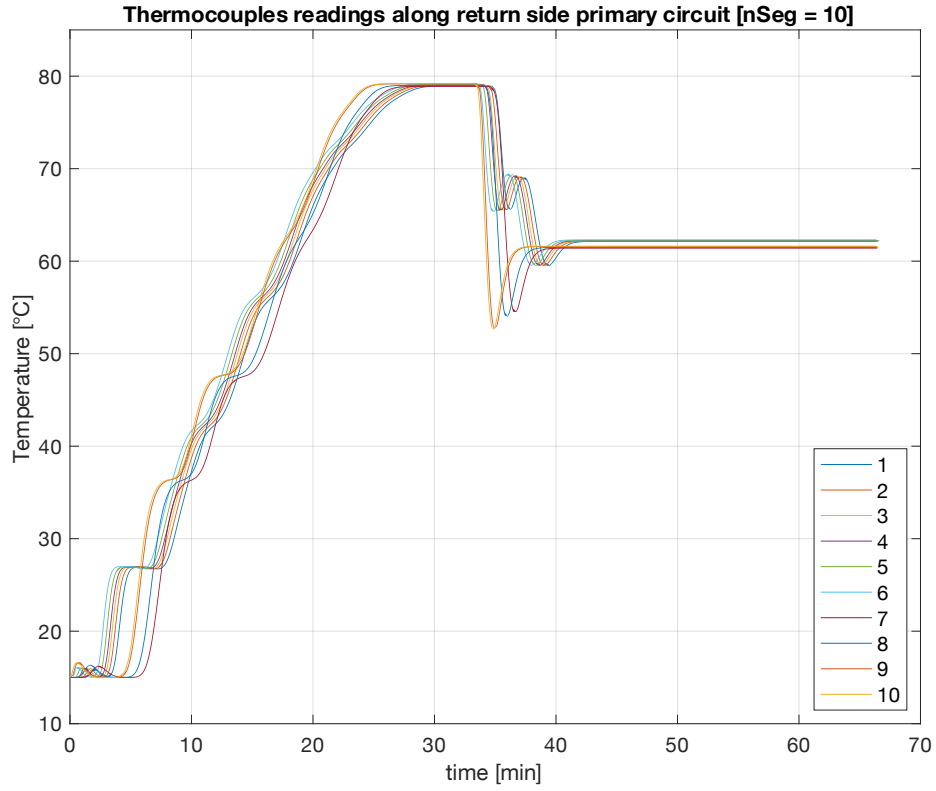


Figure 4-17 SIM 3 - Temperatures along return side primary circuit [nSeg = 10]

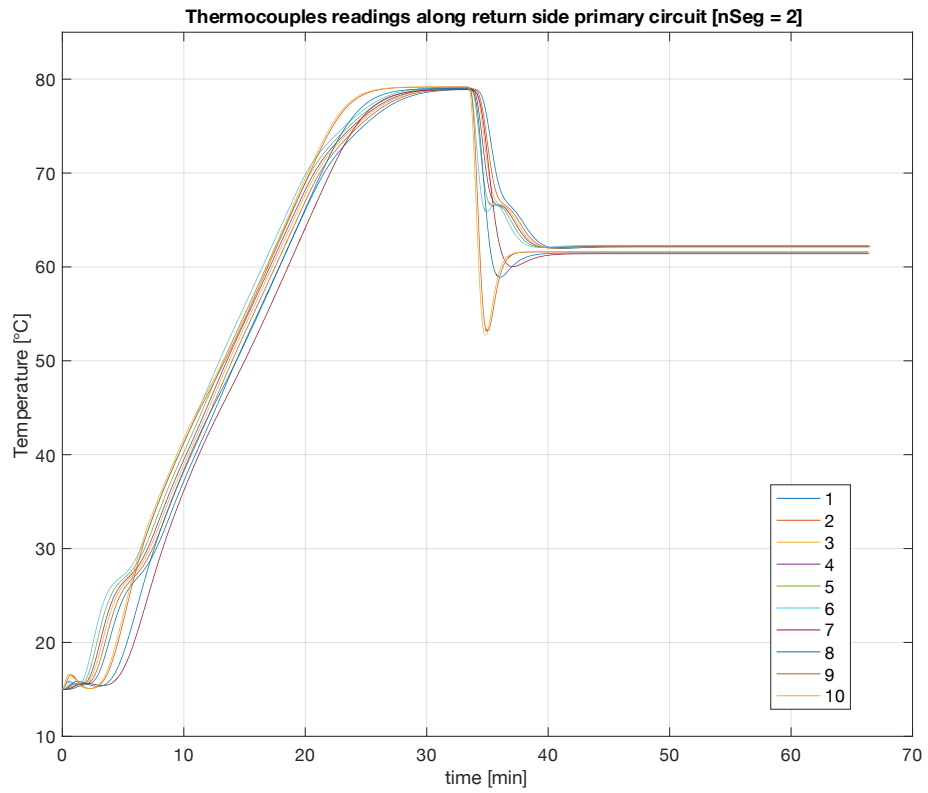


Figure 4-18 SIM 3B - Temperatures along return side primary circuit [nSeg = 2]

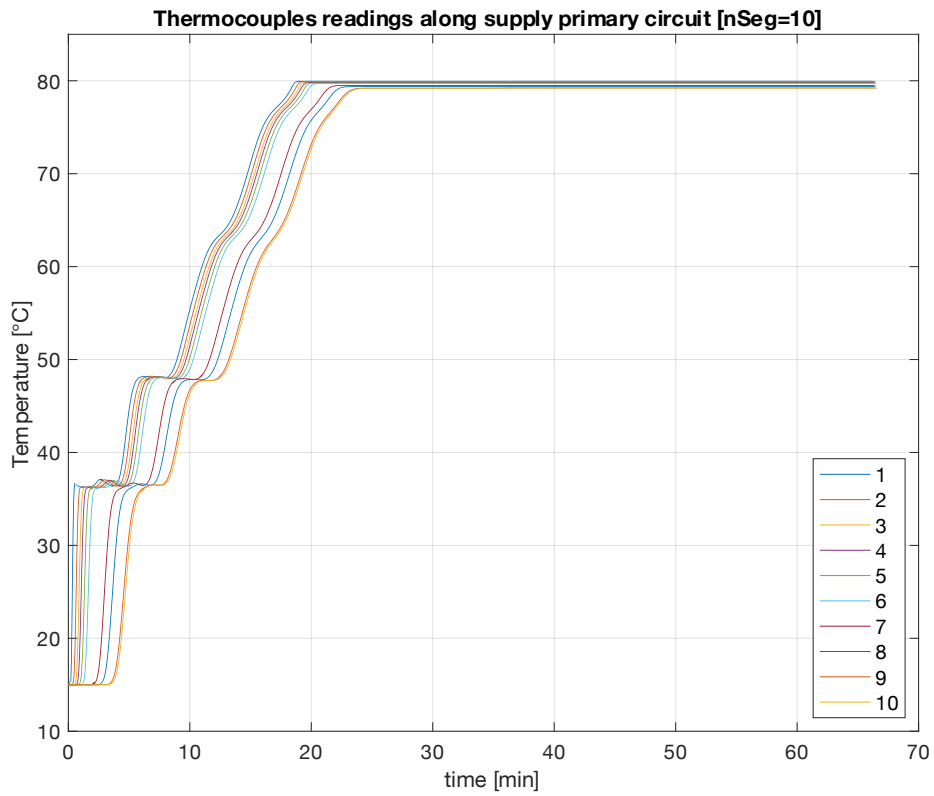


Figure 4-19 SIM 3 - Temperatures along supply side primary circuit [nSeg = 10]

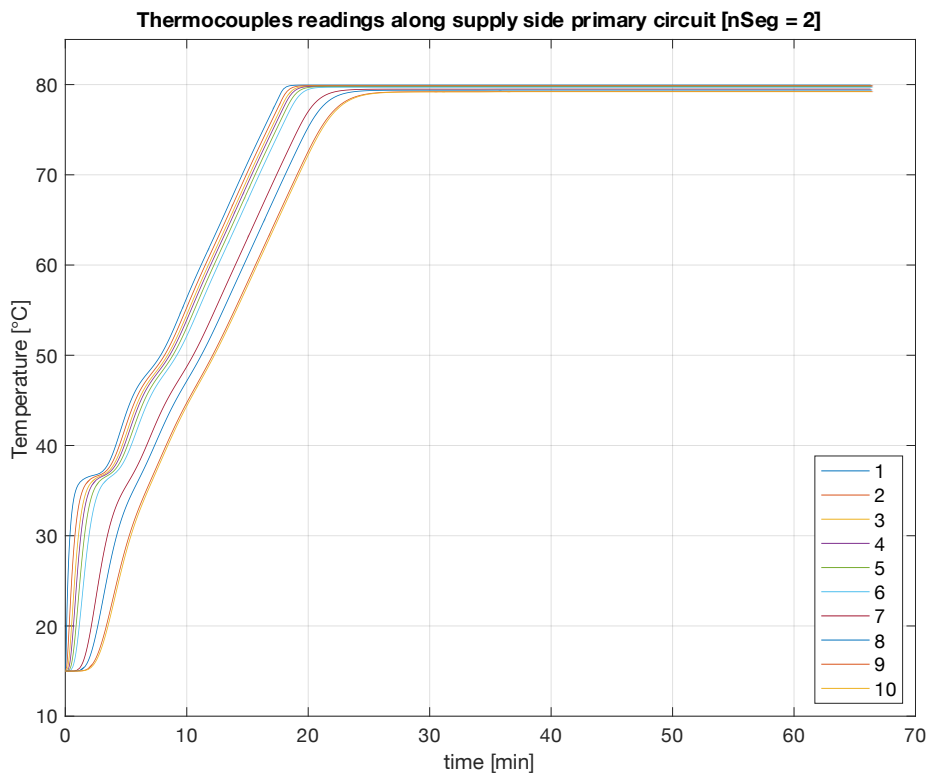


Figure 4-20 SIM 3B - Temperatures along supply side primary circuit [nSeg = 2]

4.3.2. Simulation 4: investigating temperatures on the return side

As anticipated discussing the results of SIM 2, a further analysis of the particular behaviour of temperature readings from the return side of the primary circuit was done in simulation 4. By looking at fig. 4-18 as well as Fig. 4-9 and 4-10 from the previous section, a different trend of temperature is detected from the two nodes. As explained before, this behaviour is supposedly coming from the difference in mass flow rates and temperatures in those two parts of the system. The thermocouples further from the water heater, namely thermocouples no. 7, 8, 9 and 10 in fig. 4-18, show a higher drop in temperature when the substations are connected to the primary circuit. This is due to a lower mass flow rate flowing in that part of the primary circuit, compared to the part in which are placed the other thermocouples.

In particular, the aforementioned thermocouples measure the temperature of the cold mass flow rate coming from substation 2 only, while the other ones, namely from no. 1 to 7, measure the temperature of both the mass flow rates from substation 1 and 2. In addition, as soon as the substations' valves are opened, the drop in temperature that should be expected downstream the junction of substation 1 is mitigated by a segment of hot water that is still present in that instant between node that junction and the one of substation 2. In this way, despite both substations sending back to the primary circuit water at the same temperature, in the two parts of the return side, this temperature difference is noticed.

However, at first glance, that drop in temperature could be an indicator of numerical instability. For this reason, an alternative setup for the primary circuit was tested in SIM 4, where the mass flow rate in the primary circuit is increased from 0.45 kg/s to 1 kg/s and a bypass valve connecting the supply and return side of the primary circuit is introduced. In the following scheme, the additional valve is highlighted with a dashed line.

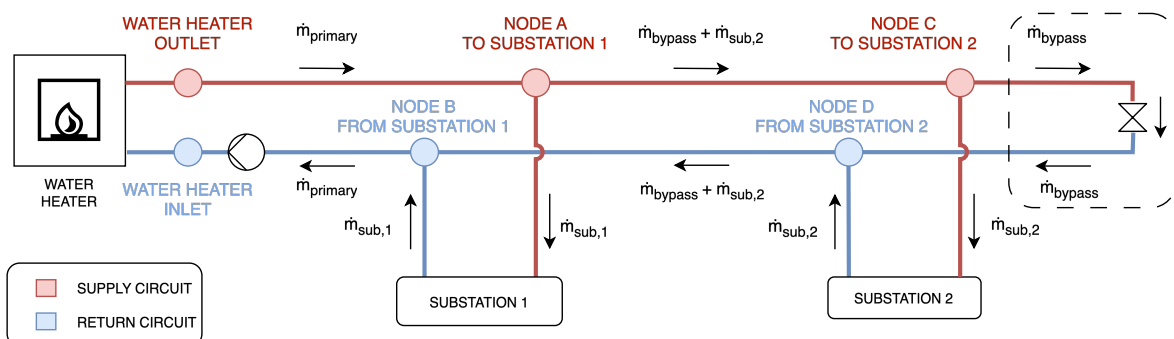


Figure 4-21 Alternative primary layout with additional bypass valve

Table 4-6 SIM 4 parameters

Simulation	4
Simulation length	4000 sec
Preheating	2000 sec
T_{start}	15 °C
$T_{\text{setpoint,water-heater}}$	80 °C
\dot{m}_{primary}	1 kg/s
$\dot{m}_{\text{secondary}}$	0.384 kg/s
$Q_{\text{air-heater}}$	16.08 kW

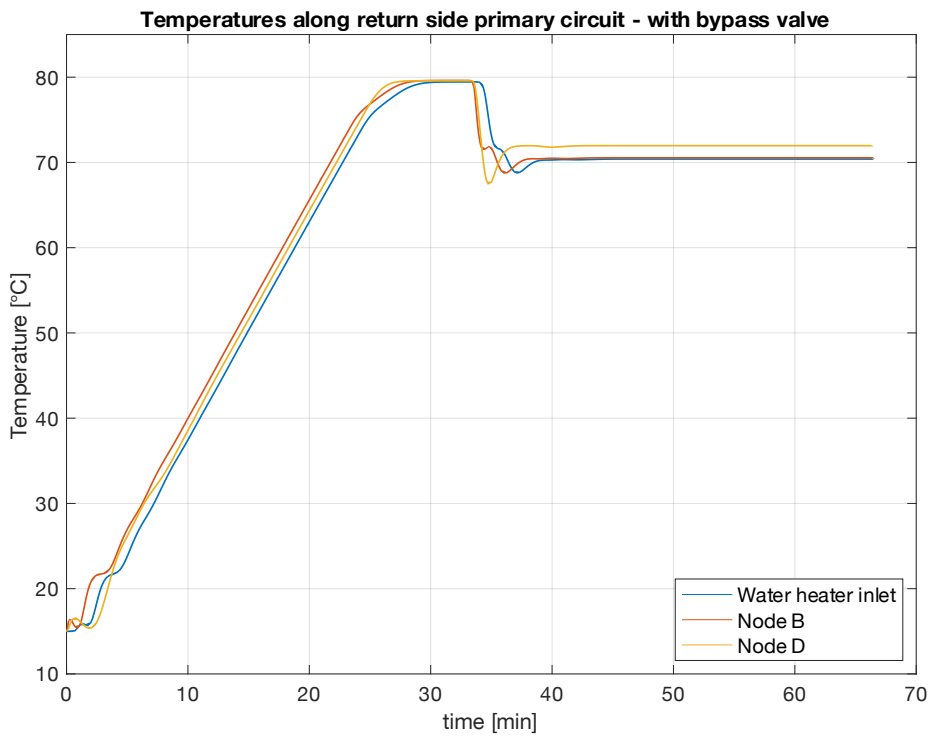


Figure 4-22 SIM 4 - temperatures along primary circuit return side with modified primary configuration

Fig. 4-22 shows the temperatures detected on the return side of the primary circuit with this new configuration. Comparing it with Fig. 4-9 and 4-10 from previous simulations, the drop in temperature detected at node D is noticeably contained, as an additional flow of hot water is being recirculated with the bypass valve connecting the return and supply side of the primary. At node B the detected temperature is slightly lower as the cold water from substation 1 enters the primary circuit.

4.4. Model 3: sensible thermal energy storage study

This section is dedicated to the study of the performance of the sensible thermal storage, which is included in the secondary circuit supported by substation 2. To accomplish the task, a purpose-built model was created containing only the TES and an ideal cooler component to allow its discharge. In this way, it was possible to analyse the performance of the component limiting the influence of other variables and lowering the complexity of the configuration.

In the first place, a simulation was done to assess the impact of the discretization level of the TES component on the results, similarly to what has been done with pipes in the previous section. Afterwards, the focus shifted to the analysis of the available experimental data, gathered during a discharge test on the TES installed in the system. In this simulation, the model was initialized in such a fashion trying to recreate the conditions present during the experimental test.

4.4.1. *Simulation 5: comparing with experimental data*

This part of the study is the only one that relies on data gathered during an actual operation of the system. This experiment was not performed during the course of this project, as it took place before the TES was even placed in the EC laboratory. The test was conducted in a different location, where the TES was connected to an air heater and discharged through its top outlet with a constant mass flow rate, to assess the quantity of energy supplied for 2 hours. The air heater maintained an almost constant power draw, generating an average $\Delta T=10^{\circ}\text{C}$ drop on the water side. Before beginning the discharge cycle, the TES was supposedly charged to a $T_{\text{start}}=80^{\circ}\text{C}$ by a natural gas water heater. However, by analysing the data gathered, the TES proved not to be fully charged, with readings from the thermocouples ranging between 76°C and 74.5°C . This flawed partially the trustworthiness of the test, as it was not conducted with controlled initial conditions.

For this reason, setting up the digital model in order to replicate this test turned out to be difficult, requiring a one-by-one initialization of the 70 nSeg of which the TES component is made of. The initialization consisted of assigning an initial temperature value to each one of them, trying to replicate the temperature distribution at the beginning of the discharge test, as described by the experimental data.

Model 3 was set up according to the description of the experimental test, by connecting the TES to an ideal cooler set at the same average power drawn by the air heater of the real test, $P_{\text{cooler}}=20.8 \text{ kW}$, maintaining the same average temperature drop and the same mass flow rate as the experimental ones. In the following table (4-7), a summary of simulation 5 parameters is available.

Table 4-7 SIM 5 parameters

Simulation	5
Simulation length	120 min
T_{top}	76 °C
T_{middle}	76 °C
T_{bottom}	74.5 °C
\dot{m}	0.473 kg/s
$Q_{dissipated}$ (average)	20.8 kW

Fig. 4-23 shows the trend of the temperature detected at the TES supply and return comparing with the results of the simulation, while Fig. 4-25 and 4-24 report the temperature detected by the thermocouples placed on the side of the vessel, as in the experiment or the simulation respectively. While difficult, due to the incomplete charging of the TES and due to a poor resolution of experimental data (temperatures were collected every 15 minutes, with 0.5 °C sensitivity), it is still possible to notice the stratification effect, as water in the highest level remains constant.

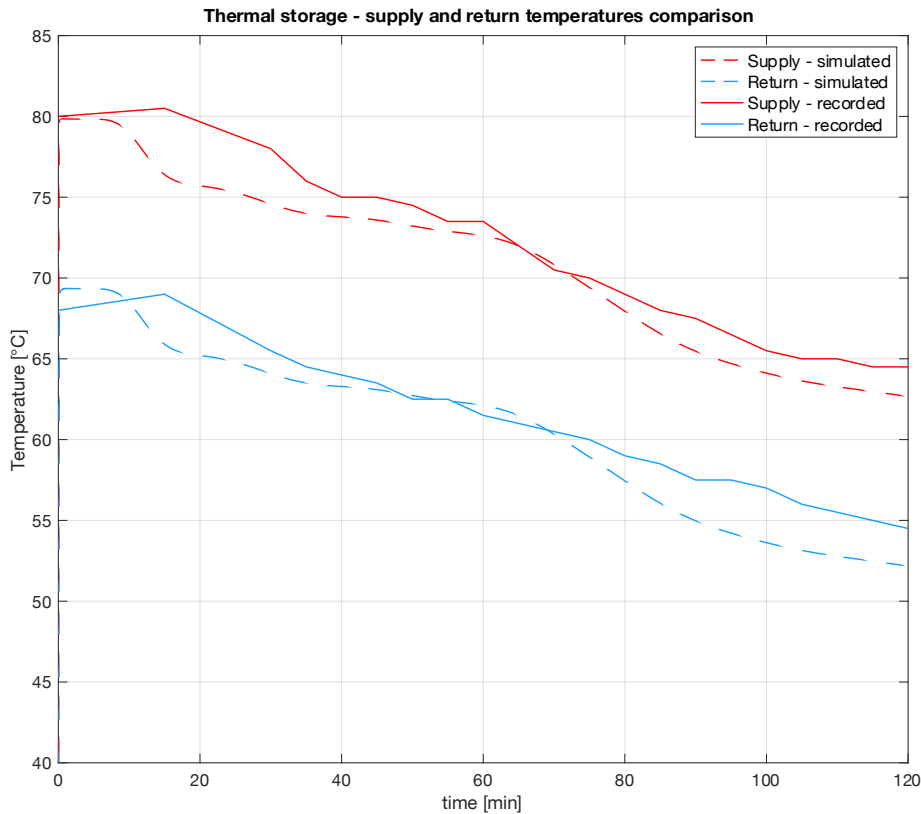


Figure 4-23 SIM 5 – TES supply and return temperature – comparison with experimental data

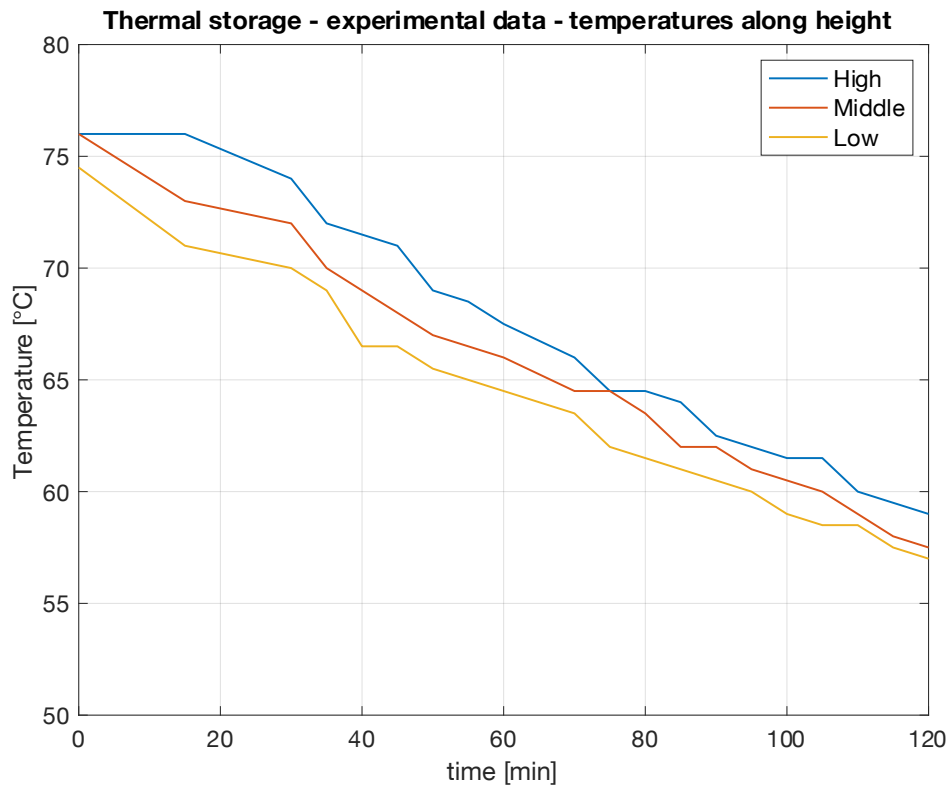


Figure 4-25 TES experimental test - temperature evolution along height

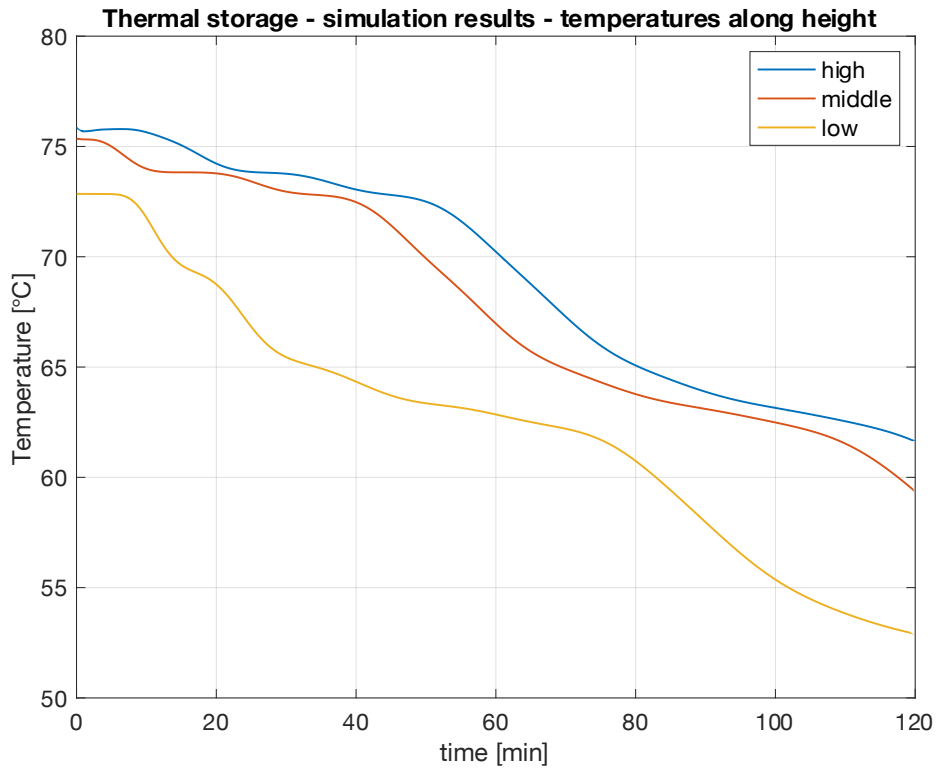


Figure 4-24 SIM 5 - temperature evolution along height

Comparing Fig. 4-24 and 4-25, a different behaviour on the temperature trends is noticeable. In particular, the temperatures detected during simulation express more clearly the stratification effect present in the TES, while the thermocouples' output from the real experiment show a different condition. First of all, they report a similar trend for the entire duration of the test, proving that the water in the vessel is mixing rapidly in between the layers. This is especially noticeable when comparing the trend of the lowest-level thermocouple between the simulated and real case. As it is placed closer to the bottom inlet, where colder water is returning from the air heater, it is supposed to detect the temperature decrease before the other two, which are placed closer together in the upper part of the vessel. This trend is clearer in the simulation output rather than in the experimental data and it is probably due to a wrong measurement of the thermocouple placement or to an overestimated stratification effect and an underestimated mixing effect in the simulated model.

In conclusion, recalling the uncertainties present in the experimental data and the following difficult initialization of the model, these differences are expected, while Fig. 4.23 still proves a good approximation of the real data by the simulation.

4.4.2. *Simulation 6: the effect of discretization level of the TES*

Like what was experienced in simulating model 2, where a high number of pipes connected in series showed the importance of choosing the right discretization level, special care to the selection of nSeg for the TES was dedicated in this section. The number of segments defines the level of discretization with which the model is simulated. During simulation, the vessel is subdivided into a number of volumes, which take into account both the buoyancy effect of differently dense water, which in turn generates the stratification along the height of the TES, and the heat transfer, due to mass flow rate and heat conduction between adjacent layers.

For this reason, the TES was modelled, repeating the same configuration from the previous simulation, testing different numbers of discretization (nSeg). As in the previous simulation, the vessel was connected to a cooler providing a constant $\Delta T=10^{\circ}\text{C}$ drop on the return. Water flows from the uppermost level into the air heater with the help of a circulation pump and re-enters the TES via the bottom inlet. Unlike SIM 5, the same value of temperature was set during initialization for all the layers, representing a fully charged TES. The comparison and a graphical explanation of the model behaviour are available in the following images, while the following table (4-8) reports the summary of SIM 6 parameters.

In Figure 4-26 the numbering of the layers is shown, with the uppermost layer called 1 and the bottom one corresponding to the value of nSeg set. For example, in the case of nSeg = 70, the lowermost layer will be referred to as 70.

In Figures 4-27 and 4-28, the temperatures recorded in the less discretized case ($nSeg = 4$) and the most discretized one ($nSeg = 70$) are shown.

Table 4-8 SIM 6 parameters

Simulation	6
Simulation length	240 min
Tstart	80 °C
\dot{m}	0.473 kg/s
Qcooler	20.8 kW

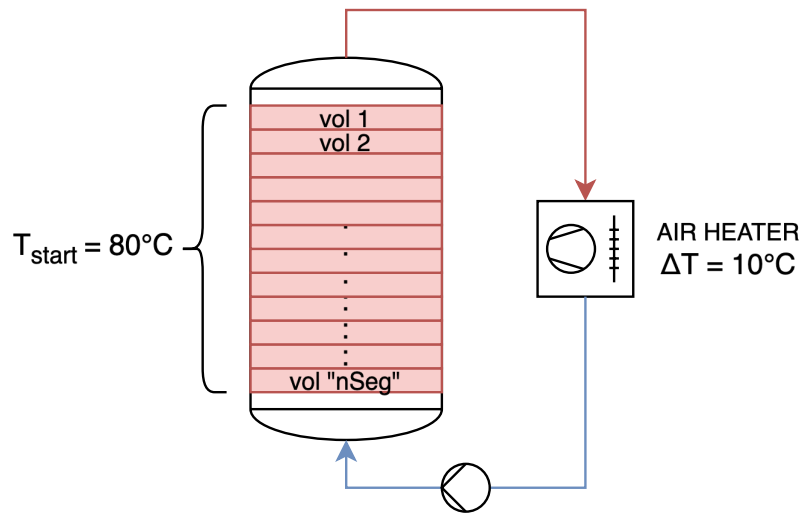


Figure 4-27 TES model configuration

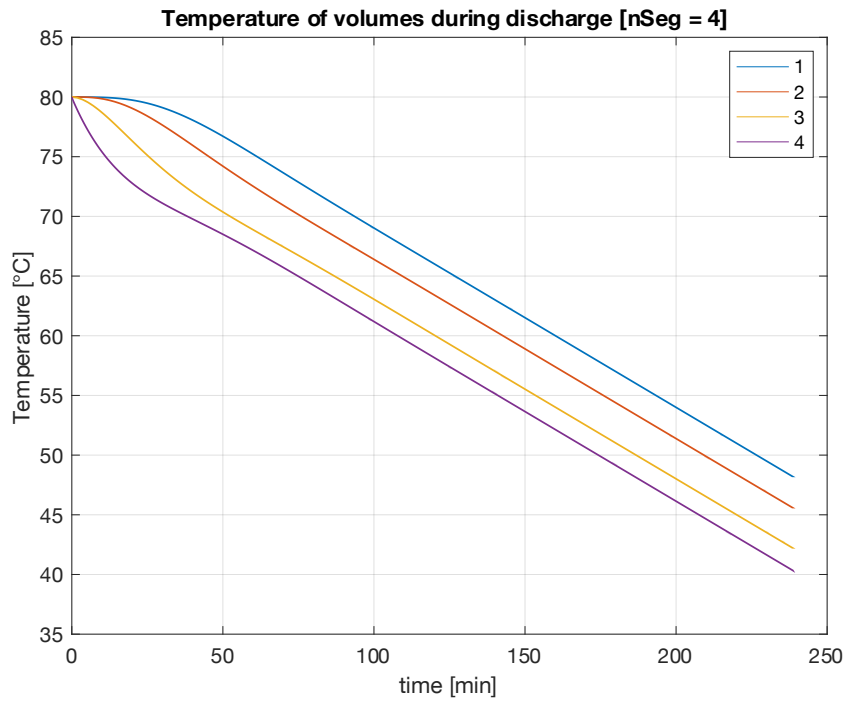


Figure 4-26 SIM 6 - temperature evolution along height [nSeg = 4]

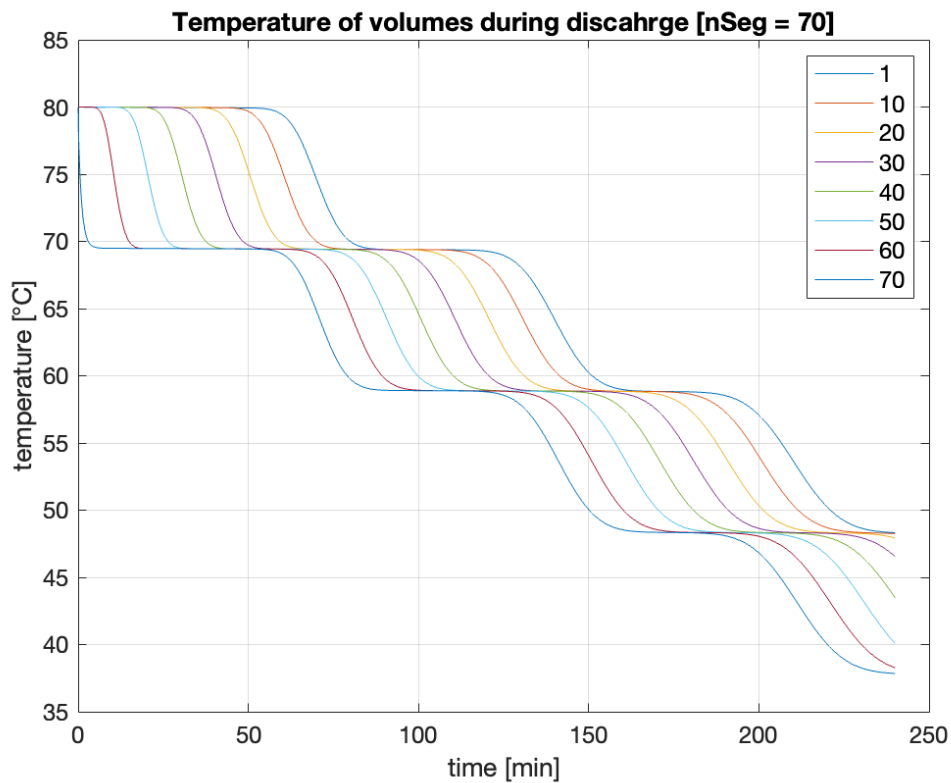


Figure 4-28 SIM 6 - temperature evolution along height [nSeg = 70]

By looking at fig. 4-27 and 4-28 the difference in the behaviour of the TES is very clear. In the less discretized case, where only 4 volumes are used during simulation, the temperature gradually decreases at the same time and rate in all the layers, with minimal differences noticeable especially comparing the uppermost and lowermost layers at the beginning of the simulation. The model still shows the stratification effects, as the temperature difference at the top and bottom is constant throughout the duration of the test. In this configuration, each layer contains a higher volume of water compared to the case with higher discretization. As cold water enters from the bottom, it mixes with a higher volume of hot water still present, making the temperature of the layer itself decrease less rapidly, if compared to a layer containing less water. In addition, the lower number of layers, makes the heat conduction in between them more present, with the highest one detecting a decrease in temperature more quickly than the other case.

The configuration with the maximum level of discretization reports a very different behaviour. The temperature of the lowest layer instantly drops at the value of return temperature, which, at the beginning of the test is 70°C. The top layer is not influenced by the cold water entering from the bottom, as it displays a steady temperature equal to the initial value of 80°C. As the test proceeds, colder water reaches higher and higher layers, eventually reaching the top one, which starts registering a decrease in temperature only after more than 50 minutes. Due to the high level of discretization, each layer covers a smaller volume, so it reacts instantly

as colder water enters it. At the same time, the higher number of layers makes the effect of heat conduction propagate more slowly along the height of the TES, compared to the less discretized case.

This behaviour is generated by the ideal stratification effect that is being simulated in the TES model, due to the high discretization. In real operation, the mixing between the layers should play a more important role, limiting the stratification effect and resulting in less harmonic behaviour. In addition, the oscillatory effect that can be seen in Fig. 4-28 is from the fact that water is re-entering the vessel with a constant temperature drop of 10°C generated by the cooler. As the supply temperature is kept constant, so is the return temperature, generating these periods in the output signal. A graphical explanation of this effect is available in the following picture, fig. 4-29.

In conclusion, the modelling of the TES proved to be challenging, both because of the lack of documentation about the component and the scarce experimental data available. On one hand, a lower discretization level seems to increase the mixing effect in the vessel while limiting the modelling of the stratification effect. On the other, a higher discretization level overestimates the effect of stratification, reporting an ideal behaviour that is unlikely found in real operations. As anticipated in section 3-3, the component features a parameter, “*tau*” that is supposed to modify the mixing effect between the layers, but, at the time of writing, it has not been already implemented. Additional practical tests should be carried out with a higher level of accuracy, to support a more precise and reliable modelling of the TES.

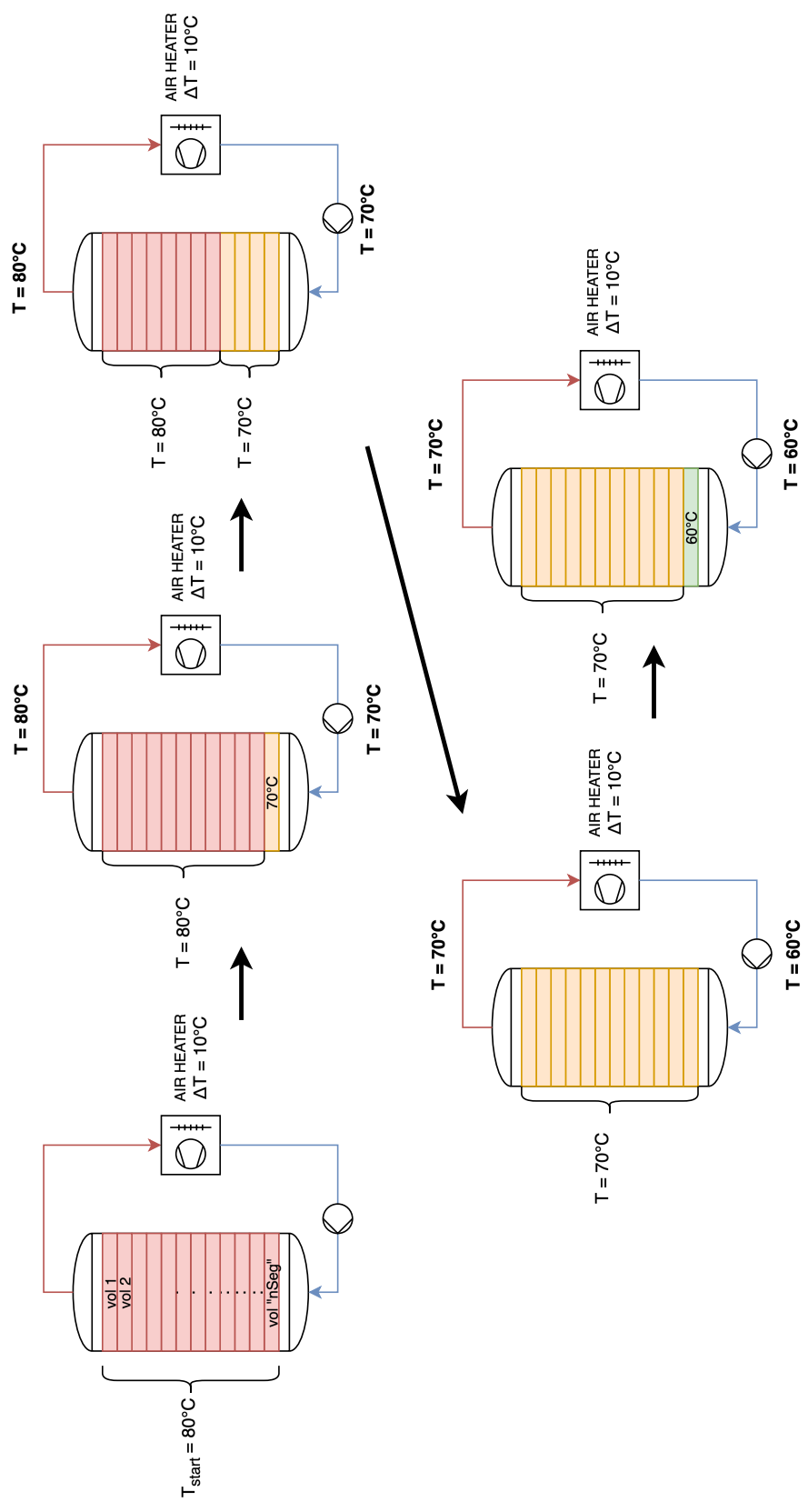


Figure 4-29 SIM 6 - TES behaviour

4.5. Model 4: the complete model

4.5.1. Simulation 7

Simulation 7 is the last simulation that is reported in this chapter. It was the test bench for Model 4, which benefits from the results obtained in the previous tests, assembling all the components into a complete system layout. A longer simulation was run, both to test the stability of the suite when dealing with longer runtimes and to allow enough time to model a charge and a discharge cycle for the TES.

As the TES is present in the secondary circuit 2, a different scenario was considered. Just like in the scenarios tested from SIM 2 up to SIM 4, the system undergoes an initial preheating phase of about 30 minutes in which the primary network reaches the supply set point. Then, the regulation valve of substation 2 is opened and the TES is charged for about 3 hours with a lower mass flow rate than the one used in normal operating conditions. During this phase, hot water supplied by the substations enters the vessel from the top inlet, while cold water is circulated back at the substation from the bottom outlet. The vessel has an initial temperature of 40°C, to simulate a partially discharged TES. After the charging phase, the substation is excluded from the secondary circuit and the discharging phase begins. In this period, hot water from the charged TES leaves from the top port towards the air heater, substituting the substation. As thermal power is dissipated by the air heater, cold water is recirculated back at the TES, entering from the bottom port. In this way the stratification effect is better exploited.

At the same time, substation 1 is activated and start operating normally, supplying hot water to the air heater. Substation 1 is supplied with hot water by the primary network, as usual. In this way, activating both air heaters at the same time, a comparison between the temperature of air at the outlet could be done.

In table 4-9 a summary of SIM 7 parameters is available.

Table 4-9 SIM 7 parameters

Simulation	7
Simulation length	20.800 sec (5h 45m approx.)
$T_{TES,START}$	40 °C
$\dot{m}_{TES-CHARGE}$	0.200 kg/s
$\dot{m}_{TES-DISCHARGE}$	0.384 kg/s
$\dot{m}_{PRIMARY}$	0.45 kg/s
$\dot{m}_{SECONDARY\ CIRCUIT\ 1}$	0.384 kg/s
$T_{setpoint,WH}$	80 °C

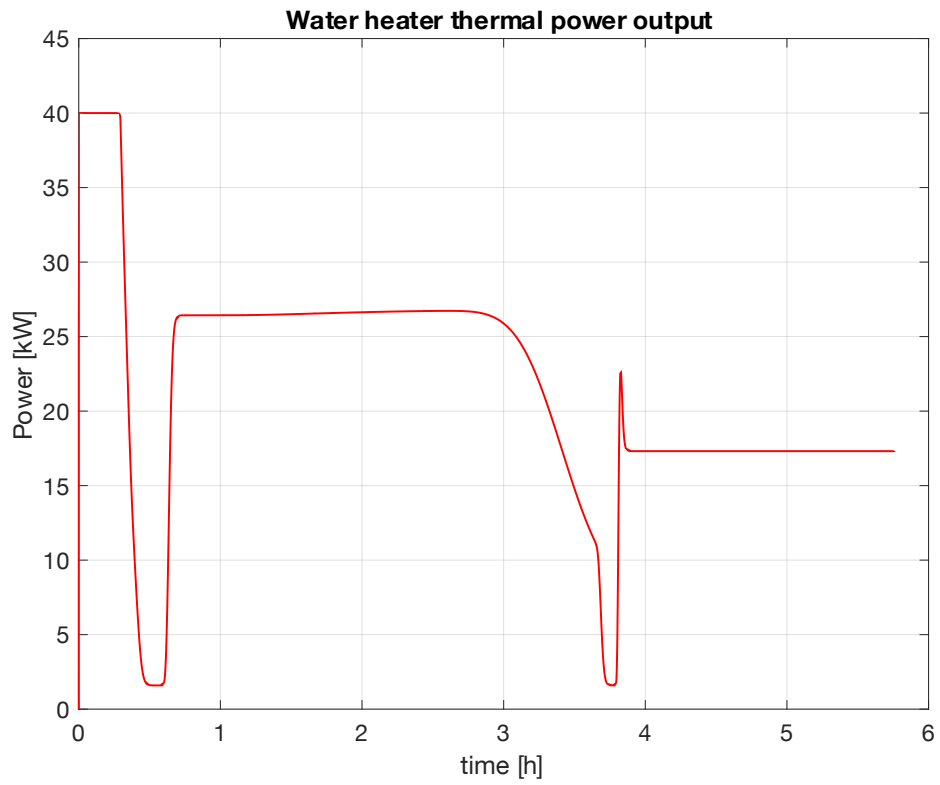


Figure 4-31 SIM 7 - Water heater power output

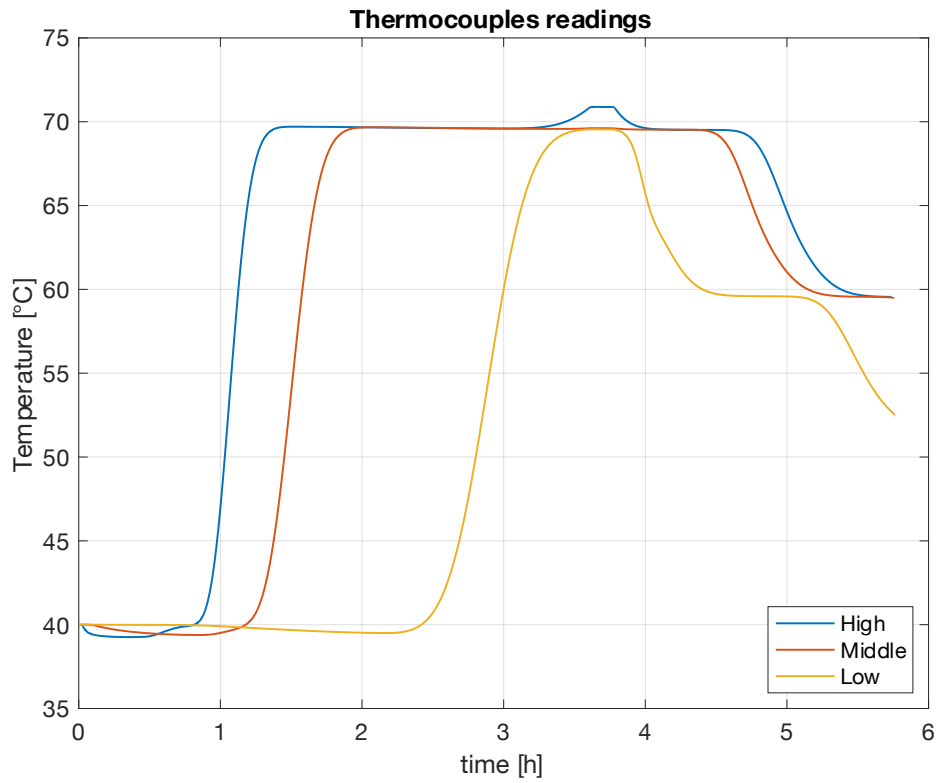


Figure 4-30 SIM 7 - TES thermocouples reading

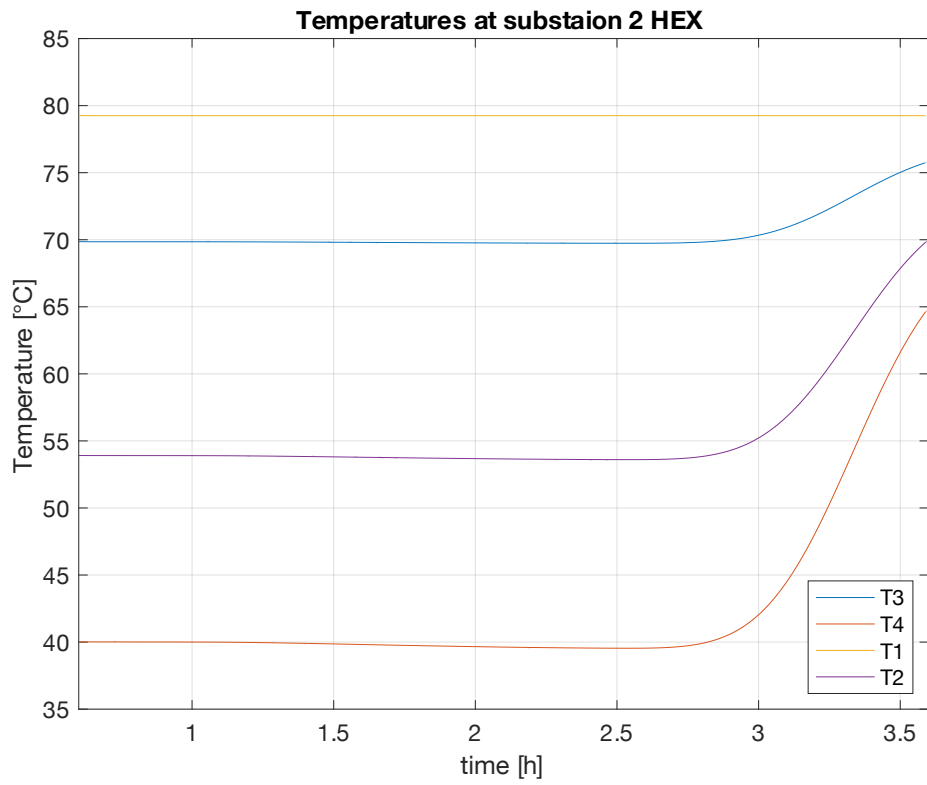


Figure 4-33 SIM 7 - Temperatures at substation 2 HEX

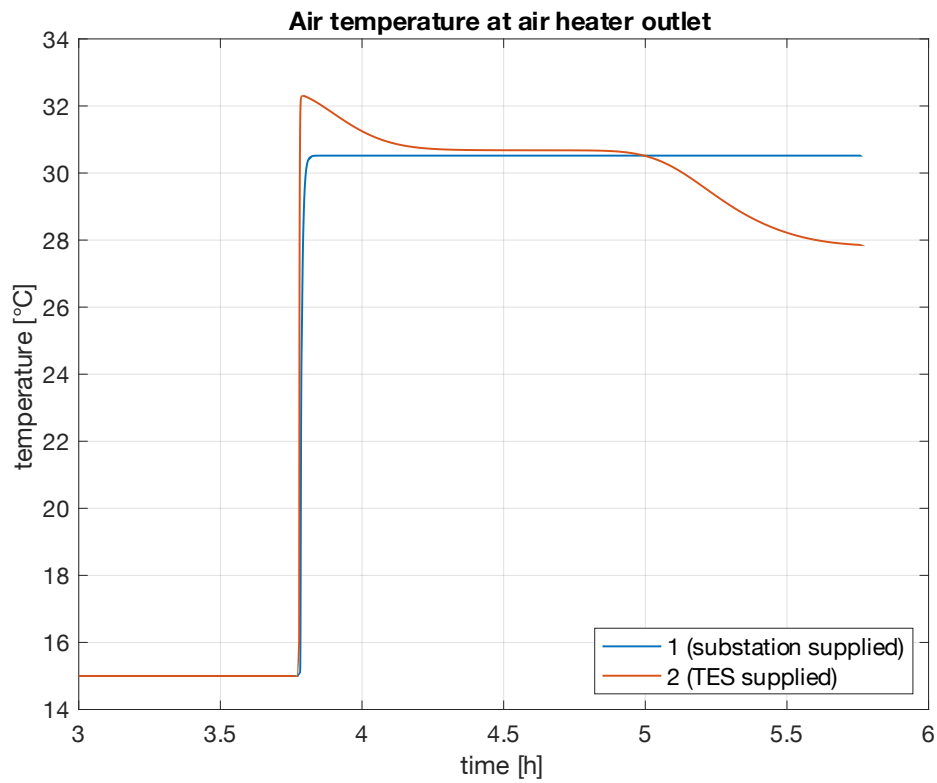


Figure 4-32 SIM 7 - Air temperature at air heater output

In figure 4-31, the curve of power output of the water heater is shown. The different phases are clearly visible. The first constant segment is due to the primary circuit preheating, while both substations are still inactive. Then the output reduces to a minimum before ramping up as the substation 2 is activated to charge the TES. The curve stabilizes as TES is being charged, only to decrease smoothly as the temperature target is being reached in the TES. This behaviour is better understood by looking at fig. 4-32, where the temperatures on the two sides of the substation 2 HEX are shown. As the TES is reaching the target temperature, the lower layers increase in temperature, after almost all the water present at the initial time (at 40°C) has been circulated.

After another brief minimum, right after the deactivation of substation 2, the WH power curve stabilizes between 15 and 20 kW, as soon as the substation 1 is activated and starts dissipating power through the air heater.

In figure 4-30 the temperature readings from the three thermocouples placed along the side of the TES are shown. As expected, the uppermost sensor detects the increase in temperature faster than the other, as hot water is being poured at the top and takes some time to mix, due to the stratification effect explained in the previous section. The opposite effect is visible during the discharge phase, when the lowest placed thermocouple registers a decrease in temperature due to cold water coming back from the air heater.

Finally, the temperature of heated air at the air heaters' outlet is compared in Fig. 4-33. The one at the air heater in secondary circuit 1 reports a constant behaviour as the substation 1 is being operated normally, supplied with hot water from the primary circuit. The other air heater is being supplied with hot water from the TES. At first a higher air temperature is registered, as the top layers in the TES have reached temperature above the target of 70°C. After the first layers have been discharged, a constant output is detected, due to the stratification effect. While cold water is being recirculated back into the TES, indeed, is kept at the lowest layers for the same effect. After about an hour and a half, the temperature drops below the one registered at the air heater 1, as the TES can no longer supply water at the target temperature of 70°C to the air heater.

With this simulation, the complete model was tested, representing both a charge and discharge phase, testing the operation of the actuators and the stability of the model when exposed to sudden changes.

4.6. Observations

In the last sections different scenarios were tested and the simulations' results showcased. As previously explained, these tests, carried out under designated condition, only served the purpose of demonstrating the feasibility of this modelling approach, laying the cornerstone on which eventually building a more comprehensive and capable digital twin. Through the various simulations, the models enable the analysis of critical system variables such as temperatures and thermal energy exchanged.

Despite the lack of reliable and detailed data about the system's performance, the creation of a complete model representing the behaviour of all the critical components was accomplished. However, many obstacles were encountered during the development highlighting a few weaknesses in the digital components employed, leaving room for further improvements.

First of all, components such as pipes and TES, based on a discretized design, posed the problem of determining the correct configuration, which can only be addressed through a thorough analysis in which feedback from the real system is essential. For instance, as discussed in the specific section, the digital TES reported an ideal stratification effect, which is not expected in the real one. A further analysis is also recommendable on the pipe component, which impacted heavily on computational performance, generating a possible issue when modelling larger systems.

In the second place, a special care and further analysis should be dedicated to the valves and other actuators that manage pressure levels throughout the system. Many simulations crashed due to issues related to pressure-related components. For instance, when a valve was closed to exclude the substation, some part of the circuits can be decoupled from their "boundary" pressure component, generating instability and eventual failure of the simulation.

In addition to these, the water heater component should be further investigated, as the one employed feature a highly simplified design, making the prediction of real behaviour more difficult.

Moreover, the model could be further enhanced including a more advanced control system, eventually replicating the ones present in the real system, such as temperature-based controls and variable mass flow rates.

In conclusion, the path towards a better modelling should begin with an extensive data collection about real operation cycles of the systems. With these data the components could be fine-tuned and modify to mimic the real ones, validating the work that has been done so far.

5. Conclusions

In this thesis the concept of the digital twin was investigated, and a possible interpretation was provided considering an experimental DH network a case study. As further discussed in the specific section, the digital twin concept can play a central role in accelerating the research in the energetic field, both to experiment with new concepts and improve the design and operation of current systems.

In this context, OpenModelica modelling and simulation environment, coupled with the various models provided by the Modelica Buildings Library proved to be a powerful and capable foundation to model such physical systems. Despite being an open-source software and, in turn, lacking a full support of some advanced Modelica libraries, considerable results were obtained and with the active support of the Modelica community, even better ones can be expected in the future.

The creation of a true digital model, however, requires constant feedback from the real system, the lack of which proved to be one of the weak points of the approach followed in this project.

In conclusion, the models created could be the basis for a more extensive “twinning” process of the real system, eventually creating a capable tool to support the research at the Energy Center laboratory, providing a cost-effective way to predict the system’ behaviour and study new configurations.

Ringraziamenti

Giunto alla fine di questo ambizioso percorso di studi, mi è ancora più chiaro quanto sia stato fondamentale l'aiuto e il supporto di tutte le persone che hanno scelto di starmi vicino, condividendo le gioie e i dolori di questi anni.

Vorrei innanzitutto esprimere la mia più sincera gratitudine verso Giulia e Gianmarco, che mi hanno seguito e guidato in questo progetto di tesi, senza i quali non avrei mai potuto risolvere i dubbi e superare le incertezze incontrate lungo la strada. Questa tesi è tanto mia quanto vostra, dunque, grazie di cuore!

Il ringraziamento più grande di tutti va alla mia famiglia, a mio papà, a mia mamma, a mio fratello, a mia nonna Carla e a tutti coloro che mi hanno protetto durante i momenti più bui e che mi hanno fatto rialzare dopo ogni caduta, facendosi da parte e regalandomi giorno dopo giorno il loro affetto e il loro sostegno. Grazie dal profondo del mio cuore!

Un abbraccio forte e un caloroso ringraziamento vanno a Tata e a Vito e a tutta la mia famiglia di Gavirate, senza i quali non sarei diventato la persona che sono adesso. Vi voglio bene!

Un grazie e un abbraccio vanno alla mia più cara amica, Valentina, che non hai mai smesso di stare al mio fianco, nonostante tutte le difficoltà e i cambiamenti che entrambi ci siamo trovati ad affrontare. Grazie!

Durante il mio percorso ho avuto la fortuna di conoscere delle persone fantastiche, che mi hanno aiutato e accompagnato sempre, esame dopo esame, progetto dopo progetto. Un ringraziamento speciale a Marta, la miglior compagna di banco e amica che potessi desiderare, Grazie!

Grazie a Rob, a Nick, a Lucio, a Fra e a Ste! Siete fantastici!

Grazie a Daniele, che ha sempre saputo alleggerirmi in questi tempi difficili oltre ad essere stato un formidabile coinquilino. Grazie!

Grazie anche a Francesca, a Clara, ad Ila, a Ciano, a Dundu, e a tutti coloro che non ho potuto menzionare qui.

References

- [1] D. Jones, C. Snider, A. Nassehi, J. Yon and B. Hicks, "Characterising the Digital Twin: A systematic literature review," *CIRP Journal of Manufacturing Science and Technology*, no. 29, pp. 36-52, 2020.
- [2] The Modelica Association, "The Modelica Language," [Online]. Available: modelica.org/language/. [Accessed January 2024].
- [3] EUROSTAT, "Heating and cooling from renewables gradually increasing," 2023. [Online]. Available: <https://ec.europa.eu/eurostat/web/products-eurostat-news/w/DDN-20230203-1>.
- [4] European Commission, "Energy Efficiency Directive," [Online]. Available: https://energy.ec.europa.eu/topics/energy-efficiency/energy-efficiency-targets-directive-and-rules/energy-efficiency-directive_en. [Accessed February 2024].
- [5] European Commission, "REPowerEU," [Online]. Available: https://commission.europa.eu/strategy-and-policy/priorities-2019-2024/european-green-deal/repowereu-affordable-secure-and-sustainable-energy-europe_it. [Accessed February 2024].
- [6] European Commission, "Clean Energy For All Europeans Package," [Online]. Available: https://energy.ec.europa.eu/topics/energy-strategy/clean-energy-all-europeans-package_en. [Accessed February 2024].
- [7] European Commission - Directorate for Energy, L. Kranzl, M. Fallahnejad and R. e. a. Büchele, "Renewable space heating under the revised Renewable Energy Directive : ENER/C1/2018-494 : final report," European Commission, Directorate-General for Energy, 2022.
- [8] B. V. Mathiesen, N. Bertelsen, N. C. A. Schneider, L. S. García, S. Paardekooper, J. Z. Thellufsen and S. R. Djørup, "Towards a decarbonised heating and cooling sector in Europe: Unlocking the potential of energy efficiency and district energy," Aalborg Universitet, 2019.
- [9] IEA, "World Energy Investment 2020," IEA, Paris, 2020.
- [10] Gestore dei Servizi Energetici (GSE); Ministero della Transizione Ecologica, "Valutazione del Potenziale Nazionale e Regionale del Riscaldamento Efficiente," GSE - Direzione Studi e Monitoraggio di Sistema, Roma, 2021.

- [11] European Commission - Directorate for Energy, Tilia, T. Wien, IREES, Öko-Institut and E. ISI, “Overview of District Heating and Cooling Markets and Regulatory Frameworks under the Revised Renewable Energy Directive,” European Commission - Directorate for Energy, 2021.
- [12] Gestore dei Servizi Energetici (GSE), “Teleriscaldamento e Teleraffrescamento 2020 - nota di approfondimento giugno 2022,” GSE - Direzione Studi, Monitoraggio e Relazioni internazionali, Roma, 2022.
- [13] European Commission Directorate-General for Energy, S. Lettenbichler, J. Corscadden and A. Krasatsenka, “Advancing district heating & cooling solutions and uptake in European cities : overview of support activities and projects of the European Commission on district heating & cooling,” Publication Office of the European Union, 2023.
- [14] European Science Communication Institute, “W.E. District - Heating & Cooling Solutions,” [Online]. Available: <https://www.wedistrict.eu>. [Accessed February 2024].
- [15] Sustainable Energy Planning Research Group Department of Planning, Aalborg University, “Heat Roadmap Europe,” [Online]. Available: <https://heatroadmap.eu/contact/>. [Accessed February 2024].
- [16] Interreg North-West Europe, “HeatNet NWE,” [Online]. Available: <https://www.nweurope.eu>. [Accessed February 2024].
- [17] J. Martinez, F. Bava, J. Romani and C. e. a. Bosio, “WEDISTRICT replicability towards 4th-5th generation of DHC,” 2023.
- [18] H. Lund, S. Werner, M. Chang, S. Svendsen and J. E. e. a. Thorsen, “The status of 4th generation district heating: Research and results,” *Energy*, no. 164, pp. 147-159, 2018.
- [19] S. Paaedekooper, B. V. Mathiesen, M. Chang, R. Uni and L. e. a. Grundahl, “Quantifying the impact of low-carbon heating and cooling roadmaps,” Aalborg Universitet, 2018.
- [20] European Commission, “REPowerEU at a Glance,” October 2022. [Online]. Available: https://commission.europa.eu/strategy-and-policy/priorities-2019-2024/european-green-deal/repowereu-affordable-secure-and-sustainable-energy-europe_en. [Accessed January 2024].
- [21] Governo Italiano; Presidenza del Consiglio dei Ministri, “Italia Domani - Piano Nazionale di Ripresa e Resilienza,” [Online]. Available: <https://www.italiadomani.gov.it/content/sogei-ng/it/it/home.html>. [Accessed February 2024].

- [22] European Environment Agency, “Decarbonising heating and cooling — a climate imperative,” February 2023. [Online]. Available: <https://www.eea.europa.eu/publications/decarbonisation-heating-and-cooling/decarbonising-heating-and-cooling>. [Accessed January 2024].
- [23] J. Wu, Y. Yang, X. Cheng, H. Zuo and Z. Cheng, “The Development of Digital Twin Technology Review,” in *2020 Chinese Automation Congress*, 2002.
- [24] H. Sebastian and A. Reiner, “Digital Twin - Proof of concept,” *Manufacturing Letters*, no. 15, pp. 64-66, 2018.
- [25] The Modelica Association, “The Modelica Association,” [Online]. Available: modelica.org/association/. [Accessed January 2024].
- [26] D. M. M. Tiller, “Modelica by Example,” [Online]. Available: mbe.modelica.university. [Accessed January 2024].
- [27] The Modelica Association, “Modelica Tools,” [Online]. Available: modelica.org/tools/. [Accessed January 2024].
- [28] Open Source Modelica Consortium, “OpenModelica Introduction,” [Online]. Available: openmodelica.org. [Accessed January 2024].
- [29] F. Peter, P. Adrian, A. Karim, A. Adeel and B. e. a. Bernhard, “The OpenModelica Integrated Environment for Modeling, Simulation, and Model-Based Development,” *Modeling, Identification and Control*, vol. 41, no. 4, pp. 241-285, 2020.
- [30] The Regents of the University of California, through Lawrence Berkeley National Laboratory, “Modelica Buildings Library,” [Online]. Available: simulationresearch.lbl.gov/modelica/index.html. [Accessed January 2024].
- [31] AIT-IES, “AIT-IES DisHeatLib,” [Online]. Available: <https://github.com/AIT-IES/DisHeatLib>. [Accessed February 2024].
- [32] B. Leitner, E. Widl, W. Gawlik and R. Hofmann, “A method for technical assessment of power-to-heat use cases to couple local district heating and electrical distribution grids,” *Energy*, vol. 182, pp. 729-738, 2019.
- [33] M. Bachmann, Y. Furst, D. Stanica and M. Kriegel, “dhcSim - A Modelica library for simple modeling of complex DHC systems,” *Energy Reports*, vol. 7, pp. 294-303, 2021.
- [34] M. Abugabbaraa, J. Lindhea, S. Javeda, H. Baggeb and D. Johanssona, “Modelica-based simulations of decentralised substations to support decarbonisation of district heating and cooling,” *Energy Reports*, vol. 7, pp. 465-472, 2021.

- [35] A. Maccarini, A. Sotnikov, T. Sommer, M. Wetter, M. Sulzer and A. Afshari, "Influence of building heat distribution temperatures on the energy performance and sizing of 5th generation district heating and cooling networks," *Energy*, vol. 275, 2023.
- [36] A. Gautier, M. Wetter and M. Sulzer, "Resilient cooling through geothermal district energy system," *Applied Energy*, vol. 325, 2022.
- [37] K. Hinkelman, S. Anbarasu, M. Wetter, A. Gautier and W. Zuo, "A fast and accurate modeling approach for water and steam thermodynamics with practical applications in district heating system simulation," *Energy*, vol. 254, 2022.
- [38] K. Hinkelman, J. Wang, W. Zuo, A. Gautier, M. Wetter, C. Fan and N. Long, "Modelica-based modeling and simulation of district cooling systems: A case study," *Applied Energy*, vol. 311, 2022.
- [39] B. Van der heijde, M. Fucjs, C. Tugores Ribas, G. Schweiger, K. Sartor, D. Basciotti, D. Muller, C. Nytsch-Geusen, M. Wetter and L. Helsen, "Dynamic equation-based thermo-hydraulic pipe model for district heating and cooling systems," *Energy Conversion and Management*, vol. 151, pp. 158-169, 2017.
- [40] Energy Center; Politecnico di Torino, "Energy Center - Politecnico di Torino," [Online]. Available: energycenter.polito.it. [Accessed February 2024].
- [41] FINTERM s.p.a., "Joannes AR-NOx H / AR-NOx BT H".
- [42] Wilo, "Wilo-Stratos MAXO," [Online]. Available: https://wilo.com/it/it/Prodotti-e-competenze/it/prodotti-ed-expertise/edifici-commerciali/riscaldamento/riscaldamento/wilo-stratos-maxo?t=0#c8ae2889e58f131940158f310b6a70d4eTL4_range_advantages. [Accessed February 2024].
- [43] AMARC DHS, "Amarc dhs products," [Online]. Available: <https://www.amarcdhs.it/product>. [Accessed February 2024].
- [44] S. Frederiksen and S. Werner, *District Heating and Cooling*, Lund: Studentlitteratur, 2013.
- [45] Alfa Laval, "Alfa Laval Shop: CB30-24H," [Online]. Available: <https://shop.alfalaval.com/it-ch/riscaldamento-a-radiatori--c003/cb30-24h--1265269->. [Accessed February 2024].
- [46] Sabiana, "Catalogo tecnico aerotermi Atlas," [Online]. Available: https://www.sabiana.it/storage/download/products/1/65e19eb291085_aerotermi-it-cat-99a4070000-rev-02-2024-spdf.pdf. [Accessed February 2024].

- [47] Wilo, "Wilo Stratos 32/1-12," [Online]. Available: <https://wilo.com/it/it/Solutions-Finder/Scelta-e-dimensionamento/Guida-comparativa-riscaldamento/it/wilo/wilo-stratos/stratos-32-1-12-pn-6-10>. [Accessed February 2024].
- [48] V. Verda and E. Guelpa, "Thermal energy storage in district heating and cooling systems: A review," *Applied Energy*, vol. 252, 2019.
- [49] H. O. Njoku, O. V. Ekechukwu and S. Onyegebu, "Analysis of stratified thermal storage systems: An overview," *Heat Mass Transfer*, vol. 50, pp. 1017-1030, 2014.
- [50] TML Industrie Loddo, «Termoaccumulo Pufferspeicher,» [Online]. Available: <https://www.tmlgroup.it/index.php?id=15&itemid=40>. [Accessed February 2024].
- [51] The Modelica Association, "Modelica Standard Library," [Online]. Available: <https://github.com/modelica/ModelicaStandardLibrary>. [Accessed February 2024].
- [52] Institute of System Dynamics and Control, German Aerospace Center (DLR), "The DLR Thermofluid Stream Library," [Online]. Available: <https://github.com/DLR-SR/ThermofluidStream?tab=readme-ov-file>. [Accessed February 2024].
- [53] Lawrence Berkeley National Laboratory; University of California, "Modelica Buildings Library Documentation," [Online]. Available: <https://simulationresearch.lbl.gov/modelica/releases/v10.0.0/help/Buildings.html>. [Accessed February 2024].
- [54] M. Doninelli and Caleffi, "Le Reti di Distribuzione," Quaderni Caleffi.
- [55] M. Ancona, L. Branchini and F. Melino, "Analisi di una rete di teleriscaldamento reale e progettazione di una sottostazione di scambio termico bidirezionale per reti di teleriscaldamento," *Accordo di programma Ministero dello Sviluppo Economico - ENEA, Dipartimento di Ingegneria Industriale, Università di Bologna*, 2017.
- [56] Open Source Modelica Consortium (OSMC), "OpenModelica User's Guide," [Online]. Available: <https://openmodelica.org/doc/OpenModelicaUsersGuide/1.22/>. [Accessed February 2024].
- [57] Interreg NWE - HeatNet, "HeatNet NWE," [Online]. Available: <https://guidetodistrictheating.eu/about/what-is-district-heating/>. [Accessed February 2024].

- [58] I. G. Trovato, "Studio Termotecnico Trovato," [Online]. Available: <https://www.studiotermotecnicotrovato.it/blog-hvac/teleriscaldamento-un-confronto-con-impianti-innovativi/>. [Accessed February 2024].
- [59] T. Fei, X. Bin, Q. Qinglin, C. Jiangfeng and J. Ping, "Digital twin modeling," *Journal of Manufacturing Systems*, no. 64, pp. 372-389, 2022.
- [60] K. Sartor, "Modeling heat transport in district heating networks - Preliminary report," Université de Liège - Faculté des Sciences Appliquées, 2015.